LAND-ATMOSPHERE EXCHANGE OF MERCURY IN TEMPERATE WETLANDS

by

LORA M. SMITH

A dissertation submitted to the

Graduate School-New Brunswick

Rutgers, The State University of New Jersey

in partial fulfillment of the requirements

for the degree of

Doctor of Philosophy

Graduate Program in Environmental Sciences

written under the direction of

Dr. John R. Reinfelder

and approved by

_____

_____

_____

_____

New Brunswick, New Jersey

October, 2008

ABSTRACT OF THE DISSERTATION

Land-Atmosphere Exchange of Mercury in Temperate Wetlands

By LORA M. SMITH

Dissertation Director:

Dr. John R. Reinfelder

Gaseous elemental mercury (Hg^0) cycling in temperate wetlands was evaluated by performing an atmospheric deposition study in addition to in situ micrometeorological and laboratory dynamic flux chamber experiments examining New Jersey salt marsh sediments.

Mercury wet deposition was measured at an urban/suburban site in eastern central New Jersey (New Brunswick) and at a rural site in northwestern New Jersey (Belvidere). Volume-weighted mean mercury concentrations in precipitation were greater in New Brunswick (11 ng L^{-1}) than Belvidere (8.6 ng L^{-1}) and exhibited seasonality with highest concentrations in the summer. Over a seven year period (1999-2002 from Zhuang 2004, plus 2003-2006 from this study), mercury concentrations in New Brunswick precipitation decreased at a rate of 0.2 μg m^{-2} y^{-1}, while over a three year period (2002-2005) in Belvidere, mercury concentrations were constant. Annual wet deposition fluxes for New Brunswick and Belvidere were 12 and 11 μg m^{-2} y^{-1} respectively, similar to previous estimates for New Jersey. No patterns were observed

between Hg and other analyzed trace metals. Meteorological conditions also did not correlate, indicating local and regional sources.

In situ estimates of sediment-air mercury volatilization fluxes were an order of magnitude higher at the Secaucus High School Marsh (-375 to +677 ng m^{-2} h^{-1}) than at the Great Bay estuary (-34 to +81 ng m^{-2} h^{-1}). Mercury volatilization fluxes were positively correlated with solar radiation at the Great Bay estuary but only on one out of six sampling days in Secaucus, potentially a result of tides. Areally averaged annual mercury emissions from Secaucus (0.06 kg y^{-1}) are much lower than those from industrial sources in New Jersey, but preliminary scaling up of mercury emissions estimated for the much larger Great Bay estuary (13 kg y^{-1}) indicate that it is comparable to minor industrial sources in the State.

Laboratory flux chamber experiments showed that photochemistry is more important in sediment-air mercury volatilization than other physicochemical sediment characteristics. In the light, mercury flux from sediments was up to 50 times larger than in the dark, with the greatest emissions observed during visible + UV treatments, as observed in the natural environment.

Dedication

To John, who inspired me…

Your wise words and thoughtful criticisms cultivated a dissertation and an eager mind.

To my family, who kept me grounded…

Your undying love, support, and unfaltering faith in me paved even the most arduous roads along this journey. While I am grateful for every member of my family, I give special thanks to: Mom & Dad, Gram & Poppy, Michelle, and my most loyal companion, Brandi.

To my friends, who made me laugh until I cried…

They say that friends are the family we choose. I have managed to surround myself with an intimate group of the most intelligent, humorous, beautiful, loyal and genuine friends imaginable. I especially thank the best girlfriends a gal could ask for: Amy, Erin, and Juliet.

To Mike, who held my hand and shared my dream…

You may not have begun this marathon with me, but you have made the finish line so much sweeter. In the wise words of Gandhi, "Where there is love, there is life". I feel so alive with you by my side. Every day is a new adventure and I am forever grateful to share each and every one with you.

Acknowledgements

A number of individuals assisted me in completing this work. A study of this magnitude would not be possible without the assistance and input of a consortium of contributors. A sincere thanks to: the Department of Education (GAANN Fellowship), the Hudson River Foundation, and NJDEP for funding my work; Ed Konsevick and Joe Sarnoski of MERI, Dr. Beth Ravit and Jared Eudell of Hackensack Riverkeeper Inc., and Dr. Chuck Nieder of the Hudson River NERR/NYSDEC for sample collection; Sandy Goodrow for her GIS expertise; the members of Dr. Reinfelder's lab, past and present, especially Derek Wright; everyone in the Department of Environmental Science who provided assistance along the way; and to the members of my committee: Lisa Rodenburg (Totten), Nathan Yee, Steve Peters and especially my advisor and mentor, John Reinfelder.

Table of Contents

List of Tables

List of Figures

Chapter 1:

Introduction

1.1. Mercury in the environment

Mercury is present in the atmosphere as a result of both natural and anthropogenic activity, existing in various forms. Natural sources of mercury include volcanoes, geothermal vents, hot springs, and forest fires, along with fresh- and salt-water bodies [Nriagu 1989; UNEP 2002; EC 2003; USGS 2004]. Anthropogenic sources are more diverse as the distinctive qualities of this metal (Table 1.1) have given rise to a wide variety of uses. The mining of cinnabar, the principal mercury-containing ore, and its subsequent smelting result in considerable human-induced releases of mercury to the environment. In the metallic, elemental form, mercury can be used as an amalgam in dental fillings as well as in mining silver and gold [Carpi 2001]. This distinctive metal is used as a catalyst in chlor-alkali plants, and can be found in batteries, fluorescent light bulbs, thermometers and electrical switches [US EPA 2003]. Mercury has further potential for release to the atmosphere during waste incineration of many of the aforementioned products, yet the greatest man-made contribution to the atmospheric mercury pool remains coal-fired power plants [Pacyna & Pacyna 2000; PA DEP 2003]. Lindberg et al. [2007] report that current direct anthropogenic and truly natural sources are thought to contribute about equally to the global tropospheric pool.

The major concern regarding mercury in aquatic ecosystems is the threat of transformation to the highly toxic methylmercury species which bioconcentrates more than a million-fold in aquatic food chains [USGS 2004; Hall et al. 2005; Wangberg et al. 2007]. The organic methylmercury species is a known neurotoxin and when ingested, absorbs into the bloodstream and distributes to tissues throughout the body, including the brain [US EPA 1999].

1.2. Fate and transport

The term cycling refers to the inputs to and outputs from a system, as well as transport and transformations within the system [Zillioux et al. 1993]. Mercury contamination of remote, pristine regions has lead to the recognition that mercury is a global pollutant as its transport is dominated by atmospheric pathways [Canario & Vale 2004], a result of the high vapor pressure of this heavy metal (Table 1.1; Schroeder et al. 1991). The exchange of mercury between the atmosphere and the Earth's surface is bidirectional, with three pathways of air-surface exchange: wet deposition, particle deposition and gas exchange [Lindqvist & Rodhe 1985; Fitzgerald, 1989]. The studies conducted involved two of the three exchange pathways: wet deposition and gas exchange (volatilization), the least understood pathway (Fig. 1.1).

1.2.1. *Atmospheric deposition*

Atmospherically deposited mercury is divided into wet and dry deposition depending on depositional mechanisms. Wet deposition occurs when mercury associated with moisture (e.g. rain, snow, sleet, dew, clouds, etc.) is deposited on a surface. Dry deposition refers to atmospheric fall-out of particle-bound forms of mercury and is difficult to estimate using current methodologies.

Atmospheric mercury exists primarily (up to 99%) in the gaseous elemental form (Hg^0), with small quantities in the divalent (Hg^{2+}), monomethylmercury (CH_3Hg^+ or MMHg), dimethylmercury (DMHg), and particulate (Hg_p) forms [Slemr et al. 1985; Zillioux et al. 1993; Morel et al. 1998; Lin & Pehkonen 1999]. Since a majority of the atmospheric mercury pool is gaseous elemental, the average residence time is quite long

(between 6 and 24 months), supporting global transport [Morel et al. 1998; Schroeder & Munthe 1998; Lindberg et al. 2007; NADP 2008].

When atmospheric elemental mercury is oxidized to the more water-soluble divalent mercury (Hg^{2+}), it can be easily removed by wet deposition [Iverfeldt & Lindqvist 1986; USGS 2004]. Hg^{2+} and Hg_p, along with MMHg and DMHg, contribute to a majority of precipitation despite their low concentrations in the atmosphere [Downs et al. 1998]. The amount of mercury scavenged by precipitation depends not only upon Hg speciation, but also local and regional meteorological conditions [Keeler et al. 2006; Wangberg et al. 2007], availability of redox reactants [Munthe & McElroy 1992], season [Sorensen et al. 1994; Hoyer et al. 1995], air mass transport [Hoyer et al. 1995], and source locations and characteristics [Guentzel et al. 2001; Mason et al. 1997]. Various other atmospheric trace metals originate from the same sources as mercury and may serve as atmospheric mercury tracers.

While gaseous elemental mercury influx from point source discharges and atmospheric deposition is very well studied and monitored, little is known about the efflux of Hg^0 back into the atmosphere from land surfaces, especially wetlands. Global mercury budgets indicate that 50% of deposited mercury is subsequently re-emitted to the atmosphere [Bergan et al. 1999; Mason & Sheu 2002], but few studies and no monitoring of wetland volatilization are currently available.

1.2.2. *Wetland sediment-air gas exchange*

Wetlands include a broad range of habitats that continually or periodically (diurnally, seasonally, or occasionally) have standing water. There are three general

types of wetlands: freshwater, brackish water, and salt water. While not historically considered significant sources or sinks of mercury on a global scale, salt marshes are delicate breeding grounds for many animal species [Lee et al., 2000]. As a result, the transport and transformations of mercury are of concern in these habitats.

Atmospheric deposition is often times a significant source of mercury to wetlands [Livett 1988], both directly and indirectly (runoff; Mason et al. 1997). Many wetland sediments accumulate mercury as a result of the high reported partition coefficient (Kd) of mercury between the water column and suspended sediment particles (400,000; Fitzgerald & O'Connor 2001). In the anaerobic bottom sediments of wetlands, Hg(II) can be converted to the neurotoxic methylmercury [Hall et al. 2005].

Once deposited to land and water surfaces, mercury may be remobilized to the atmosphere by way of emission, resulting from a number of complex processes. In the water column, mercury is preferentially accumulated in suspended particles, associated with sulfides or organic matter, precipitated, and buried [Morel et al. 1998]. In tidally-influenced salt marsh sediments, resuspension of buried anoxic sediments replenishes the sediment surface with a fresh pool of reduced mercury that may be released at low tide. Also during low tide when mudflats are exposed, photochemistry is believed to be an important mechanism for the reduction of Hg^{2+} species to the volatile Hg^{0}. This process is thought to be dependent upon the levels of reducible Hg^{2+} complexes, radiation wavelength, and radiation intensity [Morel et al. 1998]. In fact, solar radiation has been identified as a stimulus for mercury re-emission over various surfaces including contaminated soils [Lindberg et al. 1995; Leonard et al. 1998; Gustin 2003; Feng et al.

2005], vegetation [Leonard et al. 1998; Lindberg et al. 2002], water bodies [Garcia et al. 2005; O'Driscoll et al. 2005], and wetlands [Zhang et al. 2002].

Various other physicochemical properties of the wetland sediments may enhance or inhibit the transport of mercury to the atmosphere. Evasional fluxes of mercury from sediments are thought to be driven, in part, by pH [Rada et al. 1993; Zillioux et al. 1993] and mercury is often bound to organic matter [Mieli 1997]. As such, the studies performed investigated various properties of the sediment to examine if a positive or negative correlation with mercury volatilization could be established.

Approaches for measuring Hg emissions from tidally-exposed salt marsh sediments include controlled laboratory exposure chambers, field flux chambers, and micrometeorological methods. The studies presented utilized in situ micrometeorological methods and laboratory flux chambers.

1.3 Research objectives

The primary goals of this research were to continue the New Jersey Atmospheric Deposition Network (NJADN) wet deposition study in New Brunswick, developing long-term trends and to estimate Hg volatilization fluxes from salt marsh sediments in the state. The three papers presented serve to assess the fate and transport of mercury via two mechanisms: wet deposition to and land-air volatilization from tidally-exposed wetland sediments to better evaluate whether New Jersey is a net sink or source of Hg to the atmosphere.

The objectives of this dissertation were to:

1. Estimate wet deposition concentrations and fluxes for mercury and other trace metals/metalloids in New Jersey and evaluate long-term trends.
2. Estimate in situ sediment-air mercury fluxes in New Jersey salt marshes and evaluate the importance of sediment mercury concentration, micrometeorology, and solar radiation to this flux.
3. Estimate Hg fluxes from salt marsh, freshwater wetland, and riverine sediment samples in laboratory flux chamber experiments and investigate the effects of photochemistry, organic matter, sediment mercury content, and other physicochemical properties on mercury flux.
4. Compare in situ and flux chamber methods and estimate theoretical in situ fluxes for chamber fluxes.
5. Provide better estimates of wet deposition fluxes and mercury volatilization fluxes from tidally-exposed wetland sediments to improve models of Hg cycling in New Jersey and the northeastern U.S.
6. Evaluate whether New Jersey is a net sink or source of mercury to the atmosphere.

References

Bergan, T., L. Gallardo, and H. Rodhe (1999), Mercury in the global troposphere: a three-dimensional model study, *Atmos. Environ., 33,* 1575-1585.

Canario, J. and C. Vale (2004), Rapid release of mercury from intertidal sediments exposed to solar radiation: a field experiment, *Environ. Sci. Technol., 38*, 3901-3907.

Carpi, A. (2001), The toxicology of mercury, Available online: http://web.visionlearning.com/carpi/Hg%20Toxicology%20Brief.pdf.

Downs, S.G., C.L. MacLeod, and J.N. Lester (1998), Mercury in precipitation and its relation to bioaccumulation in fish: a literature review, *Water Air Soil Pollut., 108,* 149-187.

EC (2003), Mercury and the environment: basic facts, Environment Canada, Available online: http://www.ec.gc.ca/mercury/bf-s-e.html.

Feng, X., S. Wang, G. Qui, Y. Hou, and S. Tang (2005), Total gaseous mercury emissions from soil in Guiyang, Guizho, China, *J. Geophys. Res., 110,* D14306, doi:10.1029/2004JD005643.

Fitzgerald, W.F. (1989), Atmospheric and oceanic cycling of mercury, Chemical Oceanography Series, Ch. 57, vol. 10. Riley, J.P. and R. Chester (Eds.), Academic Press, New York, pp. 151-186.

Fitzgerald, W.F. and J.S. O'Connor (2001), Mercury cycling in the Hudson/Raritan basin, Report to the NYAS industrial ecology, pollution prevention and the NY/NJ Harbor project, New York Academy of Sciences.

Garcia, E., M. Amyot, and P.A. Ariya (2005), Relationship between DOC photochemistry and mercury redox transformations in temperate lakes and wetlands, *Geochim. Cosmochim. Acta, 69(8),* 1917-1924.

Guentzel, J.L., W.M. Landing, G.A. Gill, and C.D. Pollman (2001), Processes influencing rainfall deposition of mercury in Florida, The FAMS Project (1992-1996), *Environ. Sci. Technol., 35,* 863-873.

Gustin, M.S. (2003), Are mercury emissions from geologic sources significant?: A status report, *Sci. Total Environ., 304,* 153-167.

Hall, B.D., H. Manolopoulos, J.P. Hurley, J.J. Schauer, V.L. St. Louis, D. Kenski, J. Graydon, C.L. Babiarz, L. B. Cleckner, and G.J. Keeler (2005), Methyl and total mercury in precipitation in the Great Lakes region, *Atmos. Environ., 39,* 7557-7569.

Hoyer, M., J. Burke, and G.J. Keeler (1995), Atmospheric sources, transport and deposition of mercury in Michigan: two years of event precipitation, *Water Air Soil Pollut., 80,* 199-208.

Iverfeldt, A. and O. Lindqvist (1986), Atmospheric oxidation of elemental mercury by ozone in the aqueous phase, *Atmos. Environ., 20,* 1567-1573.

Keeler, G.J., M.S. Landis, G.A. Norris, E.M. Christianson, and J.T. Dvonch (2006), Sources of mercury wet deposition in Eastern Ohio, USA, *Environ. Sci. Technol., 40,* 5874-5881.

Lee, X., G. Benoit, and X.Z. Hu (2000), Total gaseous mercury concentration and flux over a coastal saltmarsh vegetation in Connecticut, USA, *Atmos. Environ*., *34*, 4205-4213.

Leonard T. L., G.E. Taylor, M.S. Gustin, and G.C.J. Fernandez (1998), Mercury and plants in contaminated soils: 2. Environmental and physiological factors governing mercury flux to the atmosphere, *Environ. Toxicol. Chem., 17,* 2072-2079.

Lin, C., and S.O. Pehkonen (1999), The chemistry of atmospheric mercury: a review. *Atmos. Environ.,33,* 2067–2079.

Lindberg, S.E., W. Dong, and T. Meyers (2002), Transpiration of gaseous elemental mercury through vegetation in a sub-tropical wetland in Florida, *Atmos. Environ., 36*, 5207-5219.

Lindberg, S.E., K.H. Kim, T.P. Meyers, and J.G. Owens (1995), Micrometeorological gradient approach for quantifying air-surface exchange of mercury-vapor - tests over contaminated soils*, Environ. Sci. Technol., 29,* 126-135.

Lindberg, S.E., R. Bullock, R. Ebinghaus, D. Engstrom, X. Feng, W. Fitzgerald, N. Pirrone, E. Prestbo, and C. Seigneur (2007), A synthesis of progress and uncertainties in attributing the sources of mercury in deposition, *Ambio, 36(1),* 19-32.

Lindqvist, O. and H. Rodhe (1985), Atmospheric mercury – a review, *Tellus, 37B,* 136-159.

Livett, E.A. (1988), Geochemical monitoring of atmospheric heavy-metal pollution – theory and application, *Adv. Ecol. Res., 18,* 65-177.

Mason, R.P. and G.R. Sheu (2002), Role of the ocean in the global mercury cycle, *Global Biogeochem. Cycles, 16,* Art. No. 1093.

Mason, R.P., N.M. Lawson, and K.A. Sullivan (1997), Atmospheric deposition to the Chesapeake Bay watershed-regional and local sources, *Atmos. Environ., 31,* 3531-3540.

Meili, M. (1997), Mercury in lakes and rivers, *Metal Ions Biol. Syst., 34,* 21-51.

Morel, F.M.M., A.M.L. Kraepiel, and M. Amyot (1998), The chemical cycle and bioaccumulation of mercury, *Annu. Rev. Ecol. Syst., 29,* 543-566.

Munthe, J. and W.J. McElroy (1992), Some aqueous reactions of potential importance in the atmospheric chemistry of mercury, *Atmos. Environ., 26A,* 553-557.

National Atmospheric Deposition Program (NRSP-3) (2008), NADP Program Office, Illinois State Water Survey, 2204 Griffith Dr., Champaign, IL 61820.

Nriagu, J.O. (1989), A global assessment of natural sources of atmospheric trace metals, *Nature, 338,* 47-49.

O'Driscoll, N.J., A.N. Rencz, and D.R.S. Lean (2005), The biogeochemistry and fate of mercury in natural environments, Ch. 14, vol. 43, Sigel, A., H. Sigel, and R.K.O. Sigel (Eds.), Metal ions in biological systems, New York, Marcel Dekker, Inc., pp. 221-238.

Pacyna, J.M. and E.G. Pacyna (2000), Assessment of emissions/discharges of mercury reaching the Arctic environment, The Norwegian Institute for Air Research, *NILU Report,* Kjeller, Norway.

PA DEP (2003), Monitoring pollutants in rain, Pennsylvania Department of Environmental Protection, Available online: http://www.dep.state.pa.us/dep/deputate/airwaste/aq/acidrain/acidrain.htm.

Rada, R.G., D.E. Powell, and J.G. Wiener (1993), Whole-lake burdens and spatial distribution of mercury in surficial sediments in Wisconsin seepage lakes, *Can. J.*

Fish. Aquat. Sci.,50, 865-873.

Schroeder, W.H., G. Yarwood, and H. Niki (1991), Transformation processes involving mercury species in the atmosphere – results from a literature survey. *Water Air Soil Poll., 56,* 653-666.

Schroeder, W.H. and J. Munthe (1998), Atmospheric mercury – an overview, *Atmos. Environ., 32,* 809-822.

Slemr, F., G. Schuster, and W. Seiler (1985), Distribution, speciation and budget of atmospheric mercury, *J. Atmos. Chem., 3,* 407-434.

Sorensen, J.A., G.E. Glass, and K.W. Schmidt (1994), Regional patterns of wet mercury deposition, *Environ. Sci. Technol., 28,* 2025-2032.

UNEP Chemicals (2002), Global mercury assessment, United Nations Environment Programme, Geneva, Switzerland.

US EPA (1999), Mercury White Paper, Available online: http://www.epa.gov/ttn/oarpg/t3/memoranda/whtpaper.pdf.

US EPA (2003), Background information on mercury sources and regulations, Available online: http://www.epa.gov/cgi-bin/epaprintonly.cgi.

USGS (2004), Mercury contamination of aquatic ecosystems, United States Geological Survey, Available online: http://water.usgs.gov/wid/FS 216-95/FS 216-95.html.

Wangberg, I., J. Munthe, T. Berg, R. Ebinghaus, H.H. Kock, C. Temme, E. Bieber, T.G. Spain, and A. Stolk (2007), Trends in air concentration and deposition of mercury in the coastal environment of the North Sea Area, *Atmos. Environ., 41,* 2612-2619.

Zhang, H., S.E. Lindberg, M.O. Barnett, A.F. Vette, and M.S. Gustin (2002), Dynamic flux chamber measurement of gaseous mercury emission fluxes over soils: simulation of gaseous mercury emissions from soils using a two-resistance exchange interface model, *Atmos. Environ., 35,* 835-846.

Zillioux, E.J., D.B. Porcella, and J.M. Benoit (1993), Mercury cycling and effects in freshwater wetland ecosystems, *Environ. Toxicol. Chem., 12,* 2245-2264.

Table 1.1 Physicochemical Properties of Gaseous Elemental Mercury.

property	reported value	units	reference
atomic weight	200.59	g mol^{-1}	Lin & Pehkonen 1999a
melting point	-39	°C	Schroeder & Munthe 1998
boiling point at 1 atm	357	°C	Schroeder & Munthe 1998
density at 20°C	13.546	g cm^{-3}	Lin & Pehkonen 1999a
vapor pressure at 20°C	0.18	Pa	Schroeder & Munthe 1998
water solubility at 20°C	4.94E-05	g L^{-1}	Schroeder & Munthe 1998
Henry's Law coefficient at 20°C	729	Pa m^3 mol^{-1}	Schroeder & Munthe 1998
octanol water partition coefficient	4.2	dimensionless	Schroeder & Munthe 1998

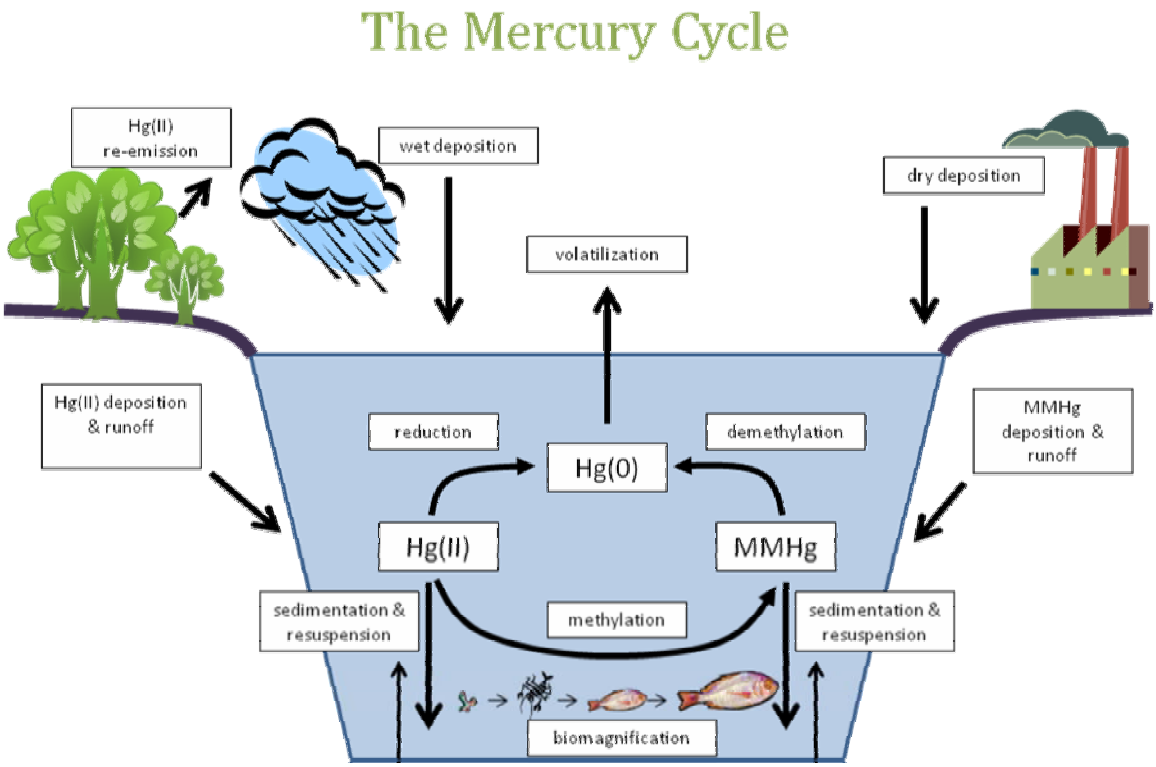

Figure 1.1 The global mercury cycle.

Chapter 2

New Jersey wet deposition:

Long-term trends in mercury and other trace elements

2.1 Introduction

Atmospheric deposition is an important pathway in the transport of trace elements from urban, impacted regions to more rural, pristine locales. Trace elements that partition to particles are rapidly removed from the atmosphere via wet and dry deposition, while elements with a significant vapor pressure (e.g., global average $P_{Hg} \approx 2 \times 10^{-13}$ atm at 20°C) at environmental temperatures (-12 to 32°C) will remain in the atmosphere much longer and may be transported over greater distances than particle-bound elements. As a result, meteorological phenomena, such as wind speed and direction, play major roles in the ultimate fate of atmospheric pollutants.

Over 90% of contaminant Hg is released into the atmosphere [USEPA 1997], where it undergoes short- or long-term transport before being deposited to the terrestrial environment [Lindqvist et al. 1991; Mason et al. 1994; Fitzgerald et al. 1998]. The atmospheric lifetime of mercury depends on chemical speciation and can range from minutes to years [Schroeder & Munthe 1998; Lindberg et al. 2007; NADP 2008]. Divalent (Hg^{2+}) and particulate (Hg_p) species will deposit near an emission source [Morel et al. 1998; Lindberg et al. 2007]. Conversely, elemental mercury (Hg^0) is readily transported in the gas phase and may travel great distances [Carpi 1997]. The US EPA [1997] estimates that 40% of mercury from combustion sources is in reactive form and deposited locally while 60% is elemental, contributing to the global atmospheric mercury load.

A variety of additional trace metals are released to the environment from the same sources (natural and anthropogenic) as mercury and may serve as atmospheric tracers of mercury emissions. For example, volcanic emissions and forest fires include a mixture of

trace elements in addition to mercury. At varying concentrations, these include: arsenic (As), cadmium (Cd), cobalt (Co), chromium (Cr), copper (Cu), manganese (Mn), nickel (Ni), antimony (Sb), vanadium (V), and zinc (Zn; Nriagu 1989). Anthropogenic emissions from coal combustion release mercury in addition to lead (Pb), chromium, manganese, antimony, and others [Nriagu & Pacyna 1988]. Arsenic, cadmium, copper, and zinc are also co-emitted with mercury during non-ferrous metal production [Themelis & Gregory 2001; Pacyna & Pacyna 2002].

Recent long term mercury wet deposition trends from 1998 – 2005 show a decreasing pattern for MDN sites in the northeastern U.S. [Butler 2008]. In fact, between time periods of 1999-2000 and 2003-2004, Sigler and Lee [2006] estimate that emissions in the Northeast have declined by 20%. However, another long term study conducted in the northeastern U.S. at Underhill, VT (1993-2003) found that Hg in wet deposition varied from year to year, with no clear increasing or decreasing trend [Keeler et al. 2005].

In order to assess the long term trend of mercury in New Jersey wet deposition, mercury and a suite of 14 metals and 2 metalloids (Mg, Al, V, Cr, Mn, Fe, Co, Ni, Cu, Zn, Pd, Ag, Cd, Pb, Sb, and As) were analyzed in 12 to 24 d integrated precipitation samples collected over seven years at an urban/suburban site in eastern central New Jersey and for three years at a rural site in northwestern New Jersey. A comparison of mercury wet deposition with a nearby suburban/rural National Atmospheric Deposition Program (NADP), Mercury Deposition Network (MDN) site in southeastern Pennsylvania was performed. Atmospheric mercury deposited to land surfaces in New Jersey and Pennsylvania is expected to have originated mostly from the Midwest and Ohio River Valley as a result of both the high density of coal-fired power plants and

waste incinerators located within this region and the prevailing westerly winds [US EPA 1997; Olmez et al. 2004; Choi et al. 2008].

This study is a continuation of work carried out as part of the New Jersey Atmospheric Deposition Network (NJADN) project [Reinfelder et al. 2004; Zhuang 2004]. The objectives of this study were: 1) to identify temporal trends in the atmospheric deposition of mercury and other trace elements in New Jersey, 2) to compare mercury wet deposition measured in New Jersey with that of an MDN site in Pennsylvania, and 3) to generate atmospheric deposition fluxes of mercury for comparison with emission fluxes from tidally-exposed wetland sediments in order to strengthen our understanding of the mercury cycle in the northeastern U.S..

2.2. Site description

2.2.1. *Rutgers Gardens, New Brunswick, Middlesex County, New Jersey*

The primary site study site was located at 40.47°N, 74.42°W in a locked and gated section of Rutgers Gardens, a 0.2 km^2 horticultural, display, and botanical garden owned and maintained by Rutgers, The State University of New Jersey (Fig. 2.1). The site is located in an urban/suburban area of east central NJ, adjacent to Westons Mill Pond, a tributary of the Raritan River. Sampling equipment was placed on a wooden platform, approximately 1 m above the ground surface.

2.2.2. *Belvidere High School, Belvidere, Warren County, New Jersey*

The comparison study site was located in the Belvidere High School recreation field (40.83°N, 75.07°W), adjacent to the Belvidere Cemetery (Fig. 2.1). Belvidere is a

rural town in northwestern NJ in close proximity to the Delaware Water Gap. At this site, the wet deposition collector was placed on the roof of a research trailer (approximately 3 m above the ground) located in a locked and gated section of the field.

2.2.3. *Valley Forge National Historic Park, Montgomery County, Pennsylvania*

Mercury concentrations in New Jersey wet deposition were compared with those from a suburban/rural site in east central Pennsylvania (40.12°N, 75.88°W). Samples from Valley Forge were collected as part of the Mercury Deposition Network (PA60; Fig. 2.1) by the United States Geological Survey (USGS). Further information on this sampling location can be accessed online via the MDN website (http://nadp.sws.uiuc.edu).

2.3. Methods

2.3.1. *Wet deposition sample collection*

Integrated 12 or 24 d wet deposition samples were collected using an MIC-B rain collector, fitted with Keeler-type [Landis & Keeler 1997] acrylic inserts to support bottle-funnel assemblies (Fig. 2.2). The MIC-B collector has a heated moisture sensor, signaling the lid to open and collect wet deposition during rain or snow events and remain closed during dry periods. Sample funnels were fabricated by removing the base of a 4 L borosilicate glass round bottle for total mercury (THg) and by removing the base of a 4 L polypropylene round bottle for trace metals (TM). The THg funnel provided a cross sectional area of 0.018 m^2 and the TM funnel, 0.017 m^2. The threaded neck of each funnel was connected to a sample bottle (1 L Teflon for THg, 1 L polypropylene for TM)

with a polyethylene adapter. A glass vapor lock and Teflon washers were fitted inside the funnel adapter for THg funnel assemblies to minimize mercury vapor loss during sample collection. Funnels, bottles, bottle-funnel connectors, glass vapor locks and washers were soaked in 10% reagent grade HCl for at least 24 hours prior to use. After removal from acid, parts were rinsed thoroughly with Q-H_2O and allowed to dry in a Class 100 laminar flow hood. Dry funnels, adapters, glass vapor locks and washers were assembled and bottles were tightly capped (Fig. 2.3). All funnel assemblies and bottles were then double bagged in plastic zip type bags and placed in a plastic container for transportation to field sites.

Integrated 5 to 15 d rain samples were collected in Valley Forge, PA. Sample collection and handling, equipment cleaning, collector troubleshooting, and shipping protocols for the NADP site in Valley Forge are detailed in the MDN Project Specific SOP provided by Frontier Geosciences, Inc. (Seattle, WA; http://nadp.sws.uiuc.edu/lib/manuals/mdnopman.pdf).

2.3.2 *Sample handling procedures*

In an effort to prevent sample contamination, the EPA Method 1669 "clean hands/dirty hands" technique was practiced [USEPA 1996]. On each sample collection day, the MIC-B rain collector was opened and powered off. With gloved hands, a clean sample funnel assembly was attached to a clean sample bottle with care taken to avoid touching interior surfaces of the clean funnel or bottle. The previous integrated THg and TM rain sample bottles were removed from the MIC-B. Funnels were separated from bottles which were capped, double-bagged, and placed in the plastic box to return to the

lab for preservation. With clean gloves, new funnel assemblies replaced those that were removed and the MIC-B was powered on, causing the collector lid to close.

2.3.3. *Sample preservation*

Upon returning to the lab, wet deposition volumes were estimated gravimetrically. On occasion, more than 1L of precipitation was collected in which case the volume of wet deposition collected in the funnel was measured in the field by decanting excess water into a graduated cylinder. This volume was then added to the total volume recorded in the lab.

Wet deposition samples for total Hg were preserved with 0.2% v/v 0.3M bromine monochloride (BrCl) to oxidize all Hg species to Hg(II). Reagents were prepared following EPA Method 1631, Revision E [USEPA 2002]. TM samples were acidified to 0.2% v/v [Landis & Keeler 1997] using concentrated Optima grade nitric acid (HNO_3) to prevent sorption of metals to colloids and other particles or bottle walls during storage. Each sample's unique identifier, volume, batch and amount of BrCl or HNO_3 used for preservation, and the analysis to be performed was recorded on the outer zip-type bag. Preserved samples were stored at 7ºC. Total Hg samples were analyzed within a month of collection while TM samples were analyzed within 6 months.

2.3.4. *Total mercury analysis*

Total mercury analysis was performed as per EPA Method 1631, Revision E [USEPA 2002]. The night prior to analysis, the Tekran model 2500 cold vapor atomic fluorescence spectrometer (CVAFS; Toronto, Canada) detector was powered on to warm

up the lamp and the sample gas lines were flushed with ultra high purity argon at a flow of 4 mL min^{-1}.

On the day of analysis, the UHP-Ar flow rate was increased to 50 mL min^{-1} on the mass flow controller and ultra high purity nitrogen (UHP-N_2) was turned on as a mercury-free carrier gas to the glass bubblers. Sensitivity on the Tekran was adjusted to 10x for wet deposition samples. The gain on the World Precision Instruments (Stevenage, England) Duo-18 Microsoft-based two channel data acquisition system was set to 1x and the time division on the Duo software was set to 300 s. This system serves as a liaison between the detector and computer to provide data in a user-friendly Excel format.

Electrical connections from two variable autotransformers (Staco Energy Products Co., Dayton, OH) to alligator clips and Nichrome resistance wire coils were checked and weakened components replaced, if necessary. If parts were replaced, it was important to first air burn the new parts as uneven heating may have occurred, causing damage to the gold traps. Next, the analytical gold coated sand traps were heated and analyzed. Any traps containing more than 0.1 ng of mercury were heated up to three times until mercury content was below 0.1 ng. If a gold trap maintained a Hg mass above this value after three heating cycles, it was not used.

While blank traps were analyzed, the following two steps were executed: 1) two 250 mL Pyrex (Corning Inc., Corning, NY) glass gas washing bottles with fritted discs (bubblers), stored in 50% reagent grade HCl for at least 24 h were emptied and thoroughly rinsed with Q-H_2O at least five times. The bubblers were then filled to approximately 125 mL with Q-H_2O and placed inside the mercury analytical class 100

clean hood and 2) two soda lime traps were constructed of 20 cm pieces of ¼ in (ID) PTFE tubing and ¼ in x ¼ in PTFE connectors that had been stored in 10% HCl for at least 12 h and were also rinsed clean with Q-H_2O and dried in the class 100 clean hood. Once dry, traps were filled with indicator free, ACS grade soda lime (4-8 mesh, Mallinckrodt Baker Inc., Phillipsburg, NJ), held in place with muffled quartz wool (Brooks Rand, Seattle, WA) end plugs and capped with Teflon connectors. Soda lime traps were then cleaned by adding 2 mL 0.5M stannous chloride ($SnCl_2$) to the bubblers, which reduces Hg from Hg^{2+} to Hg^0, and purged from solution through attached soda lime traps for 40 min.

After soda lime traps had been cleaned, four to five sets of blanks were run with 0.5 mL 0.5M $SnCl_2$ added to the Q-H_2O in each bubbler and bubbling each gold trap for 15 to 20 min at Q = 0.6 L min^{-1}. The RSD (relative standard deviation) for the blanks was between 0.8 and 22% (mean = 4.0 %; acceptable if < 35%) and the analytical detection limit was determined by 3 times the standard deviation of the $SnCl_2$ blanks as 11 pg, or approximately 0.014 ng L^{-1} (using an average sample volume of 0.8 L)

Once acceptable blanks were obtained, the instrument was calibrated by injecting mercury saturated air of known concentration, maintained as headspace gas over an elemental mercury standard, at injection volumes of 25, 50, 100 and 200 μL for a four point calibration curve. The y-intercept was set to 0; calibrations were acceptable if $r^2 > 0.999$.

The calibration was checked against an aqueous Hg standard. Two mL of the 1 ng mL^{-1} standard (diluted from ICM-642 TCLP 20 μg mL^{-1} mercury standard, Ultra Scientific, Kingstown, RI) were added to the Q-H_2O in each of the bubblers. This

corresponded to an approximate Hg mass of 2000 pg. Recoveries were 100 ± 10% of the gas calibration.

Next, one or two sets of reagent blanks were analyzed to determine the amount mercury in samples as a result of reagents used during preservation and analysis. These blanks quantified the amount of mercury in 1 mL 0.3M BrCl, 1 mL 2M NH_2OH•HCl (hydroxylamine hydrochloride), and 0.5 mL 0.5M $SnCl_2$ that were used in the samples. Reagent blanks were preferably < 15% of the sample concentration, however; if reagent blanks constituted a significant portion of the sample concentration, three or four sets were run and a standard deviation calculated to better assess uncertainty of the blank correction. Mean mercury concentrations of reagent blanks were subtracted from samples.

Bubblers were emptied of Q-H_2O mixture used for blanks and calibration and thoroughly rinsed with Q-H_2O. Brominated samples were removed from the refrigerator and treated with 1 mL 2M NH_2OH•HCl for every 1 mL 0.3M BrCl to neutralize excess BrCl in solution. Sample bottles were then inverted several times to mix and allowed to react for at least 30 minutes prior to analysis. Samples were poured into the bubblers, volumes recorded (generally 150 – 200 mL), and 0.5 mL 0.5M $SnCl_2$ added. Samples were bubbled for 15 min (Q = 0.6 L min^{-1}) onto gold-coated sand traps which were subsequently placed in line with a Tekran model 2500 (Toronto, Canada) cold vapor atomic fluorescence spectrophotometer (CVAFS) mercury detector [Fitzgerald & Gill 1979; Bloom & Crecelius 1983]. Two replicates of each sample were analyzed unless they differed by more than 10%, in which case a third or fourth replicate was run. All

replicates of each sample were run consecutively on the same bubbler to minimize variations.

2.3.5. *Trace metals analysis*

Concentrations of the following metals and metalloids: Mg, Al, V, Cr, Mn, Fe, Co, Ni, Cu, Zn, As, Pd, Ag, Cd, Sb, and Pb in wet deposition were measured by High Resolution - Inductively Coupled Plasma – Mass Spectrometry (HR-ICP-MS) on a Finnigan Element XR (Thermo Electron Corp., Waltham, MA). The Element XR was selected due to its wide linear dynamic detection range. The triple detector mode (Faraday, Analog, and Counting detector circuits) allows it to accurately measure trace (ppb) and ultra trace (ppt/ppq) up to percent quantities of elements with minimal interferences in a single analysis.

Previous work by Zhuang [2004] at Rutgers Gardens in New Brunswick provided expected concentration ranges for each of the elements investigated. As a result, we were able to synthesize a multi-element standard at tenfold the maximum expected concentration for each of the elements analyzed. This multi-element standard contained: 1000 ppb Mg, 400 ppb Al, 7 ppb V, 0.8 ppb Cr, 50 ppb Mn, 500 ppb Fe, 0.7 ppb Co, 20 ppb Ni, 30 ppb Cu, 300 ppb Zn, 1 ppb As, 0.6 ppb Pd, 0.3 ppb Ag, 1 ppb Cd, 1 ppb Sb, and 20 ppb Pb.

The Element XR has 3 resolution settings ($R = M (\Delta M)^{-1}$ at 10% peak height). Elements analyzed at low resolution (LR; R = 300) included As, Pd, Ag, Cd, Sb, and Pb. Those analyzed at medium resolution (MR; R = 4300) were Mg, Al, V, Cr, Mn, Fe, Co, Ni, Cu, and Zn. The only element scanned at high resolution (HR; R = 9300) was As,

which was also run at LR. One deviation from the Zhuang [2004] assignment of resolution was for Mg. MR rather than LR was selected because we used methane addition which forms a potentially interfering C-C dimer at LR for Mg.

Samples were analyzed in aqueous phase and introduced to the plasma using a SC-Fast PFA MicroFlow nebulizer, adapted to fit a conventional quartz cyclonic spray chamber. This nebulizer minimized cone deposition, allowing for continuous measurement and less sensitivity drift over time. The SC-Fast nebulizer was operated at a flow rate of 100 μL min^{-1}, providing low blanks. With a two minute uptake and two minute analysis, the SC-Fast provides a rapid and accurate estimate of trace elements in precipitation samples.

Analytical blanks were analyzed after every tenth trace metal sample on the ICP-MS. The average analytical blank was subsequently subtracted from all of the samples as a calculated concentration (Table 2.1). For most elements, this was less than a 5% correction except for Ag (12%) and Ni (54%). Ag is among the few elements which have large variability in analysis due to low concentration and nickel cones at the valve of the injection port (interface between the plasma and mass spectrometer) likely caused the observed nickel interference [Field & Sherrell 2003].

2.3.6. *Quality assurance*

2.3.6.1. *Field blanks*

In order to test the potential background contamination from lab cleaning and field procedures, one field blank was taken approximately every 10 samples for both total mercury and trace metals. Field blanks (FB) were collected in August 2000, February

2001, December 2001, August 2004, January 2005, February 2006, and July 2006 at Rutgers Gardens in New Brunswick (NB) and July 2004 and January 2005 at Belvidere (BV). Cleaned sampling bottles and funnel assemblies were brought to the field and assembled following sampling protocol. The assemblies were double-bagged in zip-type bags and returned to the lab where Q-H_2O was passed through the sampling train, collected in the respective bottles, and preserved according to previously described sample preservation procedures for both THg and TM.

Field blanks averaged 0.17 ng L^{-1} in New Brunswick and 0.36 ng L^{-1} in Belvidere for total mercury and were subtracted from sample concentrations. Mean field blank concentrations and the relative contribution of the FB to the overall rain sample concentration for trace elements in New Brunswick, NJ wet deposition over the seven year period (1999-2006) are shown in Table 2.1. Method detection limits were estimated as three times the standard deviation plus the mean of each trace element in field blanks and ranged from 3.0 ng L^{-1} (^{107}Ag) to 9.7 µg L^{-1}(^{27}Al). Since a majority of field blanks contributed less than 5% of the total concentrations of elements in rain, it was not necessary to do FB correction to the apparent concentration. Ag, Ni, Cu, Cr, and Zn in field blanks constituted >10% of the total concentration in rain. Silver and nickel interferences were previously mentioned. Zinc often has a high blank due to unknown laboratory sources. Chromium and copper may have also had an unknown contamination source in the lab.

2.3.6.2. *Total mercury analysis*

Total mercury samples were co-collected with the Mercury Deposition Network (MDN) on 18 July 2006 and 25 July 2006 at Rutgers Gardens when the site was acquired into the MDN as site NJ30. Sampling protocol for MDN requires that sample bottles be preserved prior to placement in the field, thus reducing volatile gaseous mercury and minimizing the loss term. For the 18 and 25 July 2006 samples, our measurements were 10 and 14% higher, respectively, than those in the MDN samples. Collocated MDN samples are expected to differ between one another by approximately 11% [Wetherbee et al. 2007], placing our samples within the error range of MDN samples. It is not clear which protocol provides the most accurate measurements.

Four duplicate (side-by-side) samples were collected in Belvidere to evaluate precision within our lab. Two samples were collected on 09 March 2004, 20 March 2004, 17 November 2004, and 19 February 2005 and analyzed for total mercury by CVAFS. All samples duplicates were within 10% of each other except 09 March 2004 which was a 14% deviation.

Precision of mercury concentration was determined for each sample. For n = 2:

$$precision = \frac{|C_2 - C_1|}{C_m} \times 100 \quad (1)$$

where C_2 and C_1 are measured sample concentrations (ng L^{-1}) and C_m is the mean sample concentration (ng L^{-1}). For n > 2:

$$precision = \frac{STD(C_1, C_2, C_i)}{C_m} \times 100 \quad (2)$$

where STD is standard deviation.

2.3.6.3. *Trace metals analysis*

Most common interferences for trace metals analyzed were resolved due to the high sensitivity (> 2 x 10^6 cps ppb^{-1} Indium) and resolving power of the Element XR (HR-ICP-MS). Accuracy of results was determined by blank analysis as described above, internal and external standardization, standard addition, and comparison with a certified reference material.

A 1ppm indium standard (^{115}In) was used as an internal standard to monitor sensitivity drift for trace metals other than mercury. Concentrations of each element in precipitation samples were calculated from indium-normalized intensities at each of the three resolutions. External standardization was performed using a multi-element standard to generate standard curves for all elements ($r^2 \geq 0.999$) and ensure analytical accuracy. A three point standard addition analysis was performed using the multi-element standard to identify matrix effects. Sample NB122805 was chosen as the standard addition sample due to low observed concentrations and was spiked with 2 mL and 5 mL of the multi-element standard. Spike recoveries were generally 100 ± 10%, except for Ag (88%) for both spikes, and Zn (86%), Sb (88%), and As (88%) for the 5 mL spike.

A NIST standard, ICM-442 CLP ICP Interference Check standard #2 (Ultra Scientific, North Kingstown, RI), was used to assess the precision and accuracy for the analyses of Ag, Cd, Co, Cr, Cu, Mn, Ni, Pb, V, and Zn. Relative standard deviations for

the CRM were < 3% and recoveries were 100 ± 10%, except for ^{107}Ag at 122% and ^{52}Cr at 55%. Concentrations for Ag in the NIST standard were beyond the linear range defined by the multi-element standard, resulting in a 22% over-estimation in the CRM. Samples within the linear range are expected to be accurate for Ag. The low recovery for Cr was a result of a pipetting error in the multi-element standard, whereby only half of the intended Cr was added. There was no suspicion of interference since the calibration curve was acceptable ($r^2 > 0.9999$). A 1 ppb Cr standard was analyzed to confirm analytical accuracy and percent recovery was near 100%. The error in the multi-element standard resulted in a factor of two offset for Cr in samples which was corrected by doubling Cr concentrations.

After correction for sensitivity variations, the concentration of each element analyzed by ICP-MS in unknown samples was calculated by dividing the normalized intensity by the mean slope of a five point calibration curve, which was analyzed three times throughout the analysis [Field & Sherrell 2003].

^{110}Pd is known to have a ^{111}Cd interference. A mathematical correction was applied to sample intensities for ^{110}Pd:

$$actual\ Pd(110) = measured\ Pd(110) - 0.9765 \times Cd(111) \quad (3)$$

The majority of RSDs for replicate samples were <10%; however, higher RSDs were found among elements which are a minor component of regional precipitation (i.e.- As, Co, Pd).

2.3.7. *Concentrations and fluxes of trace metals in wet deposition*

Seasonal and total volume-weighted mean (VWM) concentrations were calculated for each element in wet deposition samples using:

$$VWM = \frac{\Sigma x_i v_i}{\Sigma v_i} \tag{4}$$

where x_i is the elemental concentration and v_i is the precipitation volume of each sample.

The standard error of the VWM was calculated using the following equation [Gatz & Smith 1995a]:

$$(SEM)^2 = \left(\frac{n}{(n-1)(\Sigma v_i)^2} \right) \Sigma (x_i v_i - x_p v_i)^2 \tag{5}$$

where x_p is the VWM concentration.

Seasonal and annual wet deposition fluxes for each element were calculated using:

$$Flux_p = \frac{VWM_x \Sigma d_i}{\Sigma t_i} \tag{6}$$

where d_i is the rain depth (volume of precipitation divided by funnel area) of each cumulative rain sample and t_i is the length of time over which the VWM was measured.

Rain depths provided by a rain gauge at the New Brunswick site maintained by the Rutgers University Meteorology Program indicate that, on average, the rain volume method was generally lower than rain gauge values by 20%.

2.3.8. *Local meteorology*

Meteorological parameters including wind speed and direction, temperature, pressure, and relative humidity were also provided by the Rutgers University Meteorology Program from the weather station located within Rutgers Gardens (Appendix A.1). Data were provided over the range of sample dates and were used to investigate potential correlations with mercury and other trace metals in New Brunswick precipitation.

2.3.9. *Statistical analyses*

Regression analyses were performed to determine coefficients of determination r^2 and significance p for correlations at 95% confidence intervals. Means are reported ± SEM. The statistical significance between VWM concentrations was determined by calculating upper and lower 95% confidence intervals for each VWM using the SEM and observing whether the intervals overlap [Gatz & Smith 1995b]. Non-overlapping intervals indicated a significant difference [Gatz & Smith 1995b].

2.4. Results

2.4.1. *Total mercury*

Mercury precipitation concentrations in New Brunswick ranged from non-detect to 40 ng L^{-1} between 27 November 1999 and 26 July 2006 (VWM 11 ± 0.82 ng L^{-1}; Fig. 2.4; Appendix B.1). The annual wet deposition flux during the period of 27 November 1999 to 25 July 2006 in New Brunswick was 12 ± 0.87 μg m^{-2} y^{-1}.

In Belvidere, blank-corrected wet deposition Hg concentrations ranged from 1.2 to 29 ng L^{-1} (VWM 8.6 ± 0.54 ng L^{-1}; Fig. 2.5; Appendix B.2) between 15 November 2002 and 23 September 2005. Two samples collected 20 January 2004 and 1 February 2004 exceeded the upper limit of detection (>77 ng L^{-1}) and were suspected to be contaminated. As a result, these data were not included in calculations. The annual wet deposition flux in Belvidere from 15 November 2002 to 11 November 2005 was 11 ± 0.65 μg m^{-2} y^{-1}.

A comparison of mean mercury masses at the two sites for the period from 19 February 2003 through 23 September 2005, showed no correlation ($r^2 = 0.16$; Fig. 2.6). VWM concentrations in precipitation appeared greater in New Brunswick than in Belvidere (Figs. 2.4 & 2.5; Appendices B.1 & B.2); however, the relationship was not significant (overlapping 95% confidence intervals; Gatz & Smith 1995b).

While year to year, mercury concentrations varied, the overall trend for mercury in New Brunswick precipitation is gradually decreasing ($p < 0.05$; Fig. 2.4), while in Belvidere concentrations appeared constant over the three year study ($p = 0.82$; Fig. 2.5). During the same period in New Brunswick, rain depths were weakly significantly

increasing ($p < 0.01$) indicating a dilution of atmospherically deposited mercury (Fig. 2.4). When comparing two periods in NB, VWM for 1999 – 2002 was 15 ± 1.7 ng L^{-1}, and decreased by 40% during the 2003 – 2006 period when VWM dropped to 8.8 ± 0.86 ng L^{-1} (Table 2.2). The observed decrease of mercury in wet deposition over the two periods in New Brunswick was significant based on non-overlapping 95% confidence intervals [Gatz & Smith 1995b]. Comparing individual seasons between the two periods, the decreasing VWM trends were not significant. [overlapping 95% confidence intervals; Gatz & Smith 1995b].

Hg mass and rain depths were weakly positively correlated in New Brunswick ($r^2 = 0.34$, $p < 0.01$) and Belvidere ($r^2 = 0.33$, $p < 0.01$; Figs 2.7 & 2.8), with stronger correlations during summer ($r^2 = 0.40$, $p < 0.01$) and winter ($r^2 = 0.39$. $p < 0.01$) in New Brunswick and fall ($r^2 = 0.49$, $p < 0.01$) in Belvidere. Hg concentrations in precipitation were uncorrelated with sample period averaged meteorological parameters in New Brunswick: wind speed ($r^2 < 0.01$), wind direction ($r^2 = 0.03$), temperature ($r^2 = 0.07$), pressure ($r^2 < 0.01$), and relative humidity ($r^2 < 0.01$).

Seasonally, it appears that peak mercury concentrations in precipitation occur during summer months (June to August) and lowest concentrations during the winter (December to February) for all three sites. However, the observed trend was only significant during autumn in New Brunswick ($r^2 = 0.17$, $p = 0.05$). Looking at individual seasons from 1999 through 2006, the only significant decline in Hg precipitation concentrations was during autumn months ($r^2 = 0.77$, $p = 0.02$; Fig. 2.9).

2.4.2. *Trace metals*

When comparing recent data from this study (2003-2006) with the previous study (1999-2002), mean elemental fluxes appear to be decreasing (Table 2.2). In fact, the following trace metal VWM concentrations were significantly lower in the 2003-2006 interval based on non-overlapping 95% confidence intervals [Gatz & Smith 1995b]: Ag, Cd, Pb, V, Mn, Co, Ni, Cu, Zn, and As. A full dataset for trace metals is located in Appendix C.1.

Most trace metals exhibited peak VWM concentrations in precipitation during the spring (March to May), with Ag, Cd, Cu, Ni and Zn having peak VWM concentrations in the winter (December to February).

Trace metal masses in wet deposition were not correlated with precipitation depth ($0.01 \leq r^2 \leq 0.14$); log TM masses were slightly better correlated ($0.09 \leq r^2 \leq 0.52$). All log mass to precipitation depth relationships were significant and positive but relatively weak, with the strongest correlation observed with Cd ($r^2 = 0.52$, $p < 0.01$). Trace metals concentrations estimated by ICP-MS lacked a significant correlation with wind speed ($0.001 \leq r^2 \leq 0.09$), wind direction ($6E\text{-}05 \leq r^2 \leq 0.03$), and relative humidity ($6E\text{-}05 \leq r^2 \leq 0.06$). Metal concentrations were further uncorrelated with temperature, contrary to other studies [Mason et al. 2000; $0.0005 \leq r^2 \leq 0.04$]. However, atmospheric pressure was significantly correlated with Pd ($r^2 = 0.51$, $p < 0.01$; Fig. 2.10). No patterns were observed between Hg and the other analyzed trace metals in wet deposition ($5E\text{-}05 \leq r^2 \leq 0.07$).

2.5. Discussion

While global total mercury atmospheric deposition rates vary regionally and temporally, they are on the order of 10 μg m^{-2} y^{-1} [Fitzgerald et al. 1991; Zelewski & Armstrong 1996]. Reinfelder et al. [2004] report the annual precipitation fluxes of mercury in New Jersey range from 11 to 14 μg m^{-2} y^{-1}. Mercury wet deposition fluxes over each time period for both New Brunswick and Belvidere fall within the NJADN values and are elevated over the global total mercury average at 12 and 11 μg m^{-2} y^{-1}, respectively. These values are also comparable to estimated fluxes from the previous study by Zhuang [2004] and from other states in or near the northeast (Tables 2.2 & 2.3). Given that the observed fluxes are within the expected flux range for NJ precipitation, it appears the rain depths obtained from wet deposition volume are accurate.

At the MDN comparison site in the Valley Forge Historic Park, the annual mercury precipitation flux was equivalent to that in New Brunswick from 30 November 1999 to 25 July 2006 (12 ± 0.016 μg m^{-2} y^{-1}). However, the VWM concentration for mercury at Valley Forge was more similar to Belvidere (9.4 ± 0.012 ng L^{-1}). Long term mercury data for Valley Forge from 30 November 1999 through 25 July 2006 can be found in Fig. 2.11 and Appendix B.3.

It has been reported that global atmospheric deposition shows a decreasing pattern in fluxes for most trace elements in precipitation as was observed with Cd, Cu, Pb, and Zn in Paris, France [Azimi et al., 2005]. In fact, a significant decreasing pattern was observed for Hg, Cd, Cu, Pb, and Zn, in addition to Ag, V, Mn, Co, Ni, and As in New Brunswick, NJ in the 2003-2006 period as compared with the 1999-2002 period, based on non-overlapping 95% confidence intervals for VWM concentrations (Table 2.2;

Appendix B.1; Gatz & Smith 1995b). Higher, more variable mercury concentrations in New Brunswick wet deposition prior to 2003 may be explained by enhanced seasonal deposition fluxes [Vanarsdale et al. 2005], followed by significant declines in atmospheric mercury in the northeastern USA of 14 ± 4% [Butler et al. 2008]. In Belvidere, the time scale was too small to resolve such patterns (Fig. 2.5; Appendix B.2). Mercury concentrations in Valley Forge were not increasing or decreasing ($r^2 = 0.006$, $p = 0.68$) over the seven year evaluation (Fig. 2.11; Appendix B.3), suggesting the importance of local sources.

Peak mercury concentrations in precipitation occurred during summer months (June to August) and lowest concentrations during the winter (December to February), as reported elsewhere [Glass & Sorensen 1999; Mason et al. 2000; Keeler et al. 2005; Miller et al. 2005; Sakata & Marumoto 2005; Vanarsdale et al. 2005; Butler et al. 2007; Lai et al. 2007; Choi et al. 2008; Table 2.4]. While three unusually low concentrations were observed in New Brunswick samples during the spring and summer of 2002, likely a result of drought conditions, annually averaged mercury concentrations in precipitation generally show low or decreasing trends in winter and fall and high or increasing trends in spring and summer.

There are several potential explanations for the observed seasonality of mercury in precipitation samples. Lower precipitation mercury concentrations in the winter may be an effect of snow which is less efficient at scavenging particulate mercury than rain, cold temperatures that hinder atmospheric reactions, and/or local (winter) sources decreasing due to controls [Lindberg et al. 1991; Franz et al. 1998; Mason et al. 2000; Keeler et al. 2005]. Factors enhancing summertime Hg concentrations include: increased

photochemical activity and maximized air convection [Munthe et al. 1995; Keeler et al. 2005] which may aid in the long-range transport of mercury from the mid-western U.S. and China.

Other factors potentially responsible for enhanced precipitation mercury in the summer include meteorology (local and regional) and an increase in atmospheric oxidants [Keeler et al. 2005; Keeler et al. 2006]. A number of studies have shown that mercury content in wet deposition is positively correlated with precipitation amount [Glass & Sorensen 1999; Mason et al. 2000; Sakata & Marumoto 2005; Sakata et al. 2006], indicating that the mercury is not diluted by rain in longer storms as is observed for aerosol-bound trace elements. Precipitation amount and Hg mass were weakly positively correlated in New Brunswick ($r^2 = 0.34$, $p < 0.01$; Fig. 2.7) and Belvidere ($r^2 = 0.33$, $p < 0.01$; Fig. 2.8) and moderately positively correlated in Valley Forge ($r^2 = 0.57$, $p < 0.01$; Fig. 2.11). Atmospheric pressure may have played a part in the wet deposition of Pd. In fact, up to 50% of the signal of palladium in wet deposition may be explained by atmospheric pressure. During high pressure, conditions are more favorable for atmospheric deposition of emitted particles as the air is denser and winds are generally lighter [Eisenreich et al. 1981]. Meteorological factors such as wind speed, wind direction, temperature, and relative humidity had no significant effect ($6E\text{-}05 < r^2 < 0.09$) on the concentration of mercury and other trace elements in NJ wet deposition.

Enhanced soil dust generated from higher winds (crustal origin) and/or greater fuel combustion from the increase in home heating may explain some of the signal for Cd, Ni and Zn in the winter [Arditsoglou & Samara 2005]. Season-specific sources of Ag and Cu were not identified.

Mercury concentrations in wet deposition were not correlated with those of the 16 other trace metals measured in New Brunswick. Since mercury cannot be associated with other atmospheric co-pollutants analyzed, this suggests that a variety of sources are contributing to mercury in New Jersey precipitation.

2.6. Conclusions and implications

Since precipitation amount did not strongly correlate and most other meteorological conditions did not correlate with the wet deposition flux of mercury, it appears that local and regional sources of particulate and reactive gaseous mercury may better explain variations in wet deposition for New Jersey.

While mercury emissions in the United States have declined in the last decade or so due to the closure of municipal and medical waste incinerators [Butler et al. 2008], high concentrations of mercury are still found in wet deposition of northeastern states, largely derived from coal-fired power plants in the Ohio River Valley [Choi et al. 2008]. Although some years may have witnessed lesser amounts of mercury in wet deposition during this seven year study, atmospheric concentrations are expected to fluctuate in New Jersey and much of the northeastern United States for the foreseeable future.

References

Arditsoglou, A. and C. Samara (2005), Levels of total suspended particulate matter and major trace elements in Kosovo: a source identification and apportionment study, *Chemos., 59,* 669-678.

Azimi, S., V. Rocher, S. Garnaud, G. Varrault, and D.R. Thevenot (2005), Decrease of atmospheric deposition of heavy metals in an urban area from 1994 to 2002 (Paris, France), *Chemos., 61,* 645-651.

Bloom, N.S. and E.A. Crecelius, (1983), Determination of mercury in seawater at sub-nanogram per liter levels, *Mar. Chem., 14,* 49-59.

Butler, T.J., M.D. Cohen, F.M. Vermeylen, G.E. Likens, D. Schmeltz, and R.S. Artz (2008), Regional precipitation mercury trends in the eastern USA, 1998-2005: Declines in the Northeast and Midwest, no trend in the Southeast, *Atmos. Environ., 42,* 1582-1592.

Carpi, A. (1997), Mercury from combustion sources: a review of the chemical species emitted and their transport in the atmosphere, *Water Air Soil Pollut., 98 (3-4),* 241-254.

Choi, H.-D., T.J. Sharac, and T.M. Holsen (2008), Mercury deposition in the Adirondacks: A comparison between precipitation and throughfall, *Atmos. Environ., 42,* 1818-1827.

Eisenreich, S.J., B.B. Looney, and J.D. Thornton (1981), Airborne organic contaminants in the Great Lakes ecosystem, *Environ. Sci. Technol., 15(1),* 30-38.

Field, M.P. and R.M. Sherrell (2003), Direct determination of ultra-trace levels of metals in fresh water using desolvating micronebulization and HR-ICP-MS: application to Lake Superior waters, *J. Anal. Atom. Spectrom., 18,* 254-259.

Fitzgerald, W.F. and G.A. Gill (1979), Subnanogram determination of mercury by two stage gold amalgamation and gas phase detection applied to atmospheric analysis, *Analyt. Chem., 51,* 1714-1720.

Fitzgerald, W.F., R.P. Mason, and G.M. Vandal (1991), Atmospheric cycling and air-water exchange of mercury over mid-continental lacustrine regions, *Water Air Soil Pollut., 56,* 745-767.

Fitzgerald, W.F., D.R. Engstrom, R.P. Mason, and E.A. Nater (1998), The case for atmospheric mercury contamination in remote areas. *Environ. Sci. Technol., 32,* 1-7.

Franz, T.P., S.J. Eisenreich, and T.M. Holden (1998), Dry deposition of particulate polychlorinated biphenyls and polycyclic aromatic hydrocarbons to Lake Michigan, *Environ. Sci. Technol., 32,* 3681-3688.

Gatz, D.F. and L. Smith (1995a), The standard error of a weighted mean concentration – I. Bootstrapping vs. other methods: the national atmospheric deposition program, *Atmos. Environ., 29(11),* 1185-1193.

Gatz, D.F. and L. Smith (1995b), The standard error of a weighted mean concentration – II. Estimating confidence intervals, *Atmos. Environ., 29(11),* 1195-1200.

Glass, G.E. and J.A. Sorensen (1999), Six-year trend (1990-1995) of wet mercury deposition in the Upper Midwest, U.S.A., *Environ. Sci. Technol., 33,* 3303-3312.

Hall, B.D., H. Manolopoulos, J.P. Hurley, J.J. Schauer, V.L. St. Louis, D. Kenski, J. Graydon, C.L. Babiarz, L. B. Cleckner, and G.J. Keeler (2005), Methyl and total

mercury in precipitation in the Great Lakes region, *Atmos. Environ., 39,* 7557-7569.

Keeler, G.J., L.E. Gratz, and K. Al-Wali (2005), Long-term atmospheric mercury wet deposition at Underhill, Vermont, *Ecotoxicol., 14,* 71-83.

Keeler, G.J., M.S. Landis, G.A. Norris, E.M. Christianson, and J.T. Dvonch (2006), Sources of mercury wet deposition in Eastern Ohio, USA, *Environ. Sci. Technol., 40,* 5874-5881.

Lai, S. T.M. Holsen, P.K. Hopke, and P. Liu (2007), Wet deposition of mercury at a New York state rural site: concentrations, fluxes, and source areas, *Atmos. Environ., 41,* 4337-4348.

Landis, M.S. and G.J. Keeler (1997), Critical evaluation of a modified automatic wet-only precipitation collector for mercury and trace element determinations, *Environ. Sci. Technol., 31,* 2610-2615.

Landis, M.S. and G.J. Keeler (2002), Atmospheric mercury deposition to Lake Michigan during the Lake Michigan mass balance study, *Environ. Sci. Technol., 36,* 4518-4524.

Lindberg, S.E., R.R. Turner, T.P. Meyers, G.E. Taylor Jr., and W.H. Schroeder (1991), Atmospheric concentrations and deposition of mercury to a deciduous forest at Walker Branch Watershed, Tennessee, USA, *Water Air Soil Pollut., 56,* 577-594.

Lindberg, S.E., R. Bullock, R. Ebinghaus, D. Engstrom, X. Feng, W. Fitzgerald, N. Pirrone, E. Prestbo, and C. Seigneur (2007), A synthesis of progress and uncertainties in attributing the sources of mercury in deposition, *Ambio, 36(1),* 19-32.

Lindqvist, O., K. Johansson, M. Aastrup, A. Andersson, L. Bringmark, G. Hovsenius, L. Hakanson, A. Iverfeldt, M. Meili, and B. Timm (1991), Mercury in the Swedish environment – recent research on causes, consequences and corrective methods, *Water Air Soil Pollut., 55,* 1-261.

Mason, R.P., W.F. Fitzgerald, and F.M.M. Morel (1994), The biochemical cycling of elemental mercury: anthropogenic influences. *Geochim. Cosmochim. Acta, 58,* 3191-3198.

Mason, R.P., N.M. Lawson, and G.R. Sheu (2000), Annual and seasonal trends in mercury deposition in Maryland, *Atmos. Environ., 34,* 1691-1701.

Miller, E.K., A. Varnarsdale, G.J. Keeler, A. Chalmers, L. Poissant, N.C. Kamman, and R. Brulotte (2005), Estimation and mapping of wet and dry mercury deposition across Northeastern North America, *Ecotoxicol., 14,* 53-70.

Morel, F.M.M., A.M.L. Kraepiel, and M. Amyot (1998), The chemical cycle and bioaccumulation of mercury, *Annu. Rev. Ecol. Syst., 29,* 543-566.

Munthe, J., H. Hultberg, and A. Iverfeldt (1995), Mechanisms of deposition of methylmercury and mercury to coniferous forests, *Water Air Soil Pollut., 80,* 363-371.

Nriagu, J.O. (1989), A global assessment of natural sources of anthropogenic trace metals, *Nature, 338,* 47-49.

Nriagu, J.O. and J.M. Pacyna (1988), Quantitative assessment of worldwide contamination of air, water and soils by trace metals, *Nature, 333,* 134-139.

Olmez, I., G. Gullu, N.K. Aras, and S.S. Keskin (2004), Seasonal patterns of atmospheric trace element concentrations in Upstate New York, USA, *J. Radioan. Nucl.*

Chemis., 259(1), 157-162.
Pacyna, E.G. and J.M. Pacyna (2002), Global emissions of mercury from anthropogenic sources in 1995, *Water Air Soil Pollut., 137,* 149-165.
Reinfelder, J.R., L.A. Totten, and S.J. Eisenreich (2004), The New Jersey Atmospheric Deposition Network (NJADN). Final report to the New Jersey Department of Environmental Protection.
Rorabacher, D.B. (1991), Statistical treatment for rejection of deviant values: critical values of Dixon's "Q" parameter and related subrange ratios at the 95% confidence level, *Analyt. Chem., 63(2),* 139-146.
Sakata, M. and K. Marumoto (2005), Wet and dry deposition fluxes of mercury in Japan, *Atmos. Environ., 39,* 3139-3146.
Sakata, M. K. Marumoto, M. Narukawa, and K. Asakura (2006), Regional variations in wet and dry deposition fluxes of trace elements in Japan, *Atmos. Environ., 40,* 521-531.
Schroeder, W.H. and J. Munthe (1998), Atmospheric mercury—an overview, *Atmos. Environ., 32,* 809 –822.
Sigler, J.M. and X. Lee (2006), Recent trends in anthropogenic mercury emissions in the Northeast United States, *J. Geophys. Res., 111-D,* 14316.
Themelis, N.J. and A.F. Gregory (2001), Sources and materials balance of mercury in the New York-New Jersey Harbor. Report to the New York Academy of Sciences, industrial ecology for pollution prevention study of the NYAS Harbor consortium.
US EPA (1996), Method 1669: Sampling ambient water for trace metals at EPA water quality criteria levels.
US EPA (1997), Mercury study: report to Congress, EPA report 452/R-97-0003. Available online: http://www.epa.gov/ttnuatwl/112nmerc/mercury.html. 8 vols.
US EPA (2002), Method 1631, Revision E: Mercury in water by oxidation, purge and trap, and cold vapor atomic fluorescence spectrometry.
Vanarsdale, A., J. Weiss, G. Keeler, E. Miller, G. Boulet, R. Brulotte, and L. Poissant (2005), Patterns of mercury deposition and concentration in Northeastern North America (1996-2002), *Ecotoxicol., 14,* 37-52.
Wetherbee, G.A., D.A. Gay, R.C. Brunette, and C.W. Sweet (2007), Estimated variability of National Atmospheric Deposition Program/Mercury Deposition Network measurements using collocated samplers, *Environ. Monitor. Assess., 131,* 49-69.
Yatavelli, R.L.N., J.K. Fahrni, M. Kim, K.C. Crist, C.D. Vickers, S.E. Winter, and D.P. Connell (2006), Mercury, PM2.5 and gaseous co-pollutants in the Ohio River Valley region: Preliminary results from the Athens supersite, *Atmos. Environ., 40,* 6650-6665.
Zelewski, L.M. and D.E. Armstrong (1996), Mercury dynamics in sediments of Tivoli South Bay, Hudson River, NY: A report of the 1996 Tibor T. Polgar Fellowship Program.
Zhuang, Y. (2004), Atmospheric deposition and impact of mercury and other trace elements in New Jersey. Ph.D. dissertation. Rutgers, The State University of New Jersey, New Brunswick.

Table 2.1 Mean Analytical Blank, Mean Field Blank, Detection Limit, Mean Trace Metal Concentrations, and Contribution of Field Blank to Trace Metal Concentrations.

element	n[a]	mean analytical blank ($\mu g\ L^{-1}$)	mean FB ($\mu g\ L^{-1}$)	DL[b] ($\mu g\ L^{-1}$)	mean [TM][c] ($\mu g\ L^{-1}$)	[TM] < DL[d] (%)	FB → mean [TM][e] (%)
Mg	39	3.2	0.93	2.6	71	0	1
Pd	39	0.0004	0.0005	0.0019	0.017	0	3
Ag	39	0.0019	0.0006	0.0030	0.0053	14	12
Cd	39	0.0005	0.0010	0.0034	0.030	0	3
Sb	39	0.0012	0.0014	0.0046	0.11	0	1
Pb	39	0.0063	0.016	0.064	1.0	0	2
Al	39	0.47	2.0	9.7	28	4	7
V	39	0.0006	0.0041	0.013	0.46	0	1
Cr	39	0.0021	0.042	0.061	0.19	1	22
Mn	39	0.0030	0.017	0.057	2.6	0	1
Fe	39	0.21	0.88	4.2	30	0	3
Co	39	0.0006	0.0015	0.0073	0.039	1	4
Ni	39	0.28	0.058	0.27	0.41	11	14
Cu	39	0.033	0.11	0.69	1.0	12	11
Zn	39	0.081	1.3	4.0	6.1	14	21
As	39	0.0033	0.0027	0.012	0.47	0	1

[a] Number of samples analyzed.
[b]Detection limit, calculated as the mean plus three times the standard deviation of the field blank.
[c] Mean trace metal concentration.
[d] Percent of samples where the trace metal concentration is below the DL.
[e] Percent of field blank contribution to the trace metal concentration.

.

Table 2.2 Annual Wet Deposition Fluxes[a] of Trace Metals in New Jersey.

element	1999 - 2002[b]	2003 - 2006
Mg	65 ± 5.9	59 ± 7.2
Pd	10 ± 2	12 ± 0.11
Ag	25(8[c]) ± 13	14 ± 0.025
Cd	62(39[c]) ± 23	41 ± 0.31
Sb	0.085 ± 0.006	0.083 ± 0.0037
Pb	1.7 ± 0.16	1.2 ± 0.34
V	0.58 ± 0.045	0.46 ± 0.050
Cr	0.15 ± 0.015	0.14 ± 0.0023
Mn	2.5 ± 0.24	2.1 ± 4.5
Fe	47 ± 7.4	34(20[c]) ± 442(43[c])
Co	0.046 ± 0.007	0.036 ± 0.00052
Ni	0.65(0.46[c]) ± 0.019	0.47 ± 0.099
Cu	1.5(1.1[c]) ± 0.48	1.1 ± 0.28
Zn	7.8(7.0[c]) ± 1.2	6.0(4.5[d]) ± 12(0.73[d])
As	0.067 ± 0.008	0.16(0.11[c]) ± 1.9(0.034[c])
Hg	11 ± 1	12 ± 0.87
Al	35 ± 5.2	27(18[c]) ± 452(34[c])

[a]Fluxes in units of mg m^{-2} y^{-1}, except Pd, Ag, Cd, and Hg which are in units of μg m^{-2} y^{-1}.
[b]Data from Zhuang [2004].
[c]Values in parentheses represent the estimated flux if extreme high values are excluded.
[d]Values in parentheses represent the estimated flux if extreme high and low values are excluded.

Table 2.3 Mercury in Wet Deposition of New Jersey and Other States.

location	Hg VWM concentration ($ng\ L^{-1}$)	Hg flux rates ($\mu g\ m^{-2}\ a^{-1}$)	reference
New Brunswick, NJ (1999-2006)	11	12	this study
Belvidere, NJ (2002-2005)	9.0	11	this study
Valley Forge, PA (1999-2006)	9.4	12	this study
Milford, PA (2002)	8.0	9.5	Varnasdale et al. 2005
Potsdam, NY (2004)	5.5	5.9	Lai et al. 2007
Newcomb, NY (2004-2006)	4.9	6	Choi et al. 2008
Chesapeake Bay Laboratory, MD (1998-1999)	-	11	Mason et al. 2000
Underhill, VT (1993-2003)	8.9	9.7	Keeler et al. 2005
Freeport, ME (2002)	4.9	5.5	Varnasdale et al. 2005
Athens, OH (2004-2005)	9.7	13	Yatavelli et al. 2006
Steubenville, OH (2004)	14	20	Keeler et al. 2006
Bondville, IL (1999-2004)	11	9.7	Wetherbee et al. 2007
Great Lakes region (1997-2003)	10 - 60	-	Hall et al. 2005
Lake Michigan area WI, IL, MI (1994-1995)	-	11	Landis & Keeler 2002
Upper Midwest, USA (1990-1995)	-	7.4	Glass & Sorensen 1999
Indiana Dunes National Lakeshore, IN (1999-2004)	15	12	Wetherbee et al. 2007
Mammoth Cave National Park, KY (1999-2004)	8.6	11	Wetherbee et al. 2007

Table 2.4 Seasonal Wet Deposition Fluxes[a] of Trace Metals in New Jersey.

element	winter (December - February)	spring (March - May)	summer (June - August)	autumn (September - November)
Mg	66(58[b]) ± 411(131[b])	75 ± 295	44 ± 151	55 ± 166
Pd	11 ± 0.0064	18 ± 0.052	10 ± 0.0095	10 ± 0.019
Ag	32 ± 2.6	4.0 ± 0.0015	6.9 ± 0.0077	16 ± 0.35
Cd	73 ± 9.0	35 ± 0.028	41 ± 0.31	21 ± 0.047
Sb	0.081 ± 0.00020	0.086 ± 0.00020	0.11 ± 0.0026	0.082 ± 0.00041
Pb	1.0 ± 0.18	1.6 ± 0.22	2.0 ± 1.6	0.81 ± 0.061
V	0.42 ± 0.0064	0.58 ± 0.0090	0.46 ± 0.021	0.47 ± 0.018
Cr	0.094 ± 0.00089	0.11 ± 0.00063	0.17 ± 0.012	0.11 ± 0.0019
Mn	1.7 ± 0.38	3.0 ± 0.44	3.1 ± 2.2	1.4 ± 0.31
Fe	19(18[b]) ± 30(15[b])	40(31[b]) ± 176(50[b])	45(34[b]) ± 585(160[b])	39 ± 458
Co	0.037 ± 0.00061	0.039 ± 0.000058	0.045 ± 0.00032	0.033 ± 0.00014
Ni	0.75(0.36[b]) ± 0.64(0.046[b])	0.45 ± 0.020	0.41 ± 0.019	0.34 ± 0.011
Cu	1.7(0.70[b]) ± 4.1(0.24[b])	1.1 ± 0.057	1.1 ± 0.10	0.99 ± 0.078
Zn	8.2(5.0[b]) ± 23(4.1[b])	6.0± 1.5	6.3 ± 2.0	4.2 ± 1.2
As	0.043 ± 0.00017	0.42(0.071[b]) ± 0.53(0.025[b])	0.095 ± 0.00054	0.14 ± 0.024
Hg	8.4(7.0[b]) ± 10.5(2.8[b])	9.4 ± 6.6	15 (17[c]) ± 24 (21[c])	11 ± 13
Al	17(15[b]) ± 38(20[b])	38(29[b]) ± 167(56[b])	32(25[b]) ± 233(92[b])	29(21[b]) ± 187(119[b])

[a]Fluxes in units of mg m^{-2} y^{-1}, except Pd, Ag, Cd, and Hg which are in units of μg m^{-2} y^{-1}.
[b]Values in parentheses represent the estimated flux if extreme high values are excluded.
[c]Values in parentheses represent the estimated flux if extreme high and low values are excluded.

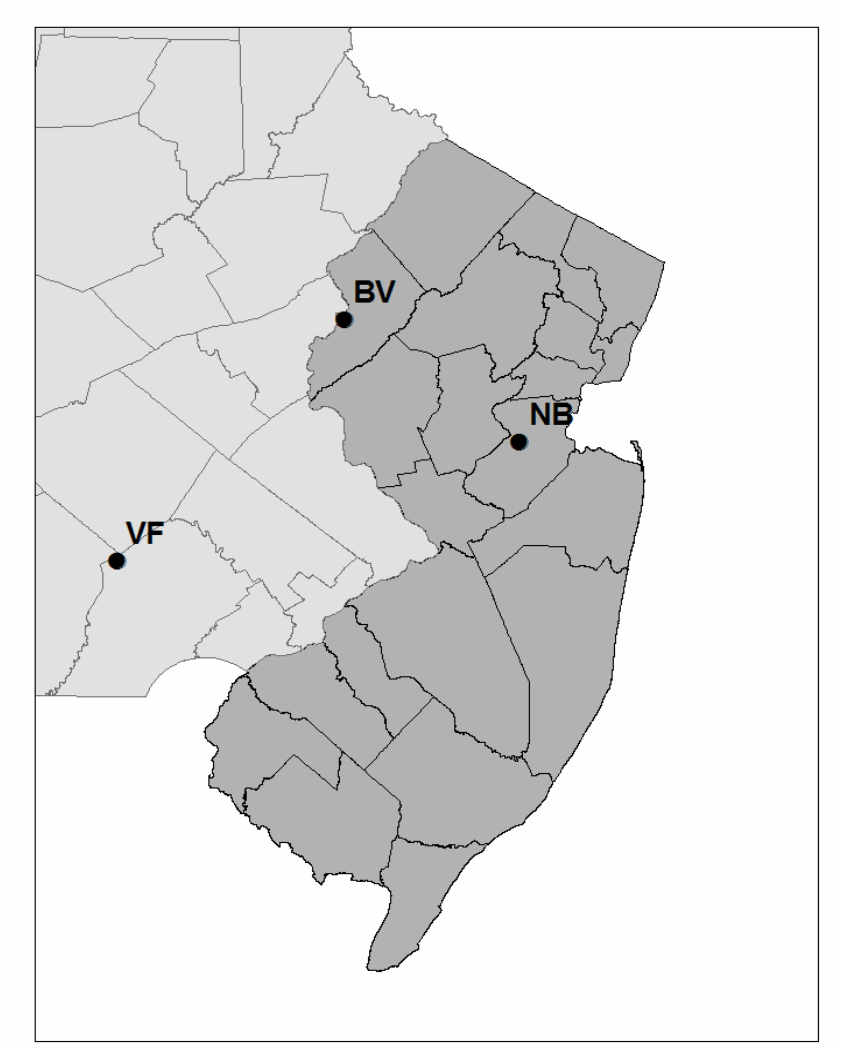

Figure 2.1 Map of wet deposition collection sites. NB is New Brunswick; BV is Belvidere; VF is Valley Forge.

Figure 2.2 A) MIC-B wet deposition collector in fenced area at Rutgers Gardens, NJ. B) Wet deposition assemblies with acrylic support inserts [Landis & Keeler 1997] inside the MIC-B wet deposition collector. Trace element funnel located far right and total mercury funnel located near right.

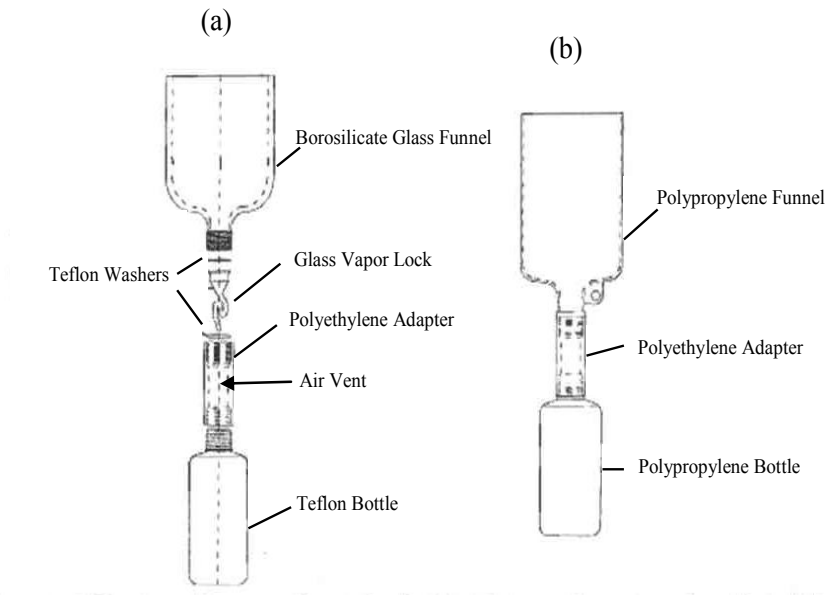

Figure 2.3 Bottle/funnel assemblies adapted from Landis & Keeler [1997]. Sampling trains for (a) total mercury and (b) trace elements.

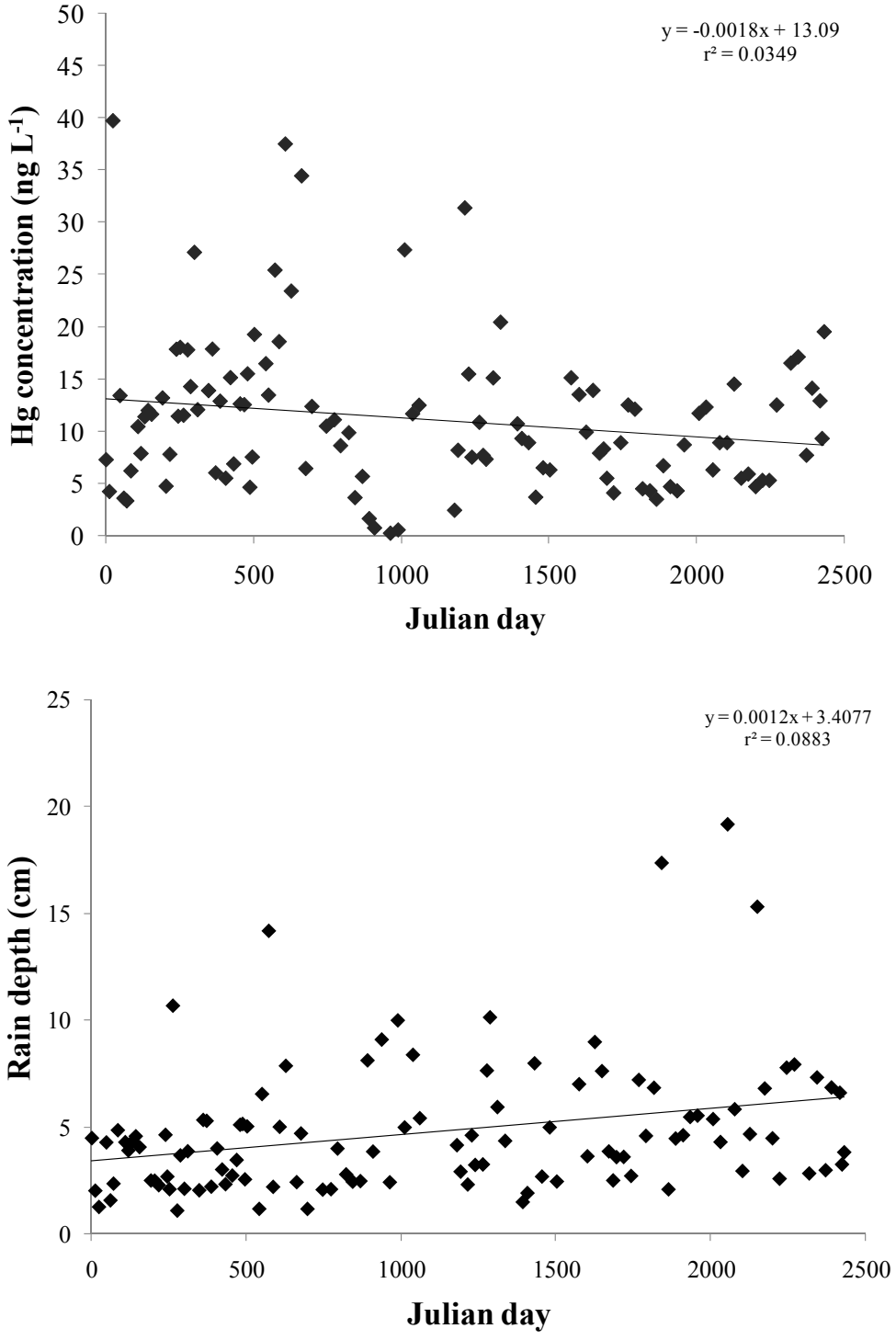

Figure 2.4 New Brunswick, NJ: top) Mercury concentrations in precipitation from 27 November 1999 through 25 July 2006 (n = 103; p = 0.15); bottom) Rain depths over same time period.

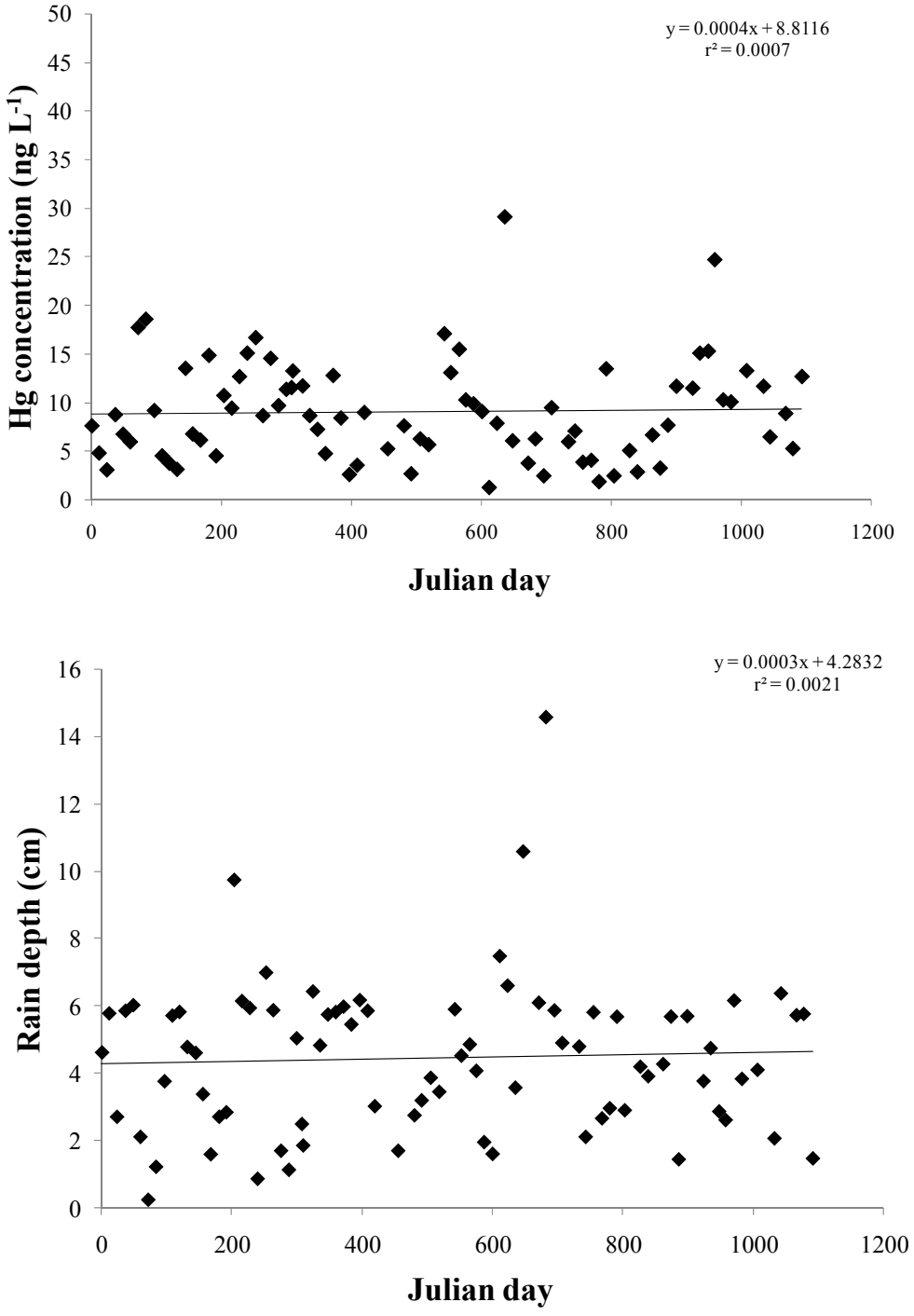

Figure 2.5 Belvidere, NJ: top) Mercury concentrations in precipitation from 15 November 2002 through 11 March 2005 (n = 81); bottom) Rain depths over same time period.

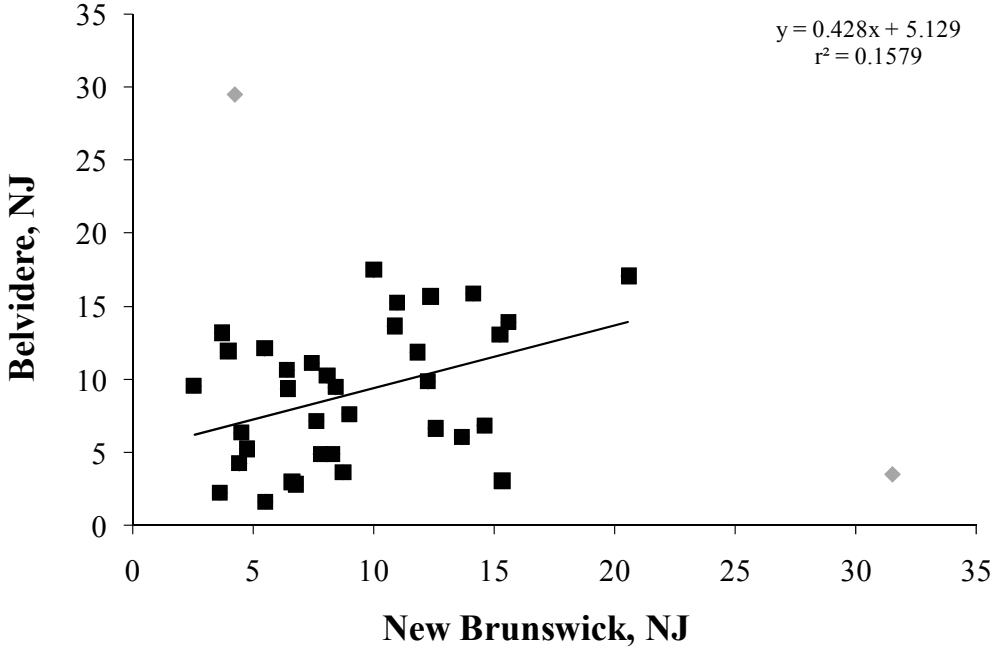

Figure 2.6 Total mercury mass (ng) comparison between New Brunswick and Belvidere (n = 35). Grey points indicate outliers using Dixon's Q at a 95% confidence interval [Rorabacher 1991].

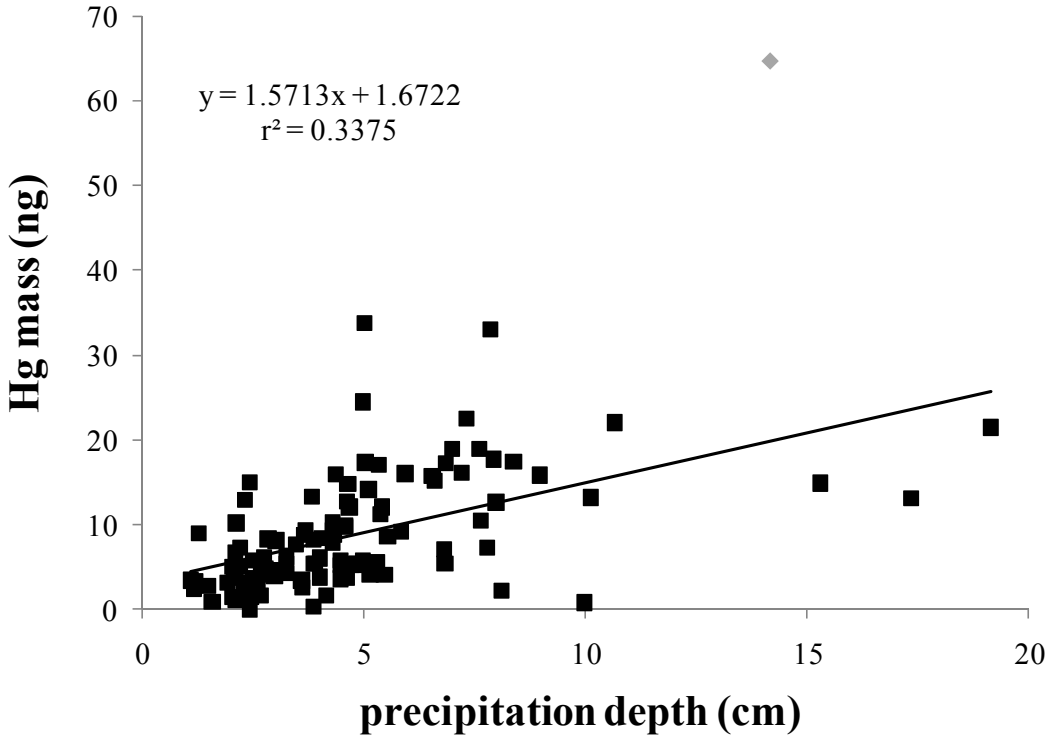

Figure 2.7 New Brunswick, NJ: Correlation between precipitation depth and Hg mass ($n = 112$; $p < 0.01$). Grey point indicates an outlier using Dixon's Q at a 95% confidence interval [Rorabacher 1991].

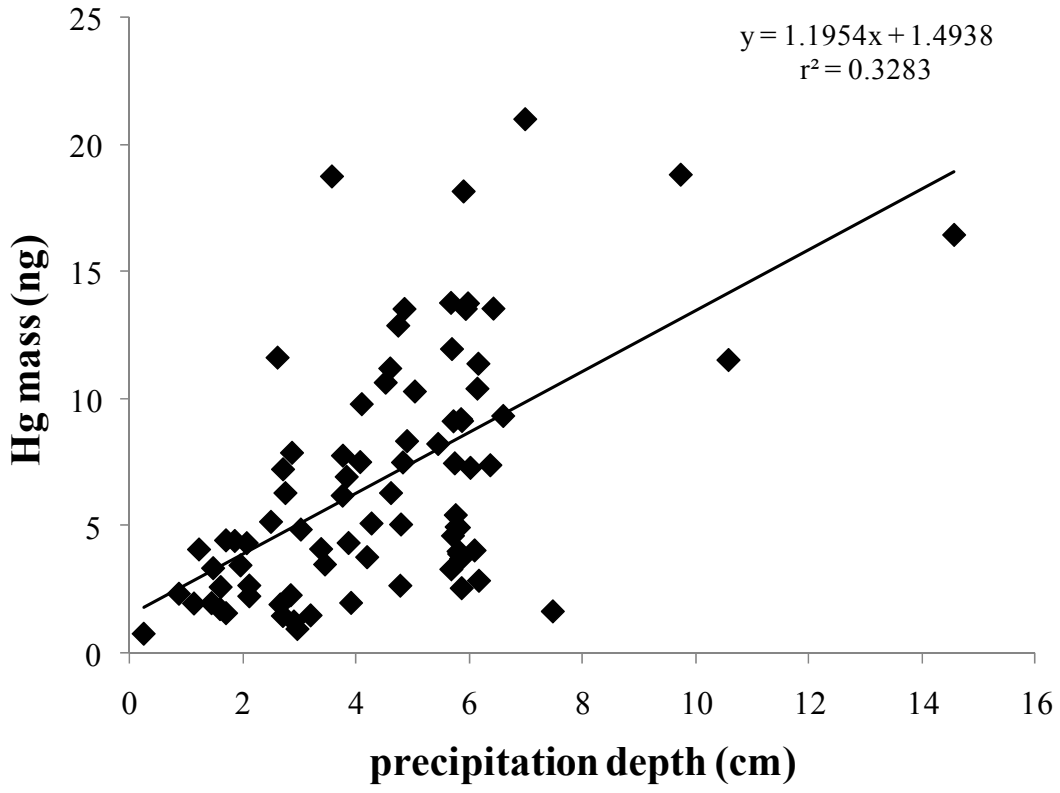

Figure 2.8 Belvidere, NJ: Correlation between precipitation depth and Hg mass ($n = 81$; $p < 0.01$).

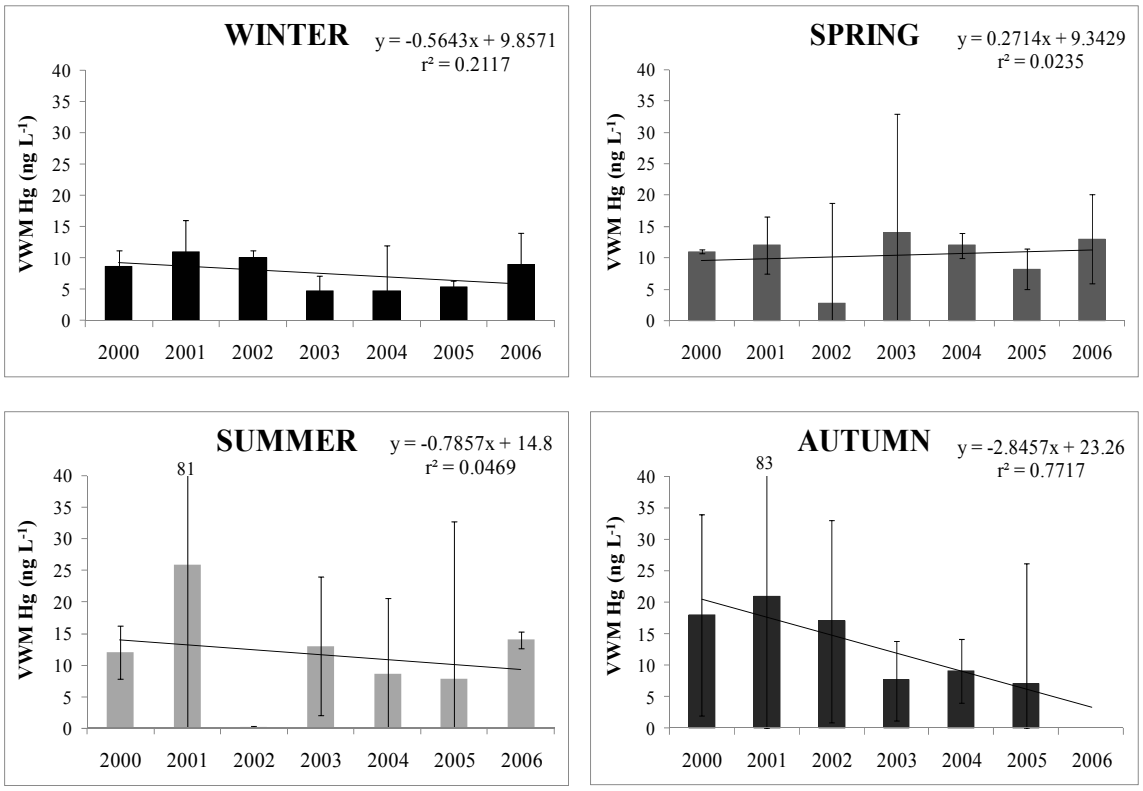

Figure 2.9 Seasonal VWM mercury concentrations in New Brunswick, NJ. Summer 2002 experienced a drought and lower than normal Hg concentrations. No data were available for Autumn 2006.

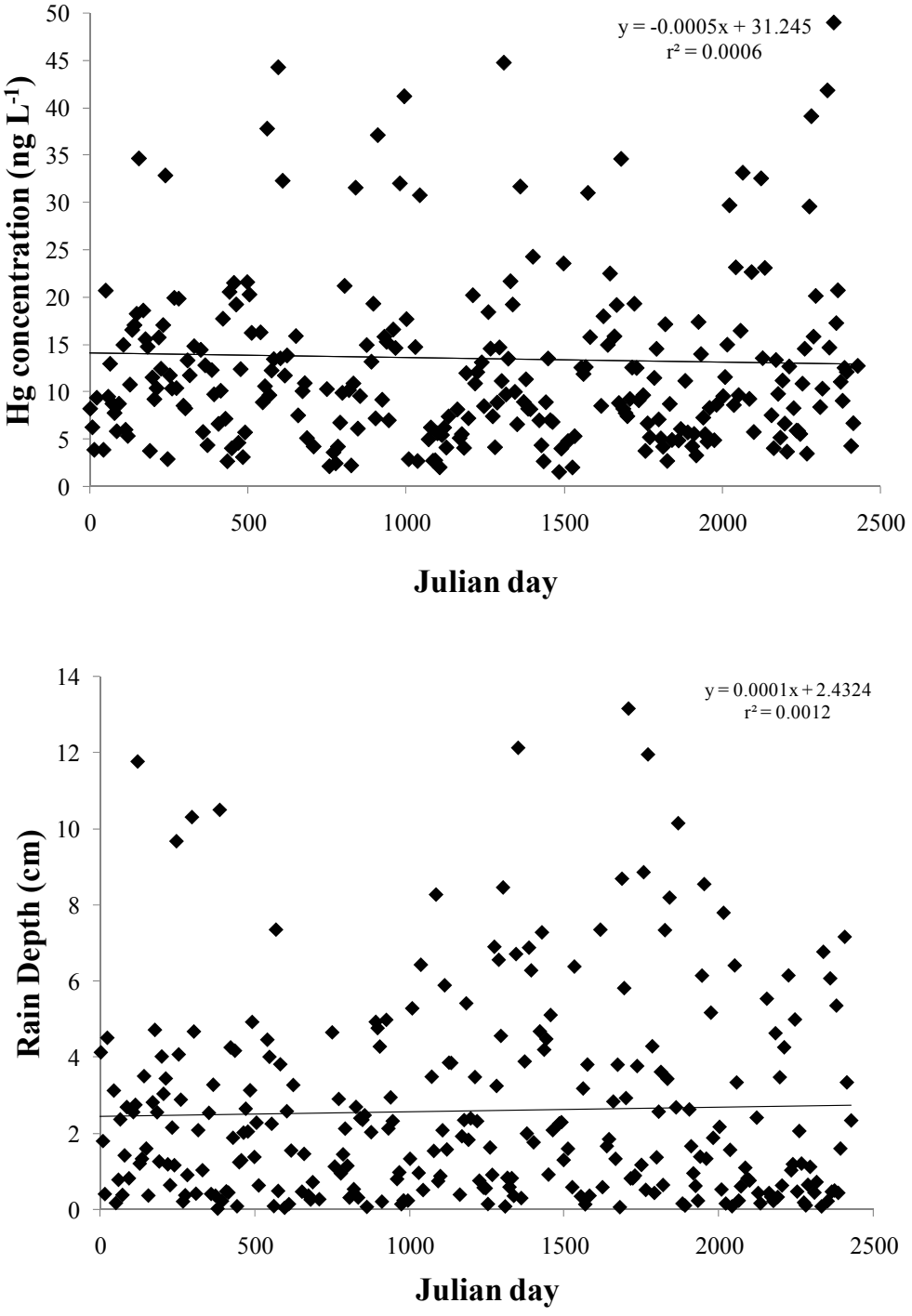

Figure 2.10 Valley Forge, PA: top) Mercury concentrations in precipitation from 30 November 1999 through 25 July 2006 (n = 271); bottom) Rain depths over same time period.

Chapter 3

Gaseous mercury emissions from tidally-exposed wetland sediments:

In situ micrometeorological study

3.1. Introduction

The land-air exchange of mercury is a global concern because of mercury's atmospheric mobility, bioaccumulation potential, and toxicity. Recent modeling studies demonstrated that the current global anthropogenic mercury emission flux is on the order of 2600 t y^{-1} [Lamborg et al. 2002] and that non-industrial emissions, including truly natural and previous anthropogenic deposition, are approximately 1800 t y^{-1} [Schroeder & Munthe 1998]. While the highest truly natural emissions are localized to regions with air-exposed, mercury-rich minerals, emission is a widely distributed phenomenon. The emission of mercury from tidally air-exposed salt marsh sediments has not been measured.

Mercury in aquatic systems accumulates in sediments [Gilmour & Henry 1991] where it is precipitated as a sulfide, associated with iron sulfides, or bound to organic matter [Mantoura et al. 1978; Drobner et al. 1990; Morse & Luther 1999]. Coastal marine sediments are covered by a thin layer of oxic sediment [Baillie 1986], but reduced mercury (Hg^0) may be formed at the sediment surface by photochemical processes or transported there from deeper in the sediment by biological activities. Although mercury is efficiently retained by aquatic sediments, water-level fluctuations may lead to the resuspension and short-term exposure of sediments to solar radiation [Carpi & Lindberg 1997; Canario & Vale 2004; Poissant et al. 2004]. In tidal systems, ebb tide brings sediments in direct contact with the atmosphere where photochemical reactions and boundary layer meteorology may enhance mercury volatilization. Additional biological processes (e.g. microbial reduction, sediment bioturbation) in wetland ecosystems may also lead to the mobilization of sediment-bound mercury [Poissant et al. 2004].

Mercury volatilization from land is dominated by the flux of elemental mercury [Kim & Lindberg 1995] and environments favoring the reduction of Hg(II), such as highly productive wetlands [Holmes & Lean 2006], are likely to support elevated Hg^0 emissions. [Bothner et al. 1980; Gobeil & Cossa 1993]. The vast area of wetlands combined with the large reservoir of mercury in wetland sediments suggests that mercury re-emission from wetland sediments has the potential to rival other natural and industrial emissions on a regional scale. However, because only a few studies have examined mercury emissions from wetlands, especially salt marsh wetlands, estimated mercury emissions from these environments are poorly constrained.

Only one previous study investigating mercury volatilization from wetland sediments has employed the micrometeorological method (Table 3.1). Sediment Hg fluxes from the Farm River salt marsh in Connecticut [Lee et al. 2000] were estimated using a micrometeorological eddy covariance system with a sonic anemometer, hygrometer, and thermometer in conjunction with a Tekran 2537A mercury vapor analyzer, as in this study. The main difference between this and the Lee et al. [2000] study was the sample gradient height (2 m, as compared to 3 m in this study). Other studies have investigated Hg emission from wetland sediments using dynamic flux chamber methods which prohibit atmospheric turbulence from reaching the sediment surface, a major limitation. This study will aid in broadening the knowledge base for Hg dynamics in salt marsh sediments under natural micrometeorological influence.

The objectives of this study were to estimate mercury volatilization fluxes from tidally-exposed salt marsh wetlands sediments and provide a preliminary scaling up for comparison with industrial mercury emissions in the state of New Jersey. To accomplish

these objectives, total gaseous mercury (TGM) emissions from two tidal estuarine wetlands in New Jersey, the non-point source mercury-impacted Secaucus High School Marsh (Secaucus, New Jersey) and the more pristine Great Bay estuary (Tuckerton, New Jersey), were estimated under ambient conditions using the micrometeorological technique [Lee et al. 2000; Lindberg & Meyers 2001; Lindberg et al. 2002; Korfiatis et al. 2003].

3.2. Site description

3.2.1. *Secaucus High School Marsh, New Jersey Meadowlands, Secaucus, New Jersey*

The Secaucus High School Marsh, at 40.80°N, 74.05°W, is a 0.15 km^2 tidally restricted estuarine wetland located in the New Jersey Meadowlands (Secaucus, Hudson County, NJ; Fig. 3.1). Secaucus High School Marsh is situated within one of the most industrial regions of the northeastern United States and its waters and sediments have accumulated a wide range of contaminants, including mercury. The vegetation was dominated by *Phragmites australis* (common reed) with small patches of *Spartina sp*. present along the banks of the Hackensack River [Tiner 1987] during field sampling in 2005. Between 2005 and 2006 the marsh was cleared to bare sediments for wetland restoration and remained bare through final experimentation in June 2007. Salinity in the Secaucus High School Marsh ranges from 3 to 12‰.

Total gaseous mercury and micrometeorological equipment were assembled on an anthropogenic berm along the eastern edge of the marsh, approximately 1 m above it. Sample location borders include: an open wetland fetch and the Hackensack River to the north, a large expanse of wetland and the Secaucus High School to the west, a residential

housing development to the south and a recreational park to the east. As a result, only data collected from the longest wetland fetch (~0.5 km; W-NW wind direction) were analyzed. For all sampling periods, except the afternoon (12:20-13:30) of 7 June 2007 when an abrupt change in wind direction occurred, winds blew over exposed wetland sediments in the direction of the sensors.

3.2.2. *Great Bay estuary, Tuckerton, New Jersey*

The Great Bay estuary near Tuckerton, Ocean County, New Jersey (39.51°N, 74.32°W; Fig. 3.1) includes an 87 km^2 salt marsh and 56 km^2 of shallow (2 m) estuarine waters [RUMFS 2008]. Our field site was located approximately 200 m northwest of the Rutgers Marine Field Station and its access road, both of which are elevated 3 m above the marsh surface. The Great Bay lies to the south and west, Little Egg Inlet (a conduit between Little Egg Harbor and the Atlantic Ocean) to the east, and the Great Bay Wildlife Management Area to the north of our field site near the Rutgers Marine Field Station. Mercury and micrometeorological monitoring equipment were placed in the center of an open area of the tidal estuarine wetland, with vegetated sediment exposed at low tide.

Given this site's proximity to the Atlantic Ocean, its waters are highly saline (22-30 ‰) [RUMFS 2008]. *Salicornia sp.* (pickleweed) and *Suaeda sp*. (sea blite) are important components of the submerged aquatic vegetation community in the Great Bay estuary although dominant plants did not cover the entire wetland area [Tiner 1987].

The region is predominantly surrounded by the New Jersey Pinelands National Reserve and other state and federal wildlife refuges, making it one of the most pristine

estuaries on the east coast [RUMFS 2008]. Mercury mainly enters the Great Bay ecosystem via atmospheric deposition. Since no known point sources of mercury are present in the Great Bay estuary, we have selected this location as our "natural background" site for comparison with the Secaucus High School Marsh.

3.3. Methods

3.3.1. *Field sampling events*

Field sampling was carried out over three to eight hour periods on 10-11 August 2005, 24-25 May 2006, and 7 and 21 June 2007 in Secaucus and continuously for 48 h on 2-4 October 2007 in Tuckerton under summer-like conditions. PAR irradiance (LI-COR model LI-250 light meter), air temperature, and wind speed were recorded at both sites (Table 3.2). In Secaucus, gaseous mercury and micrometeorological equipment was set up along the edge of the wetland to sample lower boundary layer air as it traveled approximately 0.5 km across the tidally-exposed marsh. As a result of the orientation of the Secaucus High School Marsh, sampling was only conducted in Secaucus under W-NW winds, as determined by a 03001-L Y.M. Young Wind Sentry Set (cup anemometer and wind vane at both Hg sample heights, Campbell Scientific, Logan, Utah, USA). In Tuckerton, equipment was set up in the center of an open area of tidal wetland which allowed sampling from all directions. Micrometeorological equipment was mounted on 5.7 cm diameter poles with minimal tripod support to avoid aerodynamic interference.

Total gaseous mercury was monitored at two heights in order to determine a difference in concentration over two heights ("concentration gradient") in the lower boundary layer [Edwards et al. 2005]. In August 2005, TGM was monitored at 0.2 m and

1.5 m above the top of the *Phragmites* (~2 m height) in Secaucus. For the May 2006 and June 2007 Secaucus sampling events, TGM was monitored between 0.05 m and 1 m above unvegetated sediment for the lower height and between 4.1 m and 4.4 m for the upper height. In Tuckerton, TGM was monitored at 0.2 m and 3.2 m above the marsh surface. TGM sample lines were the same length for both heights to minimize sample bias. Micrometeorological data (vertical/horizontal velocities, specific humidity) were collected near the upper sample height at 0.8 m above the top of the *Phragmites* in August 2005 and at 3.1 m and 4.4 m above the sediment surface in May 2006 and June 2007, respectively, in Secaucus. Micrometeorological data were collected at 3.0 m above the sediment surface in Tuckerton. In an effort to maximize the mercury gradient and minimize the noise-to-signal ratio, sampling heights differed between collection dates. This was, at times, limited by the height of the sampling equipment. In contrast to flux chamber flux measurements, micrometeorological methods are integrative and provide spatially averaged fluxes that include the effects of ambient air turbulence, which is an important factor driving the volatilization of gases from terrestrial surfaces.

3.3.2. *Flux calculations*

Vertical fluxes of gaseous mercury were estimated from measured vertical concentration gradients of TGM, atmospheric stability correction factors, and calculated friction velocities in a modified form of the Thornthwaite-Holzmann equation [Majewski et al. 1993; Korfiatis et al. 2003; Goodrow et al. 2005]:

$$F_{Hg} = \frac{u_* \kappa (Hg_1 - Hg_2)}{\ln\left(z_2 / z_1\right)\phi_W} \quad (1)$$

where F_{Hg} is the land-air mercury flux (ng m^{-2} h^{-1}), u_* is the friction velocity, κ is the von Karman constant, Hg_1 (lower) and Hg_2 (upper) are the TGM concentrations (ng m^{-3}) at heights z_1 (lower) and z_2 (upper) above the ground, and ϕ_W is the atmospheric stability correction factor for water vapor, though the same equation is used to estimate ϕ_H, the atmospheric stability correction factor for heat [Thornthwaite & Holzman 1939; Dyer & Hicks 1970; Majewski et al. 1991]. Both ϕ_W and ϕ_H can be used as a surrogate for ϕ_C, the atmospheric stability correction factor for a chemical, but water vapor was chosen since the krypton hygrometer measures water vapor flux and the sonic anemometer measures velocity. Errors were propagated through the variables of the flux equation. Atmospheric mercury exists primarily in the gaseous elemental form, with estimates up to 99% [Hg^0; Slemr et al. 1985; Zilloux et al. 1993; Morel et al. 1998; Lin & Pehkonen 1999], though reactive gaseous mercury may be present at greater than 1%, thus lowering the amount of Hg^0 in the immediate atmosphere. However, speciation of atmospheric mercury does not affect the resulting flux calculation.

Atmospheric stability correction factors were calculated using the Monin-Obukhov length scale for turbulent mixing [L, Obukhov 1946]:

$$L = \frac{\rho C_p u_*^{\,3} \theta}{\kappa g (H + 0.07LE)} \quad (2)$$

where ρ is the air density, C_p is the specific heat of air at constant pressure, θ is the potential temperature, g is the acceleration of gravity, H is the directly measured sensible heat flux, and LE is the latent heat flux. Turbulent mixing length scale was further used to calculate non-adiabatic atmospheric stability correction factors according to Dyer and Hicks [1970]:

$$\phi_W = \left(1 - 16\left(z/L\right)\right)^{-1/2} \tag{3}$$

where z is the height of eddy correlation measurements. Sign designation for TGM fluxes followed the convention of positive values corresponding to upward fluxes (mercury emission to the atmosphere) and negative values corresponding to downward fluxes (mercury deposition).

3.3.3. *Micrometeorology*

Micrometeorological parameters were measured using an eddy correlation system (Campbell Scientific; Fig. 3.2). The high resolution eddy correlation (EC) system is capable of resolving turbulent fluctuations in vertical and horizontal velocity, temperature, and specific humidity in the near surface atmosphere. These measurements were processed to give 10 min averaged friction velocities and sensible and latent heat fluxes. The EC system consisted of a CSAT3 three-dimensional sonic anemometer, a KH_2O ultraviolet krypton hygrometer, and a FW05 fine wire thermocouple. The CSAT3 sonic anemometer was used to determine momentum fluxes and sensible and latent heat fluxes at a rate of 10 Hz, with noise in horizontal and vertical velocities of 1 mm s^{-1} and

0.5 mm s^{-1}, respectively. Fluctuations of the moisture content in air were measured using a KH_2O Ultraviolet Krypton Hygrometer capable of measuring at rates up to 100 Hz. High precision ($\pm 0.002^{o}C$) temperature at sampling height was measured using a 0.0013 cm FW05 fine wire thermocouple. Horizontal wind speeds were also measured using a cup anemometer with a range of 0 to 50 m s^{-1} and a threshold value of 0.5 ms^{-1}.

3.3.4. *Tekran 2537A mercury vapor analyzer*

Ambient air was continuously sampled at two heights above the tidally-exposed wetland sediments using an automated mercury sampler (Tekran 2357A, Toronto, Canada). TGM was collected by gold amalgamation and analyzed by cold vapor atomic fluorescence spectrometry (CVAFS) after thermal desorption [Schroeder et al. 1995]. The Tekran sampled ambient air at a flow rate of 1.5 L min^{-1} for a period of 5 min (7.5 L sample volume) in an effort to obtain optimum instrument detection limits (0.1 ng m^{-3}). Two 5 min samples were taken at each height, one on each of the gold traps (A and B), during monitoring using a Synchronized Two-Port Sampler (Tekran, Model 1110). TGM concentrations from A and B cartridges were averaged for each of the upper and lower heights in an effort to remove minor systematic cartridge biases. The Tekran was housed in a temperature controlled tent to prevent over-heating and was calibrated regularly using internal calibrations in the field and periodically with gas injection calibrations to assure analyzer performance.

3.3.5. *Sediment mercury concentration*

Composite sediment samples were collected by shovel, placed in sealed 5 gallon HDPE containers and stored, untreated, in a cold chamber at 10ºC until analysis. Care was taken to minimally disrupt the ecosystem during sample collection.

Total mercury was determined for each of the homogenized, composite sediment samples as per EPA Method 1631 by way of aqua regia digestion. Dilute digested sediment samples were reduced with 0.5M $SnCl_2$ and bubbled onto gold-coated sand traps, passed through a dual amalgamation system, and subsequently thermally desorbed to a Tekran model 2500 (Toronto, Canada) CVAFS detector [Fitzgerald & Gill 1979; Bloom & Crecelius 1983].

Bubbler and reagent blanks were run for quality control purposes. A gas injection calibration curve was performed and compared with liquid standard spikes to determine recovery. Average recoveries were 100% ± 10%.

3.3.6 *Statistical analyses*

Percent gradients were calculated as:

$$\%gradient = \frac{Hg_1 - Hg_2}{Hg_1} \times 100 \quad (4)$$

where variables are defined as follows: ($Hg_1 - Hg_2$), vertical TGM concentration gradient (ng m^{-3}) and Hg_1, TGM concentration (ng m^{-3}) at the lower sample height [Kim & Kim 1999; Goodrow et al. 2005]. Samples with percent TGM gradients less than 2.6% (twice

the relative analytical uncertainty) in the Secaucus High School Marsh and less than 0.72% in the Great Bay estuary were assigned vertical TGM fluxes of zero.

Regression analyses were performed for each experimental run to determine coefficients of determination r^2 and significance p for correlations at 95% confidence intervals.

3.4. Results

3.4.1. *Total gaseous mercury concentrations and land-air mercury fluxes*

The results for Secaucus High School Marsh and the Great Bay estuary are summarized in Tables 3.3 and 3.4, respectively. Twenty minute gradients were averaged over one to two hours to smooth the data. Ambient TGM concentrations measured 4.3 m above the Secaucus High School Marsh ranged from 1.4 to 5.1 ng m^{-3}. The average summertime concentration of TGM at the Secaucus site (2.5 ng m^{-3}) was similar to that observed in Bayonne, New Jersey 18 km to the south [Goodrow et al. 2005]. Ambient TGM concentrations measured 3.2 m above the marsh surface at the Great Bay estuary site ranged from 2.3 to 3.4 ng m^{-3}. The average concentration of TGM at the Great Bay site (3.0 ng m^{-3}) was higher than that in Secaucus but was not significantly different ($p = 0.06$, two-tailed t-test for unequal variances). Secaucus ambient TGM concentrations were more variable than those at the Great Bay. Indeed, the highest ambient TGM concentrations (4.9 to 5.1 ng m^{-3}) were recorded in Secaucus on 11 August 2005, a day when daytime air temperatures ranged from 35 to 37°C.

Surface gaseous mercury concentration differences over height at the Secaucus site varied from -1.4 to 1.0 ng m^{-3} and were positive (higher near the sediment surface) in

16 out of 20 measurement events. In two time periods, vertical TGM gradients were negative indicating net absorption of atmospheric TGM by the marsh, and in two others, TGM concentration differences between the upper and lower sample heights were not significant. The two gradients with insignificant differences were recorded on 11 August 2005 when ambient TGM concentrations were elevated, potentially due to extreme heat. Estimated daytime land-air mercury fluxes ranged from -375 to +677 ng m^{-2} h^{-1} at the Secaucus High School Marsh during the study period.

Positive gaseous mercury concentration differences were observed in 17 out of 28 measurement periods at the Great Bay site and negative gradients were observed in five of these periods. Six gradients at the Great Bay site were below detection. TGM concentration gradients at the Great Bay site exhibited a diurnal pattern with the highest positive gradients occurring during midday and the lowest gradients measured at night (Fig. 3.3). Land-air TGM fluxes at the Great Bay site ranged from -34 to +81 ng m^{-2} h^{-1} in October 2007. Small fluxes of <10 ng m^{-2} h^{-1} accounted for about half of all values in the Great Bay estuary. By comparison, only 10% of estimated mercury fluxes in Secaucus were <10 ng m^{-2} h^{-1}. Negative fluxes were only observed in the presence of the *Phragmites* in Secaucus and at night at the Great Bay site, indicating net movement of mercury from the air to the plant/marsh surface. In Secaucus, the observed negative fluxes also coincided with elevated ambient air concentrations of > 3 ng m^{-3}, potentially suppressing Hg volatilization and enhancing deposition.

Cumulative mercury fluxes were positively correlated with cumulative solar radiation from 3 October 2007 8:35 through 4 October 2007 17:35 at the Great Bay site ($r^2 = 0.97$, $p < 0.01$) and from 24 May 2006 10:45 through 25 May 2006 16:55 at the

Secaucus site ($r^2 = 0.97$, $p < 0.01$; Fig. 3.4). No significant correlations were found between mercury fluxes and wind speed or air temperature at either site.

3.4.2. *Total mercury concentrations in salt marsh sediments*

The concentrations of total mercury in composite, homogenized sediments at the two field sites were 7.1 mg kg^{-1} and 0.45 mg kg^{-1} in the Secaucus High School Marsh and the Great Bay estuary, respectively.

3.5. Discussion

3.5.1. *Abiological factors driving mercury volatilization from wetlands sediments*

When comparing mercury volatilization fluxes for Secaucus High School Marsh and the Great Bay estuary it appears that mercury concentration in surface sediments may be an important factor controlling the flux. The sediment THg concentration estimated at the Great Bay site (0.5 mg kg^{-1}) was toward the high end of that observed in pristine Florida Everglades sediments where total mercury concentrations range from 0.08-0.43 mg kg^{-1} [Cai et al. 1997]. The estimated concentration of total mercury in Secaucus High School Marsh sediments (7 mg kg^{-1}) is similar to that of the contaminated areas of the Savannah River in South Carolina where sediment total mercury concentrations are as high as 10 mg kg^{-1} [Kaplan et al. 2002]. This ten-fold higher mercury concentration in Secaucus sediments than at the Great Bay site supported up to ten-fold higher sediment-air fluxes of gaseous mercury in Secaucus (Tables 3.3 and 3.4).

Another important factor driving mercury volatilization from salt marsh sediments is the photochemical reduction of Hg(II) in surface sediments.

Micrometeorological mercury volatilization fluxes determined for the Secaucus High School Marsh and the Great Bay estuary showed clear diurnal trends with peak emissions in the mid- to late afternoon and small bidirectional fluxes of Hg^0 overnight and into the morning (Tables 3.3 and 3.4; Figs. 3.3 and 3.4). The observed diurnal pattern is similar to that of previous studies [Kim et al. 1995; Canario & Vale 2004; Feng et al. 2005] and is likely due to photochemical reduction of Hg(II) [Carpi & Lindberg 1997]. Estuarine sediments are rich in organic carbon and sulfide and Hg(II) is usually present in photochemically active forms including organic matter-bound mercury [Zhang & Lindberg 1999] and solid phase HgS [Nriagu 1994]. While the observed correlations of mercury volatilization fluxes and PAR irradiance are evidence that photochemistry plays an important role in mercury volatilization from salt marsh sediments, other physical factors may also be important.

Low nighttime fluxes of mercury, as were observed in this study, may result from a stable, stratified atmospheric boundary layer which causes transport to be dominated by molecular diffusion rather than turbulent mixing [Kim et al. 1995]. However, in this study, meteorological parameters did not exhibit diurnal trends, indicating that they did not play a major role in controlling mercury volatilization fluxes. For example, for the period of 11:55 on 3 October 2007 to 4:25 on 4 October 2007, friction velocities and atmospheric stability correction factors were relatively constant (Table 3.4). Over this same period, however, the vertical gaseous mercury gradient decreased from 0.4 ng m^{-3} to 0 ng m^{-3} indicating that the source of volatile mercury in the sediments was effectively turned off over night (Table 3.4, Fig. 3.3).

In addition to solar radiation, air temperature is considered an important environmental factor driving the re-emission of mercury from terrestrial surfaces [Feng et al. 2005]. Positive correlations of mercury emission fluxes and temperature have been observed [Canario & Vale 2004], yet mercury volatilization flux is often independent of air temperature [Gustin et al. 1997; Gustin et al. 2002; Bahlmann et al. 2004; Feng et al. 2005]. For example, mercury fluxes in both Secaucus and the Great Bay decreased in the afternoon as sunlight decreased, but ambient air temperatures remained relatively constant (Tables 3.2 to 3.4). In this study, temperature was uncorrelated with TGM flux in Secaucus and was weakly negatively correlated in the Great Bay ($r^2 = 0.24$, $p < 0.01$).

3.5.2. *Biological factors affecting mercury volatilization*

Several studies have indicated that plants serve as a conduit, moving inorganic and organic mercury from soils, through their root systems to the foliage, and through the stomata before reaching the atmosphere [Bargagli et al. 1986; Barghigiani & Bauleo 1992; Hanson et al. 1995; Lindberg 1996; Leonard et al. 1998a]. This movement is bi-directional [Hanson et al. 1995] as foliar surfaces may act as sources or sinks of Hg^0, depending on atmospheric concentration.

Size, species, and genotype of vegetation may affect the extent to which vegetation facilitates the transfer of mercury to the atmosphere [Leonard et al. 1998a]. Photosynthesis occurs most rapidly during midday sun, coincident with peak Hg fluxes, so it is difficult to separate the effects of direct sediment photoreduction from plant-induced processes in the natural environment. In the absence of strong midday solar radiation, our results from 10 August 2005 suggest that the tall grass *Phragmites* may

absorb gaseous mercury from the atmosphere (Table 3.3). In the Great Bay, the waxy exterior of *Salicornia* is expected to render it insignificant in gas exchange [S. Peters, personal communication, 2 July 2008]. Note: *Phragmites* were only present in the Secaucus High School Marsh during field sampling in 2005. Between field studies in 2005 and 2006, the vegetation had been cleared to bare sediment for wetland restoration purposes.

Bioturbation has the potential to facilitate the transport of elemental mercury from reduced sediment layers to the surface [Canario & Vale 2004; Robbins & Edgington 1975; Kramer et al. 1991] and was clearly occurring at both sites. However, at the Great Bay site, bioturbation as well as microbial mercury reduction from non-photosynthetic bacteria appear to be of minor importance compared with photoreduction since no mercury was emitted to the atmosphere at night. Photosynthetic organisms such as cyanobacteria are the only organisms that have the potential to photoreduce Hg. The California EPA [2008] suggest that cyanobacteria are most productive in warm, slow-moving water, rich in nutrients such as fertilizer and manure runoff and septic tank overflows. These conditions were not present and algal mats were not observed in either Secaucus or the Great Bay, indicating that abiological photoreduction was the dominant pathway in this study.

3.5.3. *Comparison of mercury emissions from salt marsh wetlands with fluxes from point source emissions and other land surfaces*

While scaling up of mercury flux measurements to regional scales is limited by our understanding of the physical, chemical, and biological processes occurring in

complex wetland sediments, we provide a first estimate toward the direct sediment-air component of the mercury cycle. The potential contribution of salt marsh wetlands to regional mercury emissions was evaluated by comparing mean estimated fluxes for impacted and background wetlands in this study with major industrial emissions in New Jersey [NJ DEP 2005]. Observed land-air volatilization fluxes of mercury were an order of magnitude higher at the Secaucus High School Marsh compared with the Great Bay estuary. However, given its larger area, the Great Bay estuary is expected to be a larger source of mercury to the atmosphere than Secaucus. Annual mercury emissions were estimated by multiplying the mean estimated Hg flux at each study site (85 ± 29 ng m^{-2} h^{-1} and 17 ± 4 ng m^{-2} h^{-1} in Secaucus and Tuckerton, respectively) by the surface area listed in the Site Description section. Secaucus estimates were only made during the day. Assuming a 12 h day/night schedule, estimated annual mercury emissions were divided by two in Secaucus, providing an annual source of 0.06 ± 0.02 kg y^{-1} to the atmosphere while those in the Great Bay are expected to provide approximately 13 ± 3 kg y^{-1}. When compared to regional mercury emissions for New Jersey (Table 3.5), estimated annual emissions from the small (0.15 km^2) Secaucus High School Marsh are much lower than industrial emissions in New Jersey. This trend is expected to be real since summertime mercury fluxes are expected to be elevated over the annual average. Mercury emissions from the larger (87 km^2) Great Bay estuary are potentially on the order of small industrial sources in the state, but the effects of seasonality were not studied and may minimize this estimate.

Relatively few micrometeorological studies have been performed investigating the direct volatilization of mercury from sediment/soil surfaces to the atmosphere. The

extremely high average annual mercury volatilization fluxes for the Steamboat Springs geothermal region in Nevada [Gustin et al. 1999] reflects elevated levels of mercury not necessarily characteristic of background soils (Table 3.1). When compared with another local salt marsh wetland (Farm River, CT; Lee et al. 2000), mercury emission rates in Secaucus and Great Bay are elevated although sediment mercury concentrations in Secaucus are enhanced over background sediments. Nonetheless, uncontaminated Great Bay estuary sediments supported potentially higher fluxes than the contaminated Walker Branch watershed humid soils in Tennessee (Table 3.1). Thus, while contaminated soils may support mercury volatilization fluxes greater than those of impacted wetlands, fluxes may be significant in larger wetlands with greater surface area. Mercury volatilization fluxes from salt marsh sediments (>17 ng m^{-2} h^{-1}) in this study are more than ten-fold higher than the average mercury emission flux from land (~1 ng m^{-2} h^{-1}; Fitzgerald & Mason 1996), implying that further study of gaseous mercury emission from wetlands is necessary.

3.6. Conclusions and Implications

We conclude that mercury sediment concentration and solar radiation are likely the most important factors controlling in situ volatilization of mercury from tidally-exposed sediments. Our results suggest that pulses of gaseous elemental mercury are released to the atmosphere from tidally-exposed, estuarine wetlands where organic matter-rich sediments are exposed to solar radiation and come in direct contact with the atmosphere.

The magnitude of the land-air mercury fluxes estimated for contaminated (Secaucus High School Marsh) and relatively pristine (Great Bay estuary) salt marsh sediments suggests that mercury emission fluxes for large wetlands have the potential to rival smaller scale industrial emissions and demonstrates that the emission of mercury from tidally-exposed wetland sediments is likely an important pathway in regional and perhaps global mercury biogeochemical cycles.

It should be stressed that these estimations are based on extrapolating a relatively small dataset and lack the robustness necessary to make absolute conclusions regarding salt marsh wetlands as atmospheric sources of mercury. While the data are limited, the information disseminated warrants further investigation into the volatilization of gaseous elemental mercury from salt marsh sediments.

References

Bahlmann, E., R. Ebinghaus, and W. Ruck (2004), Influence of solar radiation on mercury emission fluxes from soils, *Mater. Geoenviron., 51,* 787-790.

Baillie, P.W. (1986), Oxygenation of intertidal estuarine sediments by benthic microalgal photosynthesis, *Estuar. Coast. Shelf S., 22,* 143-149.

Bargagli, R., C. Barghigiani, and B.E. Maserti (1986), Mercury in vegetation of the Mount Amiata area (Italy), *Chemos., 15,* 1035-1042.

Barghigiani, C. and R. Bauleo (1992), Mining area environmental mercury assessment using *Abies alba*, *Bull. Environ. Contam. Toxicol., 49,* 31-36.

Bloom, N.S. and E.A. Crecelius (1983), Determination of mercury in seawater at sub-nanogram per liter levels, *Mar. Chem., 14,* 49-89.

Bothner, M.H., R.A. Jahnke, M.L. Peterson, and R. Carpenter (1980), Rate of mercury loss from contaminated estuarine sediments, *Geochim. Cosmochim. Acta, 44,* 273-285.

Cai, Y., R. Jaffe, and R. Jones (1997), Ethylmercury in the soils and sediments of the Florida Everglades, *Environ. Sci. Technol., 31(1),* 302-305.

California EPA (2008), Blue-green algae (cyanobacteria) fact sheet, Available online: http://www.swrcb.ca.gov/bluegreenalgae/docs/workshop110805/shortfactcdcsheet.pdf.

Canario, J. and C. Vale (2004), Rapid release of mercury from intertidal sediments exposed to solar radiation: A field experiment, *Environ. Sci. Technol., 38,* 3901-3907.

Carpi, A. and S.E. Lindberg (1997), The sunlight mediated emission of elemental mercury from soil amended with municipal sewage sludge, *Environ. Sci. Technol.,* 31(7), 2085-2091.

Drobner, E., H. Huber, C. Wachterhauser, D. Rose, and K. Stetter (1990), Pyrite formation linked with hydrogen evolution under anaerobic conditions, *Nature, 346,* 742-744.

Dyer, A. J. and B. B. Hicks (1970), Flux-gradient relationships in the constant flux layer, *Quart. J. Roy. Meteor. Soc., 96*, 715–721.

Edwards, G.C., P.E. Rasmussen, W.H. Schroeder, D.M. Wallace, L. Halfpenny-Mitchell, G.M. Dias, R.J. Kemp, and S. Ausma (2005), Development and evaluation of a sampling system to determine gaseous mercury fluxes using an aerodynamic micrometeorological gradient method, *J. Geophys. Res., 110,* D10306, doi:10.1029/2004JD005187.

Feng, X., S. Wang, G. Qui, Y. Hou, and S. Tang (2005), Total gaseous mercury emissions from soil in Guiyang, Guizho, China, *J. Geophys. Res., 110,* D14306, doi:10.1029/2004JD005643.

Fitzgerald, W.F. and G. A. Gill (1979), Subnanogram determination of mercury by two-stage gold amalgamation and gas phase detection applied to atmospheric analysis, *Anal. Chem., 51(11),* 1714-1720.

Fitzgerald, W. and Mason, R. (1996), The global mercury cycle: oceanic and anthropogenic aspects, in W. Baeyens, et al (eds.), *Global and Regional Mercury Cycles: Sources, Fluxes and Mass Balances*, 85-108, Kluwer Academic Publishers, Netherlands.

Gilmour, C.C. and E.A. Henry (1991), Mercury methylation in aquatic systems affected by acid deposition, *Environ. Pollut., 71,* 131-169.

Gilmour, C.C., E.A. Henry, and R. Mitchell (1992), Sulfate stimulation of mercury methylation in freshwater sediments, *Environ. Sci. Technol., 26,* 2281-2287.

Gobeil, C. and D. Cossa (1993), Mercury in sediments and sediment pore water in the Laurentian Trough, *Can. J. Fish. Aquat. Sci., 50,* 1794-1800.

Goodrow, S., R. Miskewitz, R.I. Hires, S.J. Eisenreich, W.S. Douglas, and J.R. Reinfelder (2005), Mercury emissions from cement-stabilized dredged material, *Environ. Sci. Technol., 39,* 8185-8190.

Gustin, M.S., G.E. Taylor, Jr., and R.A. Maxey (1997), Effect of temperature and air movement on the flux of elemental mercury from substrate to the atmosphere, *J. Geophys. Res., 102,* 3891-3898.

Gustin, M.S., H. Biester, and C.S. Kim (2002), Investigation of the light-enhanced emission of mercury from naturally enriched substrate, *Atmos. Environ., 36,* 3241-3254.

Gustin, M.S., S.E. Lindberg, F. Marsik, A. Casimir, R. Ebinghaus, G. Edwards, C. Fitzgerals, J. Kemp, H. Kock, T. Leonard, M. Majewski, J. Owens, L. Poissant, P. Rasmussen, F. Schaedlich, D. Schneeberger, J. Sommar, R. Turner, A. Vette, D. Wallschlaeger, and Z. Xiao (1999), Nevada STORMS project: Measurement of mercury emission from naturally enriched surfaces, *J. Geophys. Res., 104,* 21,831-21,844.

Hanson, P.J., S.E. Lindberg, T.A. Tabberer, J.G. Owens, and K.-H. Kim (1995), Foliar exchange of mercury vapor: Evidence for a compensation point, *Water Air Soil Pollut., 80,* 373-382.

Holmes, J. and D. Lean (2006), Factors that influence methylmercury flux rates from wetland sediments, *Sci. Total Environ., 368,* 306-319.

Kaplan, D.I., A.S. Knox, and J. Myers (2002), Mercury geochemistry in a wetland and its implications for in situ remediation, *J. Environ. Eng., 128(8),* 723-732.

Kim, K.-H. and M.-Y. Kim (1999), The exchange of gaseous mercury across soil- air surface interface in a residential area of Seoul, Korea, *Atmos. Environ., 33,* 3153-3165.

Kim, K.-H. and S.E. Lindberg (1995), Design and initial tests of a dynamic enclosure chamber for measurements of vapor-phase mercury fluxes over soils, *Water Air Soil Pollut*., *80*, 1059–1068.

Kim, K.-H., S.E. Lindberg, and T.P. Meyers (1995), Micrometeorological measurements of mercury vapor fluxes over background forest soils in eastern Tennessee, *Atmos. Environ., 29(2)*, 267-282.

Korfiatis, G.P., R.I. Hires, J.R. Reinfelder, L.A. Totten, and S.J. Eisenreich (2003), Monitoring of PCB and Hg air emissions in sites receiving stabilized harbor sediment, *Report to the New Jersey Marine Sciences Consortium and New Jersey Department of Transportation Office of Maritime Resources*.

Kramer, K.J.M., R. Misdorp, G. Berger, and R. Duijts (1991), Maximum pollutant concentrations at the wrong depth: A misleading pollution history in a sediment core, *Mar. Chem., 36,* 183-198.

Lamborg, C.H., W.F. Fitzgerald, J. O'Donnell, and T. Torgersen (2002), A non-steady-state compartmental model of global-scale mercury biogeochemistry with

interhemispheric atmospheric gradients, *Geochim. Cosmochim. Acta., 66,* 1105-1118.

Lee, X., G. Benoit, and X.Z. Hu (2000), Total gaseous mercury concentration and flux over a coastal saltmarsh vegetation in Connecticut, USA, *Atmos. Environ*., *34*, 4205-4213.

Leonard, T.L., G.E. Taylor, M.S. Gustin, and G.C.J. Fernandez (1998a), Mercury and plants in contaminated soils: 1. Uptake, partitioning, and emission to the atmosphere, *Environ. Toxicol. Chem.,* 17, 2063-2071.

Leonard, T.L., G.E. Taylor, M.S. Gustin, and G.C.J. Fernandez (1998b), Mercury and plants in contaminated soils: 2. Environmental and physiological factors governing mercury flux to the atmosphere, *Environ. Toxicol. Chem., 17,* 2072-2079.

Lin, C. and S.O. Pehkonen (1999), The chemistry of atmospheric mercury: a review. *Atmos. Environ., 33,* 2067–2079.

Lindberg, S.E. (1996), Forests and the global biogeochemical cycle of mercury: The importance of understanding air/vegetation exchange processes, in *Global and regional mercury cycles: Sources, fluxes and mass balance*, vol. 21, pp. 359-380, Kluwer, Dordrecht, The Netherlands.

Lindberg, S.E. and T.P. Meyers (2001), Development of an automated micrometeorological method for measuring the emission of mercury vapor from wetland vegetation, *Wet. Ecol. Manag*., *9(4),* 333-347.

Lindberg, S.E., W. Dong, and T. Meyers (2002), Transpiration of gaseous elemental mercury through vegetation in a sub-tropical wetland in Florida, *Atmos. Environ*., *36*,5207-5219.

Majewski, M., M. McChesney, and J. Seiber (1991), A field comparison of two methods for measuring DCPA soil evaporation rates, *Environ. Toxicol. Chem., 10,* 301–311.

Majewski, M., R. Desjardins, P. Rochette, E. Pattey, J. Sieber, and D. Glotfelty (1993), Field comparison of an eddy accumulation and an aerodynamic-gradient system for measuring pesticide volatilized fluxes, *Environ. Sci. Technol., 27,* 121-128.

Mantoura, R.F.C., A. Dickson, and J.P. Riley (1978), The complexation of metals with humic materials in natural waters, *Estuar. Coast. Shelf S., 6,* 387-408.

Marsik, F.J., G.J. Keeler, S.E. Lindberg, and H. Zhang (2005), Air-surface exchange of gaseous mercury over a mixed sawgrass-cattail stand within the Florida Everglades, *Environ. Sci. Technol., 39,* 4739-4746.

Meyers, T.P., M.E. Hall, S.E. Lindberg, and K. Kim (1996), Use of the modified Bowen-ratio technique to measure fluxes of trace gases, *Atmos. Environ., 30(19),* 3321-3329.

Morel, F.M.M., A.M.L. Kraepiel, and M. Amyot (1998), The chemical cycle and bioaccumulation of mercury, *Annu. Rev. Ecol. Syst., 29,* 543-566.

Morse, J.W. and G.W. Luther (1999), Chemical influences on trace metal-sulfide interactions in anoxic sediments., *Geochim. Cosmichim. Acta, 63*, 3373-3378.

NJ DEP: Mercury Task Force (2005), Mercury Emissions, http://www.nj.gov/dep/dsr/trends2005/pdfs/mercury.pdf.

Nriagu, J.O. (1994), Mechanistic steps in the photoreduction of mercury in natural-waters, *Sci. Total Environ., 154,* 1-8.

Obukhov, A.M. (1946), Turbulence in an atmosphere of non-homogeneous temperature, *Trans. Inst. Theoret. Geophys., USSR*, *1*, 95-115.

O'Driscoll, N.J., L. Poissant, J. Canario, J. Ridal, and D.R.S. Lean (2007), Continuous analysis of dissolved gaseous mercury and mercury volatilization in the Upper St. Lawrence River: Exploring temporal relationships and UV attenuation, *Environ. Sci. Technol., 41,* 5342-5348.

Poissant L, and A. Casimir (1998), Water–air and soil–air exchange rate of total gaseous mercury measured at background sites, *Atmos. Environ., 32(5),* 883 –93.

Poissant, L., M. Pilote, X. Xu, and H. Zhang (2004), Atmospheric mercury speciation and deposition in the Bay St. Francois wetlands, *J. Geophys. Res., 109,* D11301-D11302.

Robbins, J.A. and D.N. Edgington (1975), Determination of recent sedimentation rates in Lake Michigan using Pb-210 and Cs-137, *Geochim. Cosmochim. Acta, 39,* 285-304.

Rutgers Marine Field Station website (2008), Locations and facilities, Available online: http://marine.rutgers.edu/rumfs/RUMFShomepage.htm.

Schroeder, W.H., G. Keeler, H., Kock, P. Roussel, D. Schneeberger, and F. Schaedlich (1995), International field intercomparison of atmospheric mercury measurement methods, *Water Air Soil Pollut., 80,* 611-620.

Schroeder,W.H. and J. Munthe (1998), Atmospheric mercury: An overview, *Atmos. Environ., 32,* 809-822.

Slemr, F., G. Schuster, and W. Seiler (1985), Distribution, speciation and budget of atmospheric mercury, *J. Atmos. Chem., 3,* 407-434.

Thornthwaite, C.W. and B. Holzman (1939), The determination of evaporation from land and water surfaces, *U.S. Mon. Weather Rev., 67,* 4-11.

Tiner, R.W. (1987), *A Field Guide to Coastal Wetland Plants of the Northeastern United States,* 285 pp., Univ. of Mass. press, Massachusetts.

Zhang, H. and S.E. Lindberg (1999), Processes influencing the emission of mercury from soils: A conceptual model, *J. Geophys. Res., 104,* 21,889-21,896.

Zillioux, E.J., D.B. Porcella, and J.M. Benoit (1993), Mercury cycle and effects in freshwater wetland ecosystems, *Environ. Toxicol. Chem., 12,* 2245-2264.

Table 3.1 Average Annual Land-Air Gaseous Mercury Volatilization Fluxes Estimated by Micrometeorological Methods for Wetland Sediments and Two Soils[a].

site name	media	TGM flux ($ng\ m^{-2}\ h^{-1}$)
Secaucus High School Marsh, NJ[a]	intertidal salt marsh sediment	85
Great Bay estuary, NJ[a]	intertidal salt marsh sediment	17
New Haven, CT (Farm River salt marsh)[b]	intertidal salt marsh sediment	-0.5
Walker Branch, Oak Ridge, TN[c]	acid humid soil	8 - 18
Steamboat Springs, NV[d]	desert arid soil	490

[a] All fluxes are diurnal except Secaucus High School Marsh which is only daytime fluxes and may represent a somewhat elevated flux compared to diurnal measurements.

Table 3.2 Micrometeorological Parameters[a] Measured in the Secaucus High School Marsh and the Great Bay Estuary, New Jersey.

site	date	local time	PAR ($\mu mol\ m^{-2}\ s^{-1}$)	air temperature (°C)	wind speed ($m\ s^{-1}$)
Secaucus High School Marsh	10-Aug-05	9:20 – 10:20	519	32	1.0
		10:55 – 11:55	1550	32	0.9
		12:15 – 13:05	1680	33	2.0
		13:05 – 14:00	-	34	1.8
	11-Aug-05	9:20 – 10:50	810	35	1.1
		10:50 – 12:10	1530	37	0.7
	24-May-06	10:45 – 11:50	1710	19	3.9
		12:05 – 12:50	1790	20	4.4
		13:05 – 14:30	1870	21	3.1
		15:30 – 16:10	1770	22	1.6
		17:05 – 17:50	1635	23	1.4
		18:05 – 18:50	700	23	1.1
	25-May-06	12:20 – 13:15	1840	25	2.8
		13:20 – 14:35	2200	24	2.5
		14:40 – 15:40	1020	25	3.7
		15:45 – 16:55	935	25	2.7
	7-Jun-07	10:40 - 11:50	1300	20	2.4
	21-Jun-07	11:10 - 12:30	1670	24	2.6
		12:40 - 13:50	1760	26	3.1
		14:00 - 15:50	1688	27	4.1
Great Bay estuary	2-Oct-07	17:35 - 19:05	155	24	-
		20:55 - 22:25	0	23	-
		22:35 - 0:05	0	23	-
	3-Oct-07	0:15 - 1:45	0	25	-
		1:55 - 3:25	0	30	-
		3:35 - 5:05	0	28	-
		5:15 - 6:45	0	26	-
		6:55 - 8:25	73	24	-
		8:35 - 10:05	228	24	-
		10:15 - 11:45	450	24	-
		11:55 - 13:25	673	24	-
		13:35 - 15:05	1173	24	-
		15:15 - 16:45	1100	24	-
		16:55 - 18:25	380	24	2.1
		18:35 - 20:05	53	23	3.1
		20:15 - 21:45	0	23	1.6
		21:55 - 23:25	0	23	1.5
		23:35 - 1:05	0	25	1.9
	4-Oct-07	1:15 - 2:45	0	30	2.9
		2:55 - 4:25	0	29	2.6
		4:35 - 6:05	0	28	1.9
		6:15 - 7:45	20	25	2.2
		7:55 - 9:25	165	24	1.6
		9:35 - 11:05	405	24	1.2
		11:15 - 12:45	443	24	1.5
		12:55 - 14:25	1110	24	2.4
		14:35 - 16:05	1310	24	3.1
		16:15 - 17:35	640	24	2.6

[a] PAR is photosynthetically active radiation; dash (-) indicates no data available.

Table 3.3 Secaucus High School Marsh, NJ: Friction Velocities (u_*), Atmospheric Stability Correction Factors (ϕ_w), Average Vertical Concentration Gradients of Total Gaseous Mercury (TGM), Concentrations of Ambient TGM, and Sediment-Air TGM Fluxes[a].

date		local time	u_*	ϕ_w	TGM gradient (ng m^{-3})	ambient TGM (ng m^{-3})	TGM flux (ng m^{-2} h^{-1})
10-Aug-05	9:20	9:20 – 10:20	0.19 ± 0.06	0.59 ± 0.18	-1.44 ± 0.05	3.25 ± 0.08	-375 ± -165
	10:55	10:55 – 11:55	0.26 ± 0.08	0.65 ± 0.17	-0.83 ± 0.05	3.30 ± 0.55	-269 ± -109
	12:15	12:15 – 13:05	0.31 ± 0.09	0.69 ± 0.15	1.04 ± 0.04	1.46 ± 0.15	203 ± 74
	13:05	13:05 – 14:00	0.36 ± 0.11	0.37 ± 0.20	0.15 ± 0.05	2.62 ± 0.18	63 ± 45
11-Aug-05	9:20	9:20 – 10:50	0.23 ± 0.05	0.75 ± 0.13	0	5.05 ± 0.42	-
	10:50	10:50 – 12:10	0.20 ± 0.04	0.54 ± 0.10	0	4.87 ± 0.06	-
24-May-06	10:45	10:45 – 11:50	0.30 ± 0.02	0.46 ± 0.07	0.44 ± 0.04	2.09 ± 0.06	97 ± 19
	12:05	12:05 – 12:50	0.29 ± 0.04	0.41 ± 0.07	0.22 ± 0.05	2.31 ± 0.03	51 ± 15
	13:05	13:05 – 14:30	0.30 ± 0.05	0.40 ± 0.07	0.55 ± 0.04	1.98 ± 0.04	136 ± 34
	15:30	15:30 – 16:10	0.27 ± 0.02	0.39 ± 0.01	0.71 ± 0.04	1.82 ± 0.04	166 ± 15
	17:05	17:05 – 17:50	0.27 ± 0.02	0.55 ± 0.08	0.25 ± 0.03	1.49 ± 0.05	76 ± 16
	18:05	18:05 – 18:50	0.32 ± 0.02	0.94 ± 0.11	0.17 ± 0.03	1.38 ± 0.00	36 ± 7
25-May-06	12:20	12:20 – 13:15	0.30 ± 0.02	0.54 ±0.07	0.22 ± 0.05	2.59 ± 0.04	75 ± 20
	13:20	13:20 – 14:35	0.31 ± 0.02	0.69 ± 0.07	0.26 ± 0.06	2.92 ± 0.20	71 ± 18
	14:40	14:40 – 15:40	0.30 ± 0.02	0.70 ± 0.08	0.24 ± 0.05	2.53 ± 0.08	63 ± 15
	15:45	15:45 – 16:55	0.29 ± 0.01	0.55 ± 0.02	0.44 ± 0.05	2.39 ± 0.05	142 ± 18
7-Jun-07	10:40	10:40 - 11:50	0.24 ± 0.15	0.31 ± 0.22	0.32 ±0.05	2.44 ± 0.13	227 ± 245
21-Jun-07	11:10	11:10 - 12:30	0.30 ± 0.09	0.42 ± 0.15	0.93 ± 0.04	1.90 ± 0.10	677 ± 310
	12:40	12:40 - 13:50	0.33 ± 0.07	0.45 ± 0.10	0.49 ± 0.04	2.14 ± 0.13	364 ± 117
	14:00	14:00 - 15:50	0.36 ± 0.09	0.54 ± 0.14	0.55 ± 0.04	1.67 ± 0.12	374 ± 139

[a] Values are means ± SD for ambient TGM, u_*, and ϕ_w and means ± propagated error for TGM gradients and fluxes. Atmospheric correction factors for water vapor were calculated using the Monin-Obukhov length scale [Obukhov, 1946] according to Dyer and Hicks [1970]. Samples with TGM percent gradients <2.6% (twice the relative analytical uncertainty) were assigned vertical fluxes of zero. Hg concentrations measured at the upper sample height (4.3 m) were taken as ambient.

Table 3.4 Great Bay estuary, NJ: Friction Velocities (u_*), Atmospheric Stability Correction Factors (ϕ_w), Average Vertical Concentration Gradients of Total Gaseous Mercury (TGM), Concentrations of Ambient TGM, and Sediment-Air TGM Fluxes[a].

date	local time	u_*	ϕ_w	TGM gradient (ng m^{-3})	ambient TGM (ng m^{-3})	TGM flux (ng m^{-2} h^{-1})
2-Oct-07	17:35 - 19:05	0.33 ± 0.03	0.79 ± 0.00	0.05 ± 0.04	3.43 ± 0.05	10 ± 4
	20:55 - 22:25	0.21 ± 0.02	0.76 ± 0.05	0.08 ± 0.04	3.39 ± 0.11	12 ± 3
	22:35 - 0:05	0.17 ± 0.02	0.61 ± 0.05	0.06 ± 0.03	3.27 ± 0.13	8 ± 3
3-Oct-07	0:15 - 1:45	0.19 ± 0.02	0.68 ± 0.06	0.08 ± 0.03	3.19 ± 0.27	11 ± 3
	1:55 - 3:25	0.22 ± 0.02	0.77 ± 0.05	-0.23 ± 0.03	3.26 ± 0.05	-34 ± 4
	3:35 - 5:05	0.21 ± 0.01	0.75 ± 0.02	-0.10 ± 0.03	3.37 ± 0.07	-15 ± 3
	5:15 - 6:45	0.21 ± 0.02	0.74 ± 0.06	-0.11 ± 0.03	3.36 ± 0.24	-16 ± 3
	6:55 - 8:25	0.21 ± 0.02	0.75 ± 0.05	0.20 ± 0.03	3.23 ± 0.06	30 ± 5
	8:35 - 10:05	0.15 ± 0.04	0.57 ± 0.14	0.41 ± 0.04	3.20 ± 0.05	58 ± 21
	10:15 - 11:45	0.17± 0.04	0.64 ± 0.12	0.29 ± 0.03	3.23 ± 0.07	42 ± 12
	11:55 - 13:25	0.26 ± 0.04	0.80 ± 0.03	0.39 ± 0.03	3.09 ± 0.07	68 ± 10
	13:35 - 15:05	0.29 ± 0.02	0.79 ± 0.02	0.29 ± 0.03	3.14 ± 0.11	56 ± 5
	15:15 - 16:45	0.23 ± 0.04	0.76 ± 0.04	0.20 ± 0.03	3.14 ± 0.08	32 ± 6
	16:55 - 18:25	0.22 ± 0.03	0.74 ± 0.11	0.09 ± 0.03	3.10 ± 0.13	15 ± 4
	18:35 - 20:05	0.34 ± 0.05	0.89 ± 0.03	0	2.80 ± 0.13	-
	20:15 - 21:45	0.17 ± 0.03	0.59 ± 0.16	-0.02 ± 0.03	2.70 ± 0.02	-3 ± -2
	21:55 - 23:25	0.16 ± 0.04	0.59 ± 0.12	0	2.51 ± 0.06	-
	23:35 - 1:05	0.23 ± 0.11	0.75 ± 0.13	-0.04 ± 0.02	2.37 ± 0.05	-6 ± -4
4-Oct-07	1:15 - 2:45	0.31 ± 0.08	0.76 ± 0.28	0	2.52 ± 0.07	-
	2:55 - 4:25	0.34 ± 0.04	0.79 ± 0.04	0	2.60 ± 0.12	-
	4:35 - 6:05	0.29 ± 0.05	0.85 ± 0.13	0	2.35 ± 0.02	-
	6:15 - 7:45	0.16 ± 0.02	0.62 ± 0.11	0	2.29 ± 0.06	-
	7:55 - 9:25	0.14 ± 0.02	0.45 ± 0.13	0.04 ± 0.03	2.44 ± 0.28	6 ± 3
	9:35 - 11:05	0.13 ± 0.05	0.32 ± 0.15	0.17 ± 0.03	2.50 ± 0.06	37 ± 22
	11:15 - 12:45	0.17 ± 0.04	0.40 ± 0.11	0.21 ± 0.03	2.50 ± 0.06	48 ± 17
	12:55 - 14:25	0.27 ± 0.04	0.43 ± 0.05	0.25 ± 0.03	2.52 ± 0.05	81 ± 16
	14:35 - 16:05	0.35 ± 0.03	0.56 ± 0.04	0.15 ± 0.03	2.55 ± 0.04	51 ± 7
	16:15 - 17:35	0.33 ± 0.08	0.54 ± 0.06	0.07 ± 0.03	2.49 ± 0.05	22 ± 7

[a] Values are means ± SD for ambient TGM, u_*, and ϕ_w and means ± propagated error for TGM gradients and fluxes. Atmospheric correction factors for water vapor were calculated using the Monin-Obukhov length scale [Obukhov, 1946] according to Dyer and Hicks [1970]. Samples with TGM percent gradients <0.72% (twice the relative analytical uncertainty) were assigned vertical fluxes of zero. Hg concentrations measured at the upper sample height (3.2 m) were taken as ambient.

Table 3.5 Mean Annual Mercury Emissions to the Atmosphere from New Jersey Industrial Sources and Salt Marsh Sediments.

source category	emissions rate (kg y^{-1})
steel and iron manufacturing[a]	450
aluminum scrap processing[a]	450
coal combustion[a]	320
MSW incineration[a]	150
product volatilization[a]	140
fluorescent tube breakage[a]	110
oil refining[a]	90
landfills[a]	20
wood combustion[a]	5
medical waste incineration[a]	2
Secaucus High School Marsh	0.06[b]
Great Bay estuary	13[b]

[a] from NJ DEP [2005].
[b] estimated daytime flux for a 24 h day.

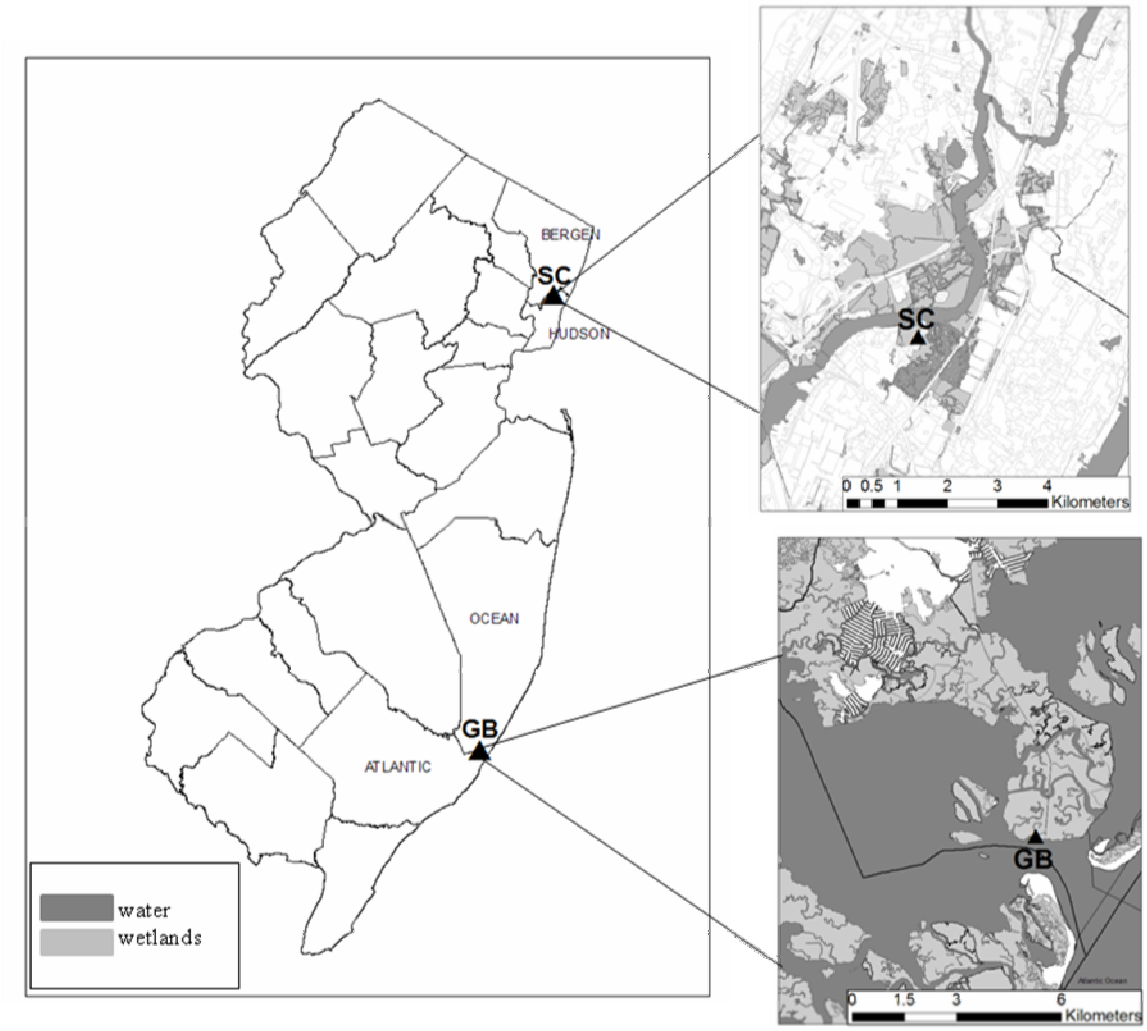

Figure 3.1 Map of in situ micrometeorological study locations. SC is Secaucus High School Marsh; GB is Great Bay estuary.

Figure 3.2 Eddy correlation system at the Secaucus High School Marsh 10-11 August 2005 (*Phragmites* removed).

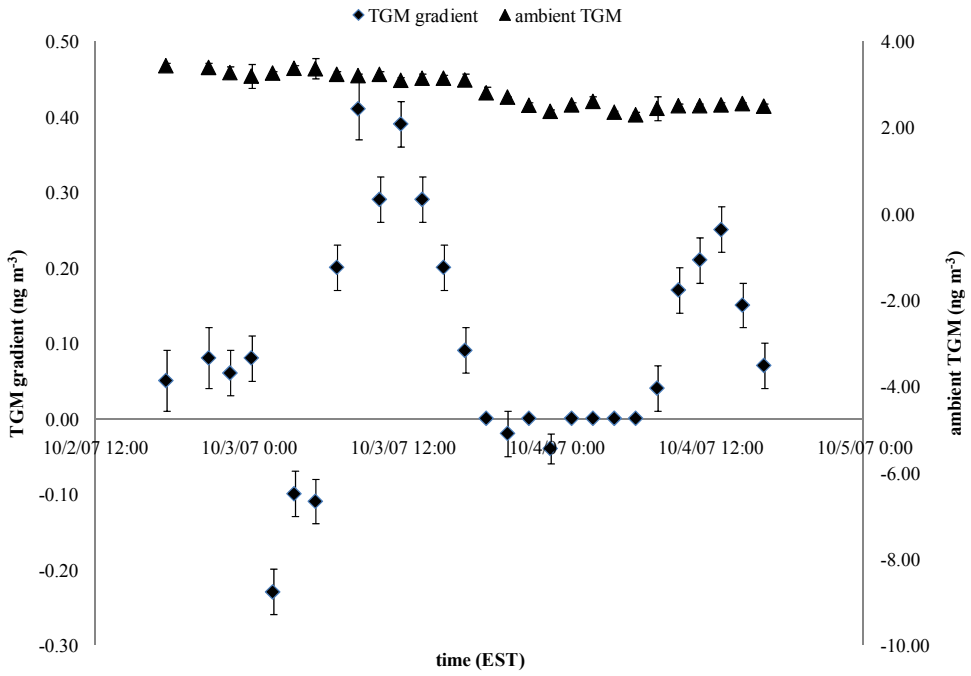

Figure 3.3 Diurnal trends in vertical TGM concentration gradient and ambient TGM observed 2-4 October 2007 in the Great Bay estuary, New Jersey. Error bars are ± 1 SD.

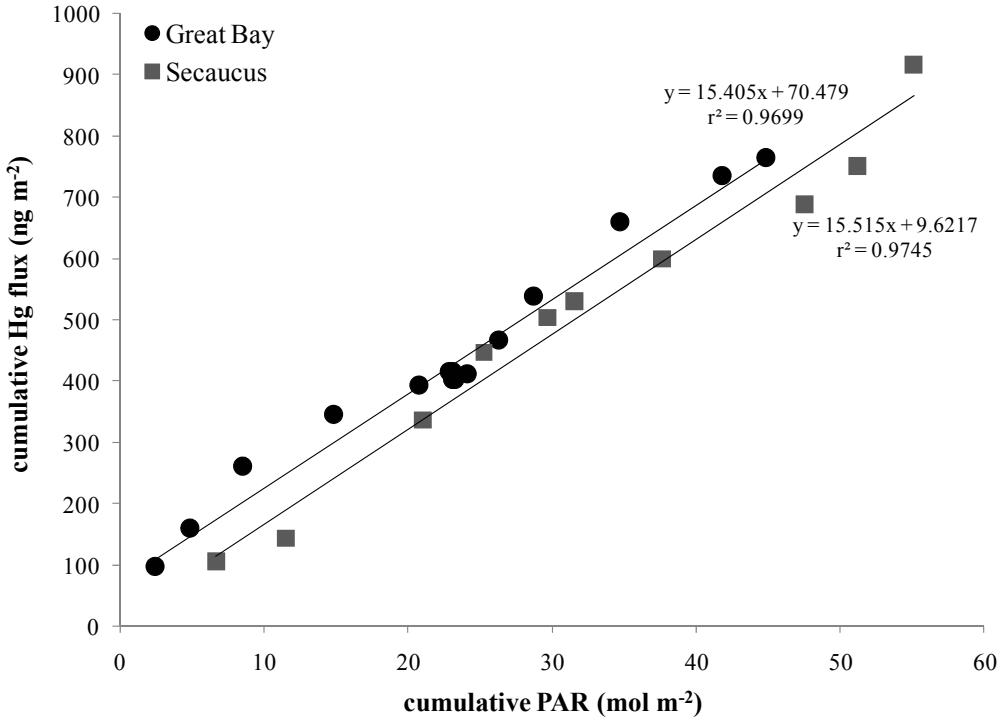

Figure 3.4 Correlation between cumulative Hg flux and cumulative solar radiation from 24 May 2006 10:45 through 25 May 2006 16:55 in the Secaucus High School Marsh ($n = 20$; $p < 0.01$) and from 3 October 2007 8:35 through 4 October 2007 17:35 in the Great Bay estuary to evaluate light effect without lag. ($n = 29$; $p < 0.01$).

Chapter 4

Gaseous mercury emissions from tidally-exposed wetland sediments: Dynamic flux chamber study

4.1. Introduction

The New York /New Jersey Harbor estuary and tributaries have received both point and non-point source mercury pollution from various pathways, since the time of the Industrial Revolution. While much research has been conducted to estimate the influx of mercury to the ecosystem from point source discharges and atmospheric deposition, little is known about the efflux of gaseous elemental mercury (Hg^0) back into the atmosphere from the various land surfaces of this region. Emissions of mercury to the atmosphere from specific industrial and municipal sources can be identified and potentially managed, but mercury emissions from contaminated ecosystems are widely dispersed and as a result, more challenging to quantify and control. Global mercury budgets indicate that 50% of deposited mercury is subsequently re-emitted to the atmosphere [Bergan et al. 1999; Mason & Sheu 2002], but at present only order-of-magnitude estimates of terrestrial emissions are available [Schroeder & Munthe 1998; Scholtz et al. 2003].

The global average natural emission rate of mercury from land surfaces has been estimated to be approximately 1 ng m^{-2} h^{-1} [Fitzgerald & Mason 1996], but field studies have shown that naturally enriched and anthropogenically contaminated soils and waters emit mercury vapor at much higher rates [Lindberg et al. 1979; Lindberg et al. 1995a; Lindberg et al. 1995b; Gustin et al. 1996; Carpi & Lindberg 1997; Carpi & Lindberg 1998; Gustin 1998; Gustin et al. 2000]. For example, measured Hg fluxes range from 8 to 45 ng m^{-2} h^{-1} for natural soils [Carpi & Lindberg 1998; Poissant & Casmir 1998; Engle et al. 2001] and from 10 to 1500 ng m^{-2} h^{-1} for contaminated soils [Lindberg et al. 1995b; Carpi & Lindberg 1997; Ferrara et al. 1998]. Since land-air mercury volatilization is

dependent upon the reduction of Hg^{2+} to Hg^0 [Kim & Lindberg 1995; Carpi & Lindberg 1997], reducing environments such as highly productive wetlands [Holmes & Lean 2006] are likely to support the most elevated Hg^0 emissions [Bothner et al. 1980; Gobeil & Cossa 1993]. In fact, with few exceptions [Lee et al. 2000], relatively high evasive fluxes of Hg have been measured in natural wetland ecosystems (30-3000 ng m^{-2} h^{-1}; Kozuchowski & Johnson 1978; Leonard et al. 1998b; Lindberg et al. 2002).

The volatilization of Hg^0 from naturally enriched or industrially contaminated soils and sediments is an important pathway in the redistribution of mercury on watershed to global scales (Fig. 4.1). The quantification of mercury emissions from wetlands and determination of the factors that affect these emissions is necessary to better estimate mechanisms important to the volatilization of mercury and provide a more robust understanding of the mercury cycle. In addition, this redistribution of mercury pollution may increase the exposure of aquatic ecosystems to reactive Hg which can be methylated [Compeau & Bartha 1985; Gilmour et al. 1992], and biomagnified in aquatic as well as terrestrial food chains [Mason et al. 1996; Burger & Gochfeld 1997; Watras et al. 1998; Gnamus et al. 2000], potentially acting as a neurotoxicant in birds and mammals [Clarkson 2002]. Therefore, it is imperative to the health of the Estuary and its inhabitants that direct sediment-air mercury fluxes are better understood in an attempt to more accurately predict effects to the local ecology and perhaps even humans.

The primary objective of this study was to measure total gaseous mercury (TGM) fluxes from a range of urban sediments in the laboratory using a dynamic flux chamber (DFC) for comparison with in situ micrometeorological fluxes. Fluxes were measured from sediments of the estuarine non-point source mercury-impacted New Jersey

Meadowlands, the non-point source impacted freshwater wetland, Tivoli South Bay in New York, and several point- and non-point source affected tributaries to the New York/ New Jersey Harbor. We estimated total gaseous mercury emissions from point and non-point source impacted wetland sediments directly to the atmosphere with the hypothesis that mercury volatilization from tidally-exposed wetland sediments within the New York /New Jersey Harbor estuary and especially the highly contaminated New Jersey Meadowlands will be enhanced over background concentrations.

A recent study identified solar radiation intensity as the single most significant meteorological parameter enhancing Hg flux from soils [Feng et al. 2005]. The effects of photochemistry on Hg volatilization from these sediments were evaluated and wetland physical-chemical properties were compared among samples. This is the first known study of mercury volatilization from tidally-exposed wetland sediments in the highly contaminated NY /NJ Harbor estuary and will provide data relevant to the mercury budgets of other coastal environments.

4.2. Sources of sediments

4.2.1. *Salt marsh wetland sediments: New Jersey Meadowlands*

Located in the heart of industrialized northeastern New Jersey, the New Jersey Meadowlands is a network of over 30 km^2 of brackish tidal marshlands in the New York/ New Jersey Harbor estuary system. The Meadowlands are an ideal site for the study of Hg volatilization from wetland sediments and vegetation in that these marshlands include the highly mercury-contaminated Berry's Creek estuary and large areas of non-point source (i.e. run-off, atmospheric deposition) impacted urban wetlands.

A tidal tributary of the Hackensack River, Berry's Creek (BCI: 40.82°N, 74.09°W; BCII: 40.81°N, 74.09°W; Table 4.1, Fig. 4.2) in the New Jersey Meadowlands (Borough of Wood-Ridge, Bergen County) has some of the most heavily mercury-contaminated sediments in the world [NJ DEP 2001]. Historic pollution from the industrial activities within the drainage area of Berry's Creek estuary has resulted in major inputs of Hg to this ecosystem and elevated concentrations of Hg in aquatic organisms [Weis et al. 1986; Konsevick 1988] and sediments [Galluzzi & Sabounjian 1980]. The estuarine section of Berry's Creek extends for 5 km downstream from a tide gate, which separates the estuarine from freshwater portions, and exhibits a decreasing downstream gradient in total and monomethylmercury (MeHg) in surface waters and sediments [Cardona-Marek et al. 2007]. Berry's Creek estuary is located downstream from the Ventron/Velsicol Superfund site, a former mercury processing plant, where as much as 289 tons of Hg was buried between 1930 and 1974 [Lipsky et al. 1980]. As a result, both freshwater and estuarine portions of Berry's Creek and other downstream ecosystems have received widespread Hg contamination.

Recent studies of Hg in Berry's Creek have addressed accumulation in sediments [Barrett et al. 2003] and macrophytes [Windham et al. 2001; Weis et al. 2003], speciation and transformations of inorganic and methylmercury in the water column [Schaefer et al. 2004; Cardona-Marek et al. 2007], and the effects of mercury on animal behavior [Weis et al. 1986; Weis et al. 2003], but none have quantified gaseous Hg emissions from tidally-exposed wetlands directly to the atmosphere within Berry's Creek or Berry's Canal.

Average sedimentation rates in the NJ Meadowlands region over the past 40 years are reported between 0.33 and 0.45 cm y^{-1} based on ^{137}Cs dating [Weis et al. 2005]. This suggests a sediment accumulation of 13 to 18 cm during that time. Although Hg is retained below fresh sediment, the gross concentrations of Hg in this region have the potential for re-introduction into the water column and the atmosphere via resuspension and bioturbation.

Sediment was also collected from the Secaucus High School Marsh in Secaucus, Hudson County, NJ (SC; Table 4.1, Fig. 4.2). This small (0.15 km^2), tidally-restricted estuarine wetland at 40.80°N and 74.05°W has also accumulated a range of contaminants, including mercury. Sediment from this site was collected and analyzed in the dynamic flux chamber in order to compare with in situ results from our micrometeorological study by way of eddy correlation.

4.2.2. *Freshwater wetland sediments: Tivoli South Bay, Dutchess County, New York*

Tivoli South Bay (TSB; Table 4.1; Fig. 4.2) extends (N-S) for about a mile between the villages of Tivoli and Barrytown, NY. TSB is a freshwater, tidal mudflat wetland located on the eastern shoreline of the Hudson River, approximately 160 km north of lower Manhattan. Tivoli South Bay is a small, shallow inlet (1.1 km^2) with exposed mudflats at low tide, fed by the Saw Kill (watershed area of 57 km^2). A freight and passenger railway right-of-way, constructed in 1851, separates the bay from the river with an embankment approximately 30 to 60 m wide and 3 m above mean sea level. Tidal exchange between the river and the bay is limited to three small bridge openings below the railway. Further, dense stands of water chestnut trees (*Trapa natans*) exist in

and around the bay. Spiny fruits of these trees can be found in bottom sediments. The physical characteristics of the bay allow it to store Hudson River sediments, with a sedimentation rate of 0.62 to 0.98 cm y^{-1} over the past 40 years [Benoit et al. 1999]. As a result, Tivoli South Bay has the potential to contain high concentrations of mercury from upstream point and non-point sources.

Point sources likely contributing to the mercury load in Tivoli South Bay include the Mercury Refining Company in Albany, NY (80 km upstream) which reclaimed mercury from batteries and had pools of mercury present on the property at the time it became a Superfund site in the early 1970s [Zelewski & Armstrong 1996]. In addition, the Hercules Paint Company in Glen Falls, NY (260 km upstream), also listed as a Superfund site, released mercury to the environment in the form of raw pigment for use in paints [Zelewski & Armstrong 1996]. Furthermore, non-point sources of mercury including agricultural chemicals and atmospheric deposition have contributed to the contamination of this freshwater wetland region [Zelewski et al. 2001]. Tivoli South Bay is therefore an ideal site to estimate mercury emissions from freshwater wetlands sediments for comparison with mercury emissions from the estuarine wetlands of the New Jersey Meadowlands. Samples were collected from northern (41.947°N, 73.943°W), central (41.945°N, 73.943°W), and southern (41.943°N, 73.943°W) regions within the bay as in a previous study of Hg at this site [Zelewski & Armstrong 1996].

4.2.3. *Non-wetland sediments*

When large areas of river banks are flooded, older sediments are resuspended, much like the process observed in tidal wetlands [Hintelmann & Wilken 1995].

Sediments from three rivers local to the NJ Meadowlands, the Hackensack, Raritan and Passaic Rivers (Table 4.1; Fig. 4.2) were also examined for mercury volatilization potential. All three rivers are tidal and feed into the New York/ New Jersey Harbor estuary before flowing to the Atlantic Ocean.

Beginning as a brook in southeastern New York (Rockland County), the Hackensack River (HK; 40.48°N, 74.09°W; Table 4.1, Fig. 4.2) flows for approximately 72 km, through a portion of the New Jersey Meadowlands, until its confluence with the Passaic River at Newark Bay (Hudson County, New Jersey). It is located due west of the lower Hudson River. The Hackensack has been impacted by operations at the former Diamond Shamrock Chemical plant, the Standard Chlorine Chemical Company, and the former Koppers Seaboard Coke and By-Products plant, in Kearny, Hudson County, NJ. Known contaminants include asbestos, benzene, cadmium, chromium, dioxins, lead, PCBs, and mercury, among others. The river has also received large amounts of non-point pollution from highway and agricultural runoff.

Upland soil was collected from a river bank along the Hackensack River (HKup; 40.48°N, 74.09°W; Table 4.1, Fig. 4.2) for a sediment-soil mercury flux comparison.

The 48 km long Raritan River (RR) becomes estuarine near its midpoint and flows to Raritan Bay. The Raritan River receives mercury from atmospheric deposition and historically, has been subject to direct contamination from a number of point sources to its tributaries (e.g. the Cornell/Dubilier Superfund site above Bound Brook) and the river itself (e.g. the Horseshoe Road Superfund site). As a result, a wide variety of chemicals can be found in the river bottom sediments. Samples were collected at 40.48°N, 74.38°W (RRI) and 40.49°N, 74.33°W (RRII) along the river's edge.

The Passaic River (PR; 40.74°N, 74.14°W) is 145 km long and meets the Hackensack River at the north end of Newark Bay. This river flows through some of the most urbanized regions of New Jersey. Currently, thirteen petroleum refineries and six chemical plants are operating on or around the river [Deason 2001]. Sediments in the final 10 km of the Passaic River leading to the mouth near Newark Bay contain considerable amounts of dioxin. The dioxins were largely produced at Diamond Shamrock Chemical Plant in Newark as a waste product during the production of Agent Orange for the Vietnam War. Additionally, unknown sources of pesticides, PCBs and metals, including mercury and lead, have accumulated in Passaic River sediments leading to a highly degraded condition of the river system.

4.3. Methods

4.3.1. *Sample collection*

Saturated sediment samples were collected between May 2005 and June 2007 using either an Ekman dredge over the side of a small fiberglass pontoon/fishing boat or a shovel alongside the wetland. Care was taken to minimally disrupt the ecosystem. Collected saturated sediments were stored, untreated, in sealed 5 gallon HDPE containers at 10ºC until flux chamber analysis or ancillary sediment chemistry was performed.

4.3.2. *Limitations of the dynamic flux chamber method for TGM flux estimation*

There are several limitations of the dynamic flux chamber method for estimating direct sediment-atmosphere mercury flux. Chamber design and low flushing rates are shown to be two major sources of potential error [Gao et al. 1997; Gustin et al. 1999;

Gillis & Miller 2000]. Many authors prefer to use Teflon for construction of the flux chamber but we used acrylic. Carpi & Lindberg [1998] used Teflon and obtained blanks similar to those in this study indicating acrylic may not have a blank problem. Low (laminar) flushing rates are thought to drastically underestimate TGM from DFC experiments [Zhang et al. 2002; Feng et al. 2005] since an artificial boundary layer may form, suppressing Hg emissions [Gustin et al. 1999] with molecular diffusion alone controlling emission. Lindberg et al. [2002] report that if a DFC is small enough, a low flow rate can be accommodated yet the dimensions of such a chamber were not discussed.

Since sediment samples are naturally wet, over time condensation would sometimes form on the interior walls of the chamber. The condensation may mimic dew and act as a Hg sink [Poissant & Casimir 1998], complicating flux estimates for some samples.

Analysis of sediment grab samples provides only a snapshot of Hg transformations in each watershed and is unable to describe dynamic processes. The complexity of the natural environment, including several environmental compartments combined with multiple variables in each, many existing in trace quantities, makes it difficult to differentiate the factors controlling Hg concentration in sediment and pinpoint the photochemical processes responsible for emissions.

Once the samples were collected, mercury in pore waters is reduced in a short period of time, escaping to the atmosphere [Canario & Vale 2004]. Mercury may have been lost during sample collection and handling. Consequently, our results may be underestimated.

While it is important to be aware of the limitations of the dynamic flux chamber, it remains the best available method for controlling a sample environment and is widely used within the scientific community.

4.3.3. *Flux chamber operation*

Dynamic flux chambers were first used as an in situ application by Schroeder et al. [1989] to measure Hg exchange at the soil/water interface. Since then, numerous studies have manipulated the design by Schroeder and colleagues to measure the flux of mercury at the air/water and soil/water interface [e.g. Xiao et al. 1991; Carpi & Lindberg 1998; Ferrara & Mazzolai 1998; Poissant & Casimir 1998; Rasmussen et al. 1998; Gustin et al. 1999; Edwards et al. 2002; Feng et al. 2002; Feng et al. 2004] but few have investigated mercury at the sediment/air interface.

In order to establish a controlled environment, enabling the manipulation of photochemistry and temperature, a sediment flux chamber was developed (Fig. 4.3) in our laboratory. The chamber was constructed of transparent acrylic and included a 100 cm long, 10 cm wide, and 5 cm deep sediment drawer (5 L sediment volume; 0.1 m^2 sediment surface area) that fit into a 120 cm long sealed chamber including 10 cm flow establishment sections at both ends and 1 cm headspace above the sediment surface. Two 30 cm x 10 cm x 5 cm inserts were placed at either end of the drawer to focus UV light over the sediment. These inserts allowed a 2 L sediment volume and a 0.04 m^2 sediment surface area. An additional insert was constructed to limit sediment depth to 1 cm in order to investigate the relative contribution of surface photochemistry to gaseous mercury volatilization. Dimensions of this insert were 100 cm long, 10 cm wide, and 4

cm deep, providing a sediment volume of 1 L and a sediment surface area matching the initial, full chamber experiments of 0.1 m^2. With a cross-sectional area of 10 cm^2 for the headspace above the sediment and an air velocity of $\leq$ 2.5 cm s^{-1}, the chamber accommodates laminar air flow with an estimated Reynolds number of 17 using the Tekran and an air velocity of $\leq$ 0.8 cm s^{-1} with an estimated Reynolds number of 5.1 using the gold traps. Note: TGM was collected on gold traps and analyzed on a Tekran model 2500 detector when the Tekran model 2537A automated analyzer was sent to the manufacturer for repairs.

Mercury in laboratory air ranged from 3.3 to 4.7 ng m^{-3}. Chamber blanks were determined by passing mercury-free air through the air-tight, acid-cleaned, Q-H_2O rinsed chamber. Blank measurements were estimated in the dark to avoid light effects. During initial tests of the sealed flux chamber without sediment, mercury concentrations in the chamber were below detection demonstrating that no mercury leaked into the chamber from the laboratory under normal operating conditions. Over time, small amounts of mercury adsorbed to the chamber walls yet blanks remained low (0.1 - 0.5 ng m^{-3}), consistent with blanks obtained in the Carpi and Lindberg [1998] and Gillis and Miller [2000] studies. The detection limit, calculated as three times the standard deviation of the blank, was 0.4 ng m^{-3} Hg for Tekran 2537A results and 0.3 ng m^{-3} for individual gold trap results.

Prior to first use and between analyses, the chamber drawer and inserts were cleaned. First, sediment (if present) was disposed. Next, the drawer was rinsed with deionized water to remove any remaining sediment. This rinse was followed with a 50% reagent grade hydrochloric acid rinse and finally a thorough Q-H_2O rinse. Once dried

with clean Chem-wipes, new weather stripping was applied to the drawer to create a tight seal with the chamber. Fresh saturated sediment was then re-loaded and sealed inside the air-tight chamber and allowed to equilibrate with room temperature overnight.

Sediment flux experiments were carried out over 2 to 3 h (gold trap) or 2 to 72 h (Tekran 2537A) by monitoring the concentration of gaseous mercury in air leaving the sediment-filled flux chamber under laminar flow conditions. Once sealed sediment had reached room temperature, the chamber headspace was flushed with mercury-free inflow air supplied by a Tekran Model 1100 zero air generator (Toronto, Canada). All of the exit air was carried through a ¼ in Teflon tube then either drawn directly into a Tekran 2537A continuous gaseous mercury analyzer or through a gold-coated glass bead trap. With the Tekran 2537A, total Hg was carried to the detector with UHP grade Argon and was measured at five minute intervals at a sampling rate of 1.5 L min^{-1} by cold vapor atomic fluorescence spectrometry (CVAFS) following thermal desorption of dual gold traps [Schroeder et al. 1995]. With the individual Hg traps, zero air was pulled through the sediment flux chamber with the assistance of a peristaltic pump (Masterflex Model 77201-62), located after the traps to prevent contamination. The gold trap was then analyzed within 24 h on a Tekran 2500 CVAFS elemental mercury detector (Toronto, Canada), also with UHP grade Argon as the carrier gas. During gold trap experiments, total Hg was measured at an average sampling rate of 0.45 L min^{-1}. This corresponds to an air sample volume of 81 L as compared with 7.5 L using the Tekran 2537A. Clearly, time-resolution was not as robust as in the set of results from the Tekran 2537A, but this was necessary in order to collect a detectable sample. In general, gold trap results were in agreement with Tekran 2537A results.

4.3.4. *Photochemistry*

Various light treatments were employed to assess the relative importance of visible and ultraviolet light (UV-A and UV-B) on total gaseous mercury volatilization from sediments.

Dark experiments were conducted to measure the baseline mercury emission from sediments without the influence of photochemistry. Dark results also represent a steady, nighttime atmosphere for comparison with in situ experiments.

For the investigation of visible + UV, visible + UV-A, and visible light effects on elemental mercury volatilization from sediments, two 40 W fluorescent bulbs were utilized providing 80 μmol m^{-2} s^{-1} visible light and 0.8 μmol m^{-2} s^{-1} UV-A (~370-400 nm) with trace amounts of UV-B to sediment loaded in the chamber. Mylar filters were used to block UV-B from the fluorescent bulbs to the sediment [Amyot et al. 1997a; Amyot et al. 1997b; Gillis & Miller 2000; Bonzongo & Donkor 2003] and Lee 226 filters were used to block both UV-A and UV-B [Lalonde et al. 2003].

The effects of UV-A and UV-B light on Hg volatilization were examined independently using a UVP model UVLM-28 ultraviolet lamp (Upland, CA). This lamp provided light at the UV-A wavelength of 365 nm with an intensity of approximately 1.5 μmol m^{-2} s^{-1} at 34 cm and at the UV-B wavelength of 302 nm with an intensity of approximately 1.2 μmol m^{-2} s^{-1} at 34 cm. Intensities were calculated based on manufacturer-provided intensities at 7.6 cm and the Inverse-Square Law. Since the UV lamp was nearly one third the length of the fluorescent light source, a set of chamber inserts were used at either end of the drawer to constrain sediments to match the UV

lamp length. As a result, only about 2 L of homogenized sediment was used during these experiments.

4.3.5. *Flux calculations*

Five-minute to three-hour sediment-air gaseous mercury concentrations (ng m^{-3}) were converted to mercury fluxes (ng m^{-2} h^{-1}) using the following equation [Xiao et al. 1991; Poissant & Casimir 1998]:

$$Flux_{Hg} = \frac{Hg \times Q}{SA} \quad (1)$$

where Hg is the TGM concentration (ng m^{-3}), Q is the flow rate of zero air (Tekran 2537A: 0.09 m^3 h^{-1}; gold trap: 0.027 m^3 h^{-1}), and SA is the surface area of the exposed sediment (5 cm and 1 cm depth chamber: 0.1 m^2, acrylic inserts for UV experiments: 0.04 m^2). Note: fluxes were measured at the chamber drawer depth of 5 cm and at a 1 cm sediment layer with the use of an acrylic drawer insert in order to estimate the relative contribution of the upper 1 cm of sediment to the observed fluxes.

4.3.6. *Sediment mercury concentrations*

Total mercury was determined for each of the sediment samples as per EPA Method 1631. Sediment (100 mg) was added to each acid-cleaned Savillex 22 mL PFA jar with 4 mL of aqua regia (3 mL Optima grade HCl; 1 mL Optima grade HNO_3) and allowed to digest overnight. Acid-cleaned 15 mL centrifuge tubes were calibrated to 10

mL with Q-H_2O and weighed. Centrifuge tubes were then emptied and dried in a clean Class 100 hood prior to being capped.

The following day, digested samples were transferred from jars to 15 mL centrifuge tubes. Bromine monochloride (BrCl; 100 µL; 0.3M) was added to each vial to oxidize Hg and volumes were brought up to 10 mL with Q-H_2O. Hydroxylamine hydrochloride (100 µL; 2M) was added to each sample 30 min prior to analysis to reduce excess BrCl in solution. Two 250 mL Pyrex (Corning Inc., Corning, NY) glass gas washing bottles with fritted discs (bubblers) were filled approximately halfway with Q-H_2O and, based on expected concentrations from previous studies, 10 -1000 µL of sample plus 0.5 mL 0.5M stannous chloride ($SnCl_2$) was added to each bubbler to reduce mercury to its elemental form (Hg^0). Samples were bubbled for 15 min onto gold-coated sand traps which were subsequently placed in line with a Tekran model 2500 (Toronto, Canada) cold vapor atomic fluorescence spectrophotometer (CVAFS) mercury detector [Fitzgerald & Gill 1979; Bloom & Crecelius 1983].

Bubbler blanks and reagent blanks were run for quality control purposes. A gas injection calibration curve was performed and compared with liquid standard spikes to determine recovery. Average recoveries were 100% ± 10%.

4.3.7. *Additional sediment characteristics*

Ambient air temperatures were recorded adjacent to the dynamic flux chamber during each experiment. Note: air temperature may not represent the effects of sediment temperature.

Sediments were centrifuged to collect pore water which was subsequently filtered (Whatman Puradisc 25 AS 0.2 μm polyethersulfone filter) for each sample. Pore water was used to determine salinity by way of a portable salinity refractometer (Vista Series Instruments Model A366ATC). A few drops of sediment pore water were placed on the refractometer prism, the cover plate closed, and refractometer held to the light. A real-time salinity reading was provided. The prism and cover plate were cleaned with Q-H_2O between samples to prevent contamination.

Since the binding capability of the sediment surface may be pH sensitive [Gonzalez & San Roman 2005], pH was determined for each pore water sample. An Orion Model 720 pH meter (Orion Research Inc., Boston, MA) was calibrated using a three-point curve. After calibration, the pH probe was then placed into each of the sediment pore water solutions, cleaning with Q-H_2O between samples. Results were provided in mV, which was converted to pH by way of the calibration curve.

Organic matter (OM) is considered one of the most important components for complexing a major percentage of inorganic Hg(II) in sediments [Lindberg & Harriss 1974; Mantoura et al. 1978; Meili 1997; Mason & Lawrence, 1999], especially in wetlands [Weber 1988]. As a result, percent organic matter (dry) and percent water content (pore water) were estimated via a standard loss on ignition (LOI) method [Schumacher 2002]. Approximately 3 g of wet sediment was placed on a pre-weighed aluminum weigh boat and weighed in triplicate. Samples were then placed in a drying oven at 105°C for 24 h and placed in a 35% humidity room to cool prior to weighing each sample in triplicate using an analytical balance. Samples were finally placed in a

muffle furnace at 550°C for 24 h and returned to the 35% humidity room to cool prior to re-weighing each sample in triplicate. Percent OM (dry) was determined by:

$$\%OM = \frac{W_d}{W_{od} - W_{wb}} \times 100 \quad (2)$$

where W_d is dry sample weight (g), W_{od} is oven dry weight (g), and W_{wb} is the average weigh boat weight (g). Soil moisture has been shown to promote TGM emission from soils [Bahlmann et al. 2004]. Percent water content was calculated as:

$$\%WC = \frac{W_w}{M_w} \times 100 \quad (3)$$

where W_w is water weight (g) and M_w is wet sample mass (g).

Another wetland constituent considered important in binding Hg^{2+}, making it less available for methylation and volatilization, is sulfide [Lindberg & Harriss 1974]. Cationic mercury in anoxic, sulfidic sediments has a strong affinity to sulfur [Drobner et al. 1990; Boszke et al. 2003] and is therefore associated with sulfur in sediments, either forming insoluble Hg sulfides [Drobner et al. 1990; Morse & Luther 1999] or being incorporated into iron sulfides including pyrite [Morse 1994], essentially unavailable for biological or photochemical oxidation. Acid-volatile sulfide (AVS) content was determined for each sample according to an amended method from Simpson [2001]. Approximately 0.05 g of dry weight sediment (0.08 to 0.19 g wet weight) was added to acid-cleaned 50 mL centrifuge tubes under anoxic conditions (UHP Nitrogen, glove bag)

using clean techniques. While in the anoxic glove bag, 50 mL of deoxygenated (bubbled with UHP Nitrogen for 1 h) Q-H_2O was then added to each tube followed by 5 mL of methylene blue reagent (MBR). The tubes were then capped and inverted 5 times to homogenize. After 5 min, each sample was centrifuged (2 min, 2500 rpm) and allowed to settle 90 min for color development. Sulfide standard solutions (3 mL) ranging in concentration from 0 to 0.10 M sodium bisulfide (NaHS) were prepared, and 60 uL MBR was added to each. After capping and inverting, standards were also centrifuged (2 min, 2500 rpm) and allowed to settle 90 min for color development. Blanks, standards and samples were subsequently analyzed on a Beckman DU-520 UV/visible spectrophotometer at 670 nm.

It has been suggested that particle size distribution (PSD) may play a role in mercury sediment chemistry as smaller, clay particles may bind charged mercury particles. PSD was determined on a Beckman Coulter LS 230 (Coulter Corp., Miami, FL) laser diffractometer. This high resolution instrument features a wide dynamic range (0.04 μm to 2000 μm), with 132 detectors, an auto aligned optical system and a precision of less than 1%. For laser diffraction, approximately 5 g of sediment was added to 5 mL of 10% (w/v) sodium hexametaphosphate $(NaPO_3)_6$ to disperse the sediment. The slurry was subsequently placed in a sonicator for 30 min to further speed dissolution. Two to three drops of the resulting solution were added per analysis to the laser diffractometer until obscuration reached 8 to 12%, with $(NaPO_3)_6$ as the eluent. While this is a good method for separating out size particles for quantification purposes, it may also disperse aggregates which may be efficient at binding mercury in sediment.

4.3.8. *Statistical analyses*

Regression analyses were performed to determine coefficients of determination r^2 and significance p for correlations at 95% confidence intervals. Means are reported ± SE.

4.4. Results

4.4.1. *Estimated total gaseous mercury sediment-air fluxes*

In the dark, TGM fluxes in the sediment-filled chamber ranged from 0.05 ng m^{-2} h^{-1} in "cleaner" TSBs sediments to 2.0 ng m^{-2} h^{-1} in heavily mercury-contaminated, Berry's Creek II sediments (Tekran 2537A; Tables 4.2 – 4.12). Data from individual Hg traps also shows that little Hg is released from sediments in the dark (0.5 – 0.6 ng m^{-2} h^{-1}; Tables 4.2 – 4.12). A clear photochemical trend was observed in all sediments (Fig. 4.4). In the light, Hg flux from sediments was found to be up to 50 times higher than in the dark. Results indicate that visible + UV provided the highest Hg emission rate from exposed sediments, followed by visible + UV-A, visible alone, UV-A alone, UV-B alone and finally dark (Tables 4.2 – 4.12). In fact, experimental results have shown that UV light, in conjunction with visible light, significantly ($p < 0.01$, one-tailed t-test for unequal variances) enhanced the volatilization of Hg from mudflat sediments over dark experiments, with a greater effect from UV-A than UV-B. This is evident as the visible + UV-A treatment (mylar filter), reduced Hg emissions from sediments by up to 30% (Fig. 4.5), similar to Bonzongo and Donkor [2003] where UV-B alone accounted for 33% of gaseous mercury production in an arctic wetland. Visible alone (Lee 226 filter) reduced Hg emissions by up to 80% (Fig. 4.6). However, for two instances in SC (Tekran 2537A) and two in PR (gold traps) the absence of UV-B radiation enhanced TGM inside the

chamber. In one case in SC (Tekran 2537A), UB-V radiation appeared to play no role in mercury volatilization.

Ultraviolet light alone was not the primary driver of mercury photoreduction as individual UV-A and UV-B experiments produced low Hg volatilization fluxes. Since different UV wavelengths were produced by each of the lamps, data from the fluorescent and UV lamps may not be directly comparable.

The top 1 cm of sediment was responsible for 73 to 91% of observed mercury volatilization fluxes as compared to the full chamber drawer (5 cm depth; Fig. 4.7).

Berry's Creek sediments consistently released considerable amounts of elemental mercury to the chamber air with peak concentrations (30 ng m^{-2} h^{-1}) witnessed downstream, furthest from the source (Table 4.11). The Raritan River was also a larger atmospheric source of mercury downstream nearest Newark Bay than in the upstream samples (Tables 4.5 & 4.8). Tivoli South Bay northern and southern samples volatilized nearly 4 times more mercury than the central samples with peak fluxes: 9.3 ng m^{-2} h^{-1}, 8.7 ng m^{-2} h^{-1}, and 2.1 ng m^{-2} h^{-1}, respectively (visible + UV; Tekran 2537A; Tables 4.2 - 4.4). The Passaic, Raritan and Hackensack Rivers and the Secaucus High School Marsh were all moderate sources of Hg^0 to the atmosphere (visible + UV: 1 – 14 ng m^{-2} h^{-1}; Tables 4.5, 4.7, 4.8, 4.9, & 4.10). Upland soils from the Hackensack River watershed area yielded moderate to high mercury concentrations (visible + UV: 9 – 26 ng m^{-2} h^{-1}), with peak flux estimates on the order of those from the most contaminated sediments in Berry's Creek.

4.4.2. *Mercury concentration in sediments*

Total Hg concentrations in estuarine and freshwater sediments ranged from 0.05 ppm (TSBs) to 51 ppm (BCI; Table 4.13), similar to other measurements in BC (59 ppm, Weis et al. 2005). There exists a slight increasing gradient in total Hg from south to north in Tivoli South Bay with TSBc and TSBn having 0.09 ppm and 0.25 ppm, respectively. Zelewski et al. [2001] reported sediment Hg content in TSB between 0.19 and 1.04 ppm, which is approximately 4 times greater than our estimates. This may indicate that newer, cleaner sediment is collecting at the sediment surface, burying historic Hg contamination. BCII was also quite enriched in Hg at 20 ppm, followed by SC (7 ppm). RR, HKup and HK have Hg contents near that of TSBn, while PR has Hg concentrations in sediment measured at 1 ppm. In comparison to other New York/ New Jersey Harbor sediments (1.3 to 2.6 ppm; Goodrow et al. 2005), Berry's Creek sediments are enriched in mercury.

4.4.3. *Additional sediment characteristics*

Temperatures ranged from 10 to 26°C during experiments (Tables 4.2 to 4.12). The 10 to 17°C range simulated nighttime temperatures while experiments between 18 to 26°C simulated daytime temperatures. The effect of temperature appeared to have an inverse relationship with sediment TGM flux, whereby colder temperatures enhanced mercury volatilization.

Pore water salinity was between 2 (TSB) and 27‰ (RRII; Table 4.13) and clearly illustrated an order of increasing estuarine influence on each of the waterways but was not correlated with mercury volatilization fluxes from sediments ($r^2 = 0.01$, $p = 0.02$).

The salinity reading for BCI and BCII was only 4‰ indicative of the upstream locations for sample collection. This falls within the typical salinity range of 0-4‰ for BC according to Cardona-Marek et al. [2007].

Sediment pore water pH was within the expected pH range of natural waters, for all but RR pore water, from 6.4 (TSBc) to 6.8 (BC; Table 4.13). RR sediment pore water had an acid pH of 5.0 to 5.7. Currently, there exists no explanation for the acidity of the Raritan River in the literature. At low pH, heavy metals are usually released from bottom sediments [Boszke et al. 2003]. We found no pH effect on mercury volatilization in this study ($r^2 = 0.07$, $p > 0.05$) as has been observed elsewhere [Bonzongo & Donkor 2003].

Sediment water content ranged from 50 (RR) – 78% (SC; Table 4.13). Interestingly, TSBc and TSBs, within 1 mile from TSBn, had water contents of 61 and 60%, respectively, while TSBn was 71%. Sediment water content was not correlated with TGM flux ($r^2 = 0.05$, $p = 0.10$).

The differences in TSB are also observed in % OM_{dry} whereby the highest was found again in TSBn at 23% (Table 4.13; Fig. 4.8). Sediment %OM_{dry} ranged from 8.0 in HK to 39 in SC and was significantly negatively correlated with Hg flux from sediments ($r^2 = 0.59$, $p < 0.01$).

Particle size distribution (PSD) analysis indicated that most sediment samples were 84-89% silt (2 - 50 μm), except for PR, which was 98% (Table 4.14). TSB and PR had low clay contents (0-2%), SC, HKup, and BCII had moderate clay contents (4-8%), and HK, BCI, RRII, and RRI had high clay contents (11-16%). There exists no correlation between the clay particle size fraction and mercury volatilization flux ($r^2 = 0.04$, $p = 0.03$).

Acid volatile sulfide content ranged from 0.89 μmol g^{-1} dry (TSBn) to 20 μmol g^{-1} dry (BCI; Table 4.13). Light-driven mercury volatilization rates had a significant strong negative correlation ($r^2 = 0.81$, $p < 0.01$) with sediment acid-volatile sulfide concentration (Fig. 4.9). A multiple linear regression of AVS and %OM against Hg flux indicates that the relationship with AVS was significant at the 95% confidence level ($p = 0.02$), while that with %OM was not ($p = 0.16$; Fig. 4.10). This suggests that the variability in the fluxes can be predominantly explained by AVS content of sediments. The significant correlation between %OM and Hg flux observed above is likely due to a weak correlation between %OM and AVS.

4.5. Discussion

4.5.1. *Factors affecting mercury volatilization from wetland sediments*

Photochemistry had the most pronounced effect on Hg emission from exposed sediments, with visible + UV treatments frequently causing the most enhanced volatilization of Hg^0 in the flux chamber (Tables 4.2 – 4.12). UV light was important for the volatilization of mercury from mudflat sediments with UV-A generally driving greater Hg^0 fluxes than UV-B. However, UV light alone was not effective in Hg efflux from sediments. Indeed, Zhang et al. [2001] demonstrated that UV light was important but not solely responsible for influencing light-enhanced emissions with a reduction of UV light.

Since virtually no Hg volatilized from sediments in the dark, heterotrophic bacteria were not major drivers of Hg^0 from sediments. Furthermore, the observed immediate change in Hg emission, following a change in light treatment suggests that

photoautotrophic bacteria are not important in reducing Hg in sediments as a lag would be expected.

In Tekran 2537A experiments, dark concentrations of Hg remained relatively constant over time, while in the light, concentrations seemed to peak and then steadily decline as is clearly illustrated in the Hackensack River (Table 4.7). This trend was also witnessed in the Tagus estuary, Portugal [Canario & Vale 2004]. Costa and Liss [1999] suggest that reaction rates are faster at the beginning of experiments and gradually slow as they progress.

For the two instances in SC (Tekran 2537A) and two in PR (gold traps) where the absence of UV-B radiation enhanced TGM inside the chamber, we suggest that UV-B may have oxidized, rather than reduced, available mercury thus rendering it unable to volatilize. This could be a result of diverse surface chemistry amongst the sediments and/or heterogeneous photochemical processes.

Temperature appears to have an inverse relationship with TGM flux, although it is difficult to determine temperature effects as temperature does not change as instantaneously as some of the changes in mercury concentrations that were measured. This observation is in contrast to previous studies that witnessed a positive correlation between the two parameters [Carpi & Lindberg, 1997; Canario & Vale 2004]. For example, TGM fluxes in TSBs and RRII were 8.7 and 14 ng $m^{-2} h^{-1}$ at approximately 10°C and only 1.1 and 1.4 ng $m^{-2} h^{-1}$ at around 20°C, respectively (Tables 4.2 & 4.8). In the Passaic River, temperature had no effect (Table 4.9). Poissant and Casimir [1998] reported that water-air transfer of Hg was significantly enhanced when the water temperature was higher than that of the air. We suggest the fluorescent lamp warmed the

chamber air slightly enough to cause a gradient between the sediment surface and overlying chamber air.

Acid volatile sulfide also appears to have an inverse relationship with mercury flux from sediments. Since more mercury will be bound as mercuric sulfide at elevated AVS concentrations and light-driven mercury volatilization decreased with higher AVS, it is unlikely that the photoreactive form of mercury in these sediments is inorganic mercuric sulfide. Comparing the two Berry's Creek sediments and the two Raritan River sediments within each estuary, the sediment sample of each pair with the highest concentration of acid volatile sulfide (AVS) had the highest mercury concentration, but lower absolute light-driven mercury volatilization rates (Tables 4.5, 4.8, and 4.11 to 4.13; Fig. 4.9). Thus, increased sulfide lowered the light driven-volatilization flux of mercury in these estuaries.

Surprisingly, sediment total mercury concentrations did not appear to be an important factor in controlling Hg volatilization from sediments in the dynamic flux chamber ($r^2 = 0.13$, $p > 0.05$). This is in stark contrast with our in situ experiments. Although samples were stored at low temperatures to preserve Hg speciation and limit mercury volatilization into containers and the surrounding air, it is possible that loss did occur over time. Additionally, sediments may not have been fully homogenized, resulting in varying degrees of mercury emission from each sediment analysis. Gustin et al. [1998] suggest a stronger correlation between Hg flux and substrate Hg concentration in the dark and far weaker in the light ($r^2 = 0.997$ as compared with $r^2 = 0.41$).

We compared organic matter content with laboratory mercury volatilization fluxes, normalized to the mercury content for each sediment sample. Excluding the high

organic matter Tivoli South Bay north and Secaucus High School Marsh samples, light-driven mercury volatilization rates were weakly significantly negatively correlated with sediment organic matter (Fig. 4.8), indicating that organic matter may play an important role in limiting light-driven mercury volatilization from sediments. Indeed, RRII with 10% OM and 0.66 ppm THg volatilized a similar amount of mercury as SC with 7.1 ppm THg and 39% OM. While OM may bind Hg(II), it can also absorb light and reduce Hg to the volatile, elemental form [Weber 1993; Costa & Liss 2000; Liu et al. 2000; Ravichandran 2004]. Therefore, the affects of organic matter on mercury volatilization may counteract one another.

With the same THg and AVS contents, it is difficult to explain why the Hackensack River upland soil sample would volatilize considerably more TGM than Hackensack River sediment. One explanation could be percent water content. The sediment sample was twice as wet as the soil sample yet volatilized only half as much mercury. In addition, the soil sample had slightly higher organic matter content. While the effects of OM are unclear, the potential exists for photoreduction of Hg as a result of binding to OM.

It has been suggested that the clay size fraction (< 2 μm) may have the ability to bind Hg, rendering it unavailable for evasion [Hintelmann & Wilken, 1995]. Further, clay particles are often coated with iron hydroxides, which may also bind inorganic Hg [Hintelmann & Wilken, 1995]. However, RRII sediments with 14% (high) clay content released considerable Hg in our experiments (Tables 4.8 & 4.13). HK and BC sediments also released variable amounts of Hg and had high clay contents at 11 and 8%, respectively. TSB sediments contain 0-1% clay, indicating that reduced Hg should

readily volatilize and in some analyses this was observed. The connection between this physical characteristic and total Hg release remains unclear.

Total gaseous mercury volatilization was not dependent upon pore water salinity or pore water pH of sediments.

4.5.2. *Estimation of local in situ mercury fluxes and potential impacts on the global Hg cycle*

Order of magnitude estimates were calculated for the expected range of in situ fluxes using the modified Thornthwaite-Holtzman equation [Majewski et al. 1993; Korfiatis et al. 2003; Goodrow et al. 2005].

$$F_{Hg} = \frac{u_* \kappa \left(Hg_1 - Hg_2 \right)}{\ln\left(z_2 / z_1 \right) \phi_W} \qquad (4)$$

Measured near surface gaseous Hg concentrations was taken as the lower Hg concentration, Hg_1, and zero was taken as the upper Hg concentration, Hg_2, since mercury-free zero air was used as the carrier gas above the sediment. As a conservative estimate of in situ Hg fluxes, we used the lowest value for friction velocities measured during in situ experiments ($\mu^* = 0.20$ m s^{-1}; typical $\mu^* = 0.10$ m s^{-1}; Tables 4.2 – 4.12; Edwards et al. 2005) and assumed a neutral atmosphere ($\phi = 1$). A 3 m vertical gradient was selected to compare with in situ gradients. Preliminary estimations of in situ sediment-air Hg fluxes (visible + UV light) from chamber experiments are 40 to 520 ng m^{-2} h^{-1} (mean = 250 ng m^{-2} h^{-1}) for "uncontaminated" sediments (TSBs, TSBc), 270 to

980 ng m^{-2} h^{-1} (mean = 400 ng m^{-2} h^{-1}) for slightly contaminated sediments (TSBn, RRI, HK), 150 to 880 ng m^{-2} h^{-1} (mean = 380 ng m^{-2} h^{-1}) for contaminated sediments (RRII, PR, SC), and 300 to 1700 ng m^{-2} h^{-1} (mean = 750 ng m^{-2} h^{-1}) for highly contaminated sediments (BCII, BCI). These are minimum flux estimates because the average in situ irradiance is higher than that used in the laboratory flux chamber and the atmospheric stability term (ϕ) is typically less than 1 during the day due to turbulent mixing. However, the use of zero air may have resulted in higher fluxes than would be observed in situ because the presence of Hg^0 in the atmosphere may lower the reduction rate of Hg^{2+} in sediment, subsequently reducing the volatilization of Hg^0 from sediment to air.

Estimates of "natural" emissions from land surfaces are approximately 1800 t y^{-1} [Schroeder & Munthe 1998]. Extrapolation of the minimum Hg flux estimate in visible + UV light (274 ng m^{-2} h^{-1}; HK; Table 4.7) from slightly contaminated tidally-exposed wetland sediments to the global mercury cycle, using a sediment Hg concentration of 0.32 ppm (HK) and assuming 10% of the Earth's land surface is covered by wetlands, yields an annual input of approximately 115 kg y^{-1} as a conservative estimate. Clearly, Hg fluxes and sediment Hg concentrations can be considerably higher with the contribution of varied anthropogenic sources, potentially up to 10% of global natural sources or greater.

4.6. Conclusions and implications

We conclude that photochemistry is the most important force driving the volatilization of mercury from tidally-exposed sediments. Our results suggest that gaseous elemental mercury is released to the atmosphere at the greatest rate in the presence of both visible and ultraviolet radiation, as in the natural environment.

The magnitude of annual sediment-air mercury emissions to the global atmosphere using conservative micrometeorological values indicates that wetlands may provide a larger portion of naturally re-emitted mercury to the global pool than earlier studies have indicated.

The amount of UV radiation reaching the Earth's surface could increase with the depletion of the ozone layer, changing the mechanisms and rates of photochemical processes occurring near the surface. This increase in ultraviolet radiation could serve to further enhance mercury volatilization from tidally-exposed wetland sediments to the global atmosphere.

References

Amyot, M., D. Lean, and G. Mierle (1997a), Photochemical formation of volatile mercury in high arctic lakes, *Environ. Toxicol. Chem., 16(10),* 2054-2063.

Amyot, M., G. Mierle, D. Lean, and D.J. McQueen (1997b), Effect of solar radiation on the formation of dissolved gaseous mercury in temperate lakes, *Geochim. Cosmochim. Acta, 61(5),* 975-987.

Bahlmann, E., R. Ebinghaus, and W. Ruck (2004), Influence of solar radiation on mercury emission fluxes from soils, *Mater. Geoenviron., 51,* 787-790.

Barrett, K., R. Bopp, T. Proctor, and P. Wei (2003), Vertical and lateral profiles of metal concentration in marsh and mudflat sediments of eight day swamp in the Hackensack Meadowlands, Meadowlands Symposium, Oct 9-10.

Benoit, G., E.X. Wang, W.C. Nieder, M. Levandowsky, and V.T. Breslin (1999), Sources and history of heavy metal contamination and sediment deposition in Tivoli South Bay, Hudson River, New York, *Estuar. Coasts, 22(2),* 167-178.

Bergan, T., L. Gallardo, and H. Rodhe (1999), Mercury in the global troposphere: a three-dimensional model study, *Atmos. Environ., 33,* 1575-1585.

Bloom, N.S. and E.A. Crecelius, (1983), Determination of mercury in seawater at sub-nanogram per liter levels, *Mar. Chem., 14,* 49-59.

Bonzongo, J.-C. J. and A.K. Donkor (2003), Increasing UV-B radiation at the earth's surface and potential effects on aqueous mercury cycling and toxicity, *Chemos., 52,* 1263-1273.

Boszke, L., A. Kowalski, G. Glosinska, R. Szarek, and J. Siepak (2003), Environmental factors affecting speciation of mercury in the bottom sediments; an overview, *Polish J. Environ. Stud., 12(1),* 5-13.

Bothner, M.H., R.A. Jahnke, M.L. Peterson, and R. Carpenter (1980), Rate of mercury loss from contaminated estuarine sediments, *Geochim. Cosmochim. Acta, 44,* 273-285.

Burger, J. and M. Gochfeld (1997), Risk, mercury levels, and birds - relating adverse laboratory effects to field biomonitoring, *Environ. Res., 75,* 160-172.

Canario, J. and C. Vale (2004), Rapid release of mercury from intertidal sediments exposed to solar radiation: A field experiment, *Environ. Sci. Technol., 38,* 3901-3907.

Cardona-Marek, T., J. Schaefer, K. Ellickson, T. Barkay, and J.R. Reinfelder (2007), Mercury speciation, reactivity, and bioavailability in a highly contaminated estuary, Berry's Creek, New Jersey Meadowlands, U.S.A. *Environ. Sci. Technol., 41(24),* 8268-8274.

Carpi, A., and S.E. Lindberg (1997), Sunlight-mediated emission of elemental mercury from soil amended with municipal sewage sludge, *Environ. Sci. Technol., 31,* 2085-2091.

Carpi, A., and S.E. Lindberg (1998), Application of a Teflon dynamic flux chamber for quantifying soil mercury flux: tests and results over background soil, *Atmos. Environ., 32,* 873-882.

Clarkson, T.W. (2002), The three modern faces of mercury. *Environ. Health Persp. 110(Suppl.)*, 11-23.

Compeau, G.C. and R. Bartha (1985), Sulfate-reducing bacteria: principal methylators of mercury in anoxic estuarine sediment, *Appl. Environ. Microbiol., 50,* 498-502.

Costa, M. and P.S. Liss (1999), Photoreduction of mercury in sea water and its possible implications for Hg^0 air-sea fluxes, *Mar. Chem., 68,* 87-95.

Costa, M. and P.S. Liss (2000), Photoreduction and evolution of mercury from seawater, *Sci. Total Environ., 261,* 125-135.

Deason, J.P. (2001), Passaic River restoration initiative: a new model for cleaning up our nation's contaminated urban rivers, *EPA Forum on Managing Contaminated Sediments at Hazardous Waste Sites*.

Drobner, E., H. Huber, C. Wachterhauser, D. Rose, and K. Stetter (1990), Pyrite formation linked with hydrogen evolution under anaerobic conditions, *Nature, 346,* 742-744.

Edwards, G.C., P.E. Rasmussen, W.H. Schroeder, K.J. Kemp, G. Dias, L. Halfpenny-Mitchell, D. Wallace, and A. Steffen (2002), Measurements of mercury fluxes from natural sources, paper presented at 2002 Canadian MITE-RN Annual Symposium, *Can. Geol. Surv.,* Ottawa.

Edwards, G.C., P.E. Rasmussen, W.H. Schroeder, D.M. Wallace, L. Halfpenny-Mitchell, G.M. Dias, R.J. Kemp and S. Ausma (2005), Development and evaluation of a sampling system to determine gaseous mercury fluxes using an aerodynamic micrometeorological gradient method, *J. Geophys. Res. 110, D10306,* doi:10.1029/2004JD005187.

Engle, M.A., M.S. Gustin, and H. Zhang (2001), Quantifying natural source mercury emissions from the Ivanhoe Mining District, north-central Nevada, USA, *Atmos. Environ., 35,* 3987-3997.

Feng, X., J. Sommar, O. Lindqvist, and Y. Hong (2002), Occurrence, emission and deposition of mercury from coal combustion in the Province, Guizhou, China, *Water Air Soil Pollut., 139,* 311-324.

Feng, X., H. Yan, S. Wang, G. Qui, S. Tang, L. Shang, Q. Dai, and Y. Hou (2004), Seasonal variation of gaseous mercury exchange rate between air and water surface over Baihu reservoir, Guizhou, China, *Atmos. Environ., 38,* 4721-4732.

Feng, X., S. Wang, G. Qui, Y. Hou, and S. Tang (2005), Total gaseous mercury emissions from soil in Guiyang, Guizho, China, *J. Geophys. Res., 110,* D14306, doi:10.1029/2004JD005643.

Ferrara, R., B.E. Maserti, M. Andersson, H. Edner, P. Ragnarson, S. Svanberg, and A. Hernandez (1998), Atmospheric mercury concentrations and fluxes in the Almaden District (Spain), *Atmos. Environ., 32,* 3897-3904.

Ferrara, R., and B. Mazzolai (1998), A dynamic flux chamber to measure mercury emission from aquatic systems, *Sci. Total Environ., 215,* 51-57.

Fitzgerald, W.F. and G.A. Gill (1979), Subnanogram determination of mercury by two stage gold amalgamation and gas phase detection applied to atmospheric analysis, *Analyt. Chem., 51,* 1714-1720.

Fitzgerald, W. and R. Mason (1996), The global mercury cycle: oceanic and anthropogenic aspects, in W. Baeyens, et al (eds.), *Global and Regional Mercury Cycles: Sources, Fluxes and Mass Balances*, 85-108, Kluwer Academic Publishers, Netherlands.

Galluzzi, P.F. and E. Sabounjian (1980), The distribution of mercury contamination in marsh sediments, channel sediments, and surface waters of the Hackensack Meadowlands, NJ, NJMC library.

Gao, F., S.R. Yates, M.V. Yates, J. Gan, and F.F. Ernst (1997), Design, fabrication, and application of a dynamic flux chamber for measuring gas emissions from soils, *Environ. Sci. Technol., 31,* 148-153.

Gillis, A. and R. Miller (2000), Some potential errors in the measurement of mercury gas exchange at the soil surface using a dynamic flux chamber, *Sci. Total Environ., 260,* 181-189.

Gilmour, C.C., E.A. Henry, and R. Mitchell (1992), Sulfate stimulation of mercury methylation in freshwater sediments, *Environ. Sci. Technol., 26,* 2281-2287.

Gnamus, A., A.R. Byrne, and M. Horvat (2000), Mercury in the soil-plant-deer-predator food chain of a temperate forest in Slovenia, *Environ. Sci. Technol., 34,* 3337-3345.

Gobeil, C. and D. Cossa (1993), Mercury in sediments and sediment pore water in the Laurentian Trough, *Can. J. Fish. Aquat. Sci., 50,* 1794-1800.

Gonzalez, M.C. and E. San Roman (2005), *Environmental photochemistry in heterogeneous media*, in Environmental Chemistry, vol. 2(M), pp. 49-75, Springer, Berlin.

Goodrow, S., R. Miskewitz, R.I. Hires, S.J. Eisenreich, W.S. Douglas, and J.R. Reinfelder (2005), Mercury emissions from cement-stabilized dredged material, *Environ. Sci. Technol., 39,* 8185-8190.

Gustin, M.S. (1998), NvMEP : Nevada Mercury Emissions Project-Mercury flux measurements: an intercomparison and assessment, Published Electric Power Research Institute Report, TR-111346.

Gustin, M.S., G.E. Taylor, T.L. Leonard and T.E. Keislar (1996), Atmospheric mercury concentrations associated with geologically and anthropogenically enriched sites in central western Nevada, *Environ. Sci. Technol., 30,* 2572-2579.

Gustin, M.S., R.A. Maxy, and P. Rasmussen (1998), Mechanisms influencing the volatile loss of mercury from soils, Symposium: Volume of Air Pollutants, Cary, NC.

Gustin, M.S., S.E. Lindberg, F. Marsik, A. Casimir, R. Ebinghaus, G. Edwards, C. Fitzgerals, J. Kemp, H. Kock, T. Leonard, M. Majewski, J. Owens, L. Poissant, P. Rasmussen, F. Schaedlich, D. Schneeberger, J. Sommar, R. Turner, A. Vette, D. Wallschlaeger, and Z. Xiao (1999), Nevada STORMS project: Measurement of mercury emission from naturally enriched surfaces, *J. Geophys. Res., 104,* 21,831-21,844.

Gustin, M.S., S. E. Lindberg, K. Austin, M. Coolbaugh, A. Vette, and H. Zhang (2000), Assessing the contribution of natural sources to regional atmospheric mercury budgets, *Sci. Total Environ., 259,* 61-72.

Hintelmann, H. and R.-D. Wilken (1995), Levels of mercury and methylmercury compounds in sediments of the polluted Elbe River: influence of seasonally and spatially varying environmental factors, *Sci. Total Environ., 166,* 1-10.

Holmes, J. and D. Lean (2006), Factors that influence methylmercury flux rates from wetland sediments, *Sci. Total Environ., 368,* 306-319.

Kim, K.-H. and S.E. Lindberg (1995), Design and initial tests of a dynamic enclosure chamber for measurements of vapor-phase mercury fluxes over soils, *Water Air Soil Pollut., 80,*1059–1068.

Konsevick, E. (1988), Berry's Creek: mercury in aquatic biota, Hackensack Meadowlands Development Commission, Lyndhurst, NJ, pp. 90.

Korfiatis, G.P., R.I. Hires, J.R. Reinfelder, L.A. Totten, and S.J. Eisenreich (2003), Monitoring of PCB and Hg air emissions in sites receiving stabilized harbor sediment, *Report to the New Jersey Marine Sciences Consortium and New Jersey Department of Transportation Office of Maritime Resources*.

Kozuchowski, I. and D.L. Johnson (1978), Gaseous emissions of mercury from an aquatic vascular plant, *Nature, 274,* 468-469.

Lalonde, J.D., M. Amyot, M.R. Doyon, and J.C. Auclair (2003), Photo-induced Hg(II) reduction in snow from the remote and temperate experimental lakes area (Ontario, Canada), *J. Geophys. Res.-Atmos., 108(D6),* Art. No. 4200.

Lee X., G. Benoit, and X.Z. Hu (2000), Total gaseous mercury concentration and flux over a coastal saltmarsh vegetation in Connecticut, USA, *Atmos. Environ., 34,* 4205-4213.

Leonard T. L., G.E. Taylor, M.S. Gustin, and G.C.J. Fernandez (1998), Mercury and plants in contaminated soils: 2. environmental and physiological factors governing mercury flux to the atmosphere, *Environ. Toxicol. Chem., 17,* 2072-2079.

Lindberg, S.E. and R.C. Harriss (1974), Mercury-organic matter associations in estuarine sediments and interstitial water, *Environ. Sci. Technol., 8,* 459-462.

Lindberg, S. E., R. C. Harriss, R. R. Turner, D. S. Shriner, and D. D. Huff (1979), Mechanisms and rates of atmospheric deposition of trace elements and sulfate to a deciduous forest canopy 510 pp., ORNL/TM-6674. Oak Ridge National Laboratory, Oak Ridge, Tennessee.

Lindberg, S. E., Meyers, T. P., and J. Munthe (1995a), Evasion of mercury vapor from the surface of a recently limed acid forest lake in Sweden, *Water Air Soil Pollut.,85,*725-730.

Lindberg, S.E., K.H. Kim, T.P. Meyers, and J.G. Owens (1995b), Micrometeorological gradient approach for quantifying air-surface exchange of mercury-vapor - tests over contaminated soils*, Environ. Sci. Technol., 29,* 126-135.

Lindberg, S.E., W. Dong, and T. Meyers (2002), Transpiration of gaseous elemental mercury through vegetation in a sub-tropical wetland in Florida, *Atmos. Environ., 36,* 5207-5219.

Lindqvist, O., K. Johansson, M. Aastrup, A. Andersson, L. Bringmark, G. Hovsenius, L. Hakanson, A. Iverfeldt, M. Meili, and B. Timm (1991), Mercury in the Swedish environment: recent research on causes, consequences and corrective methods, *Water Air Soil Environ., 55,* 23-32.

Lipsky, D., R.J. Reed, and R. Harkov (1980), Mercury levels in Berry's Creek, 76 pp., Office of Cancer and Toxic Substance, NJDEP, Trenton, NJ.

Liu, J.H., W.H. Wang, and A. Peng (2000), The photochemical reduction of divalent mercury and methyl-mercury. *J. Environ. Sci. Health Part A-Tox./Haz. Subst Eng., 35,* 1859-1868.

Majewski, M., R. Desjardins, P. Rochette, E. Pattey, J. Sieber, and D. Glotfelty (1993), Field comparison of an eddy accumulation and an aerodynamic-gradient system for measuring pesticide volatilized fluxes, *Environ. Sci. Technol., 27,* 121-128.

Mantoura, R.F.C., A. Dickson, and J.P. Riley (1978), The complexation of metals with humic materials in natural waters, *Estuar. Coast. Shelf S., 6,* 387-408.

Mason, R.P., J.R. Reinfelder, and F.M.M. Morel (1996), Uptake, toxicity, and trophic transfer of mercury in a coastal diatom, *Environ. Sci. Technol., 30,* 1835-1845.

Mason, R. and A.L. Lawrence (1999), Concentration, distribution, and bioavailability of mercury and methylmercury in sediments of Baltimore Harbor and Chesapeake Bay, Maryland, USA, *Environ. Toxicol. Chem., 18,* 2438–2447.

Mason, R.P. and G.R. Sheu (2002), Role of the ocean in the global mercury cycle, *Global Biogeochem. Cycles, 16,* Art. No. 1093.

Meili, M. (1997), Mercury in lakes and rivers. *Metal Ions Biol. Syst., 34,* 21-51.

Morse, J.W. (1994), Interactions of trace metals with authigenic sulfide minerals: implications for their bioavailability, *Mar. Chem., 46,* 1-6.

Morse, J.W. and G.W. Luther (1999), Chemical influences on trace metal-sulfide interactions in anoxic sediments., *Geochim. Cosmichim. Acta, 63*, 3373-3378.

NJ DEP (2001), Mercury Task Force Report, Trenton, NJ.

NOAA (2008), Tides and currents, Retrieved July 17, 2007, Available online: http://tidesandcurrents.noaa.gov/tides05/tab2ec2a.html.

Poissant, L., and A. Casimir (1998), Water-air and soil-air exchange rate of total gaseous mercury measured at background sites, *Atmos. Environ., 32,* 883-893.

Rasmussen, P.E., G.C. Edwards, J. Kemp, C. Hubble-Fitzgerald, and W.H. Schroeder (1998), Towards and improved natural sources inventory for mercury, in *Proceedings of metals and the environment: An international symposium,* ed. J. Skeaff, pp. 73-83, Metal. Soc. Of the Can. Inst. Of Min. Metal. And Pet., Montreal, Quebec, Canada.

Ravichandran, M. (2004), Interactions between mercury and dissolved organic matter – a review, *Chemos., 55(3),* 319-331.

Schaefer, J., J. Yagi, J.R. Reinfelder, T. Cardona, K.M. Ellickson, S. Tel-Or, and T. Barkay (2004), Role of the bacterial organomercury lyase (MerB) in controlling methylmercury accumulation in mercury-contaminated natural waters, *Environ. Sci. Technol., 38,* 4303-4311.

Scholtz, M.T., B.J. Van Heyst, and W.H. Schroeder (2003), Modeling of mercury emissions from background soils, *Sci. Total Environ., 304,* 185-207.

Schroeder, W.H., G. Keeler, H.H. Kock, P. Roussel, D. Schneeberger, and F. Schaedlich (1995), International field intercomparison of atmospheric mercury measurement methods, *Water Air Soil Pollut., 80,* 611-620.

Schroeder, W.H. and J. Munthe (1998), Atmospheric mercury—an overview, *Atmos. Environ., 32,* 809 –822.

Schroeder, W.H., J. Munthe, and O. Lindqvist (1989), Cycling of mercury between water, air and soil compartments of the environment, *Water Air Soil Pollut., 48,* 337-347.

Schumacher, B.A. (2002), Methods for the determination of total organic carbon (TOC) in soils and sediments. Office of research and development. USEPA.

Simpson, S.L. (2001), A rapid screening method for acid-volatile sulfide in sediments, *Environ. Toxicol. Chem., 20,* 2657-2661.

Watras, C.J., R.C. Back, S. Halvorsen, R.J.M. Hudson, K.A. Morrison, and S.P. Wente (1998), Bioaccumulation of mercury in pelagic freshwater food webs, *Sci. Total Environ., 219,* 183-208.

Weber, J.H. (1988), *Humic substances and their role in the environment,* in Binding and transport of metals by humic materials, Wiley, New York, pp.165-178.

Weber, J.H. (1993), Review of possible paths for abiotic methylation of mercury(II) in the aquatic environment. *Chemos., 26,* 2063-2077.

Wedepohl, K. (1995), The composition of continental crust, *Geochim. Cosmochim. Acta, 59,* 1217-1232.

Weis, J.S., L. Windham, and P. Weis (2003), Patterns of metal accumulation in leaves of the tidal marsh plants *Spartina alterniflora* (Loisel) and *Phragmites australis* (Cav. Trin ex Steud) over the growing season, *Wetlands, 23,* 459-465.

Weis, P., J.S. Weis, and J. Bogden (1986), Effects of environmental factors on release of mercury from Berry's Creek (New Jersey) sediments and its uptake by killifish (*Fundulus heteroclitus)*, *Environ. Pollut., 40,* 303-315.

Weis, P., K.R. Barrett, T. Proctor, and R.F. Bopp (2005), Studies of a contaminated brackish marsh in the Hackensack Meadowlands of northeastern New Jersey: An assessment of natural recovery, *Mar. Pollut. Bull., 50(11),* 1405-1415.

Windham, L., J.S. Weis, and P. Weis (2001), Patterns and processes of mercury release from leaves of two dominant salt marsh macrophytes; *Phragmites australis* and *Spartina alterniflora*, *Estuaries, 24,* 787-795.

Xiao, Z.F., J. Munthe, W.H. Schroeder and O. Lindqvist (1991), Vertical fluxes of volatile Hg over forest soils and lake surfaces in Sweden, *Tellus*, *43B,* 267-279.

Zelewski, L.M. and D.E. Armstrong (1996), Mercury dynamics in sediments of Tivoli South Bay, Hudson River, NY: A report of the 1996 Tibor T. Polgar Fellowship Program.

Zelewski, L.M., G. Benoit, and D.E. Armstrong (2001), Mercury dynamics in Tivoli South Bay, a freshwater tidal mudflat in the Hudson River, *Biogeochem., 52,* 93-112.

Zhang, H., S.E. Lindberg, F.J. Marsik, and G.J. Keeler (2001), Mercury air/surface exchange kinetics of background soils of the Tahquamenon River watershed in the Michigan upper peninsula, *Water Air Soil Pollut., 126,* 151-169.

Zhang, H., S.E. Lindberg, M.O. Barnett, A.F. Vette, and M.S. Gustin (2002), Dynamic flux chamber measurement of gaseous mercury emission fluxes over soils: simulation of gaseous mercury emissions from soils using a two-resistance exchange interface model, *Atmos. Environ., 35,* 835-846.

Table 4.1 General Site Information.

site	site ID	sample collection date	watershed description	latitude (ºN)	longitude (ºW)	mean tidal range[a] (m)
UNCONTAMINATED						
Tivoli South Bay (south end)	TSBs	26-Apr-06	tidal freshwater wetland	42.00	73.92	1.2
Tivoli South Bay (central)	TSBc	26-Apr-06	tidal freshwater wetland	42.02	73.92	1.2
SLIGHTLY CONTAMINATED						
Tivoli South Bay (north end)	TSBn	26-Apr-06	tidal freshwater wetland	42.03	73.92	1.2
Raritan River I (upstream)	RR1	27-Jun-05	freshwater river	40.48	74.33	1.7
Hackensack River (upland soil)	Hkup	17-Aug-05	freshwater river (adjacent)	40.78	74.10	-
Hackensack River	HK	17-Aug-05	freshwater river	40.78	74.10	1.6
CONTAMINATED						
Raritan River II	RR2	27-Jun-05	freshwater river / tidal estuary	40.48	73.38	1.7
Passaic River	PR	23-Jun-05	freshwater river	40.74	74.14	1.8
Secaucus High School Marsh	SC	21-Jun-07	tidally-restricted marsh	40.80	74.04	1.0[b]
HIGHLY CONTAMINATED						
Berry's Creek II	BC2	2-May-05	tidal estuarine wetland	40.79	74.09	1.6
Berry's Creek I (upstream)	BC1	7-Sep-04	tidal estuarine wetland	40.83	74.08	1.6

[a] from NOAA 2008

[b] isolated from tidal exchange with the Hackensack River at time of sample collection

Table 4.2 Tivoli South Bay South: Sediment-Air Mercury Volatilization Fluxes[a].

experiment date	experiment length (h:mm)	temperature (ºC)	light source	filter	TGM concentration (ng m^{-3})	chamber TGM flux (ng m^{-2} h^{-1})	theoretical in situ flux[b] (ng m^{-2} h^{-1})
6/21/2006	3:30	10	fluorescent	none	10 ± 1.2	8.7 ± 1.1	518
6/21/2006	2:30	10	none	none	0.32 ± 0.13	0.29 ± 0.12	17
6/21/2006	1:00	10	fluorescent	none	8.6 ± 0.33	7.7 ± 0.30	445
6/21/2006	0:30	10	none	none	0.53 ± 0.11	0.48 ± 0.10	27
6/21/2006	3:50	10	fluorescent	none	8.9 ± 0.56	8.0 ± 0.50	461
6/22/2006	1:30	10	none	none	0.35± 0.16	0.32 ± 0.14	18
6/22/2006	1:50	10	fluorescent	none	8.1 ± 0.22	7.3 ± 0.20	419
6/22/2006	1:10	10	none	none	0.30 ± 0.15	0.27 ± 0.14	16
6/22/2006	2:00	10	fluorescent	none	8.0 ± 0.45	7.2 ± 0.41	414
6/22/2006	1:30	10	none	none	0.21 ± 0.11	0.19 ± 0.10	11
6/22/2006	0:40	10	fluorescent	none	7.9 ± 0.16	7.1 ± 0.14	409
7/25/2006	1:05	23	fluorescent	none	1.3 ± 0.14	1.1 ± 0.13	67
7/25/2006	0:35	23	fluorescent	mylar	1.2 ± 0.08	1.1 ± 0.07	62
7/25/2006	0:50	23	none	none	0.12 ± 0.19	0.11 ± 0.17	6
7/25/2006	0:55	23	fluorescent	none	1.3 ± 0.03	1.1 ± 0.03	67
7/25/2006	1:35	23	none	none	0.13 ± 0.07	0.12 ± 0.06	7
4/17/2008	0:50	23	none	none	1.3 ± 0.31	1.2 ± 0.28	67
4/17/2008	1:50	23	fluorescent	none	2.4 ± 0.41	2.2 ± 0.37	124
4/17/2008	2:00	23	fluorescent	mylar	1.5 ± 0.09	1.4 ± 0.08	78
4/18/2008	0:40	23	none	none	0.34± 0.07	0.31 ± 0.06	18
4/18/2008	2:00	23	fluorescent	none	2.3 ± 0.40	2.0 ± 0.36	119
4/18/2008	1:20	23	fluorescent	mylar	1.3 ± 0.06	1.2 ± 0.05	67
4/18/2008	0:30	23	none	none	0.36 ± 0.19	0.32 ± 0.17	19
4/18/2008	2:00	23	fluorescent	none	1.3 ± 0.19	1.2 ± 0.17	67
4/18/2008	2:20	23	fluorescent	Lee 226	0.62 ± 0.09	0.56 ± 0.08	32
4/23/2008	1:20	23	none	none	0.10 ± 0.20	0.09 ± 0.18	5
4/23/2008	1:50	23	fluorescent	none	1.2 ± 0.25	1.0 ± 0.23	62
4/23/2008	1:50	23	fluorescent	Lee 226	0.45 ± 0.10	0.41 ± 0.09	23
4/24/2008	0:40	22	none	none	0.06 ± 0.12	0.05 ± 0.11	3
4/24/2008	1:50	22	fluorescent	none	0.79 ± 0.10	0.71 ± 0.09	41
4/24/2008	1:40	22	fluorescent	Lee 226	0.27 ± 0.12	0.24 ± 0.11	14

[a] Values are means ± propagated error for TGM concentrations and fluxes.
[b] Theoretical in situ fluxes were estimated using mean measured TGM concentrations, the von Karman constant (0.41), the lowest value for friction velocities measured during our in situ experiments ($u^* = 0.20$ m s^{-1}), and assuming a neutral atmosphere ($\phi = 1$) over a 3 m vertical gradient.

Table 4.3 Tivoli South Bay Central: Sediment-Air Mercury Volatilization Fluxes[a].

experiment date	experiment length (h:mm)	temperature (ºC)	light source	filter	TGM concentration (ng m^{-3})	chamber TGM flux (ng m^{-2} h^{-1})	theoretical in situ flux[b] (ng m^{-2} h^{-1})
7/27/2006	2:10	24	fluorescent	none	2.4 ± 0.21	2.1 ± 0.19	124
7/27/2006	0:40	24	fluorescent	mylar	1.5 ± 0.06	1.4 ± 0.05	78
7/27/2006	1:40	24	none	none	1.7 ± 0.31	1.5 ± 0.28	88
1/15/2007[c]	3:00	21	none	none	0.91	0.62	47
1/17/2007[c]	3:00	19	fluorescent	none	6.6	4.4	342
1/17/2007[c]	3:00	20	UV-A	none	3.3	2.2	171
1/18/2007[c]	3:00	20	UV-B	none	0.22	0.15	11
1/18/2007[c]	3:00	21	fluorescent	Lee 226	0.32	0.22	17
1/23/2007[c]	3:00	19	UV-A	none	1.8	1.2	93
1/23/2007[c]	3:00	20	UV-B	none	0.23	0.16	12
1/24/2007[c]	3:00	19	UV-A	none	1.1	0.74	57
1/24/2007[c]	3:00	20	UV-B	none	0.05	0.03	3

[a] Values are means ± propagated error for TGM concentrations and fluxes.
[b] Theoretical in situ fluxes were estimated using mean measured TGM concentrations, the von Karman constant (0.41), the lowest value for friction velocities measured during our in situ experiments ($u^* = 0.20$ m s^{-1}), and assuming a neutral atmosphere ($\phi = 1$) over a 3 m vertical gradient.
[c] TGM was analyzed using the gold trap method. All others were analyzed using the Tekran 2537A method.

Table 4.4 Tivoli South Bay North: Sediment-Air Mercury Volatilization Fluxes[a].

experiment date	experiment length (h:mm)	temperature (ºC)	light source	filter	TGM concentration (ng m^{-3})	chamber TGM flux (ng m^{-2} h^{-1})	theoretical in situ flux[b] (ng m^{-2} h^{-1})
6/26/2006	3:50	10	fluorescent	none	8.3 ± 0.63	7.4 ± 0.57	430
6/26/2006	1:30	10	none	none	0.49 ± 0.10	0.44 ± 0.09	25
6/26/2006	3:00	10	fluorescent	none	10 ± 0.21	9.0 ± 0.19	518
6/26/2006	2:20	10	none	none	0.30 ± 0.12	0.27 ± 0.11	16
6/27/2006	3:50	10	fluorescent	none	10 ± 0.19	9.3 ± 0.17	518
6/27/2006	1:10	10	none	none	0.35 ± 0.12	0.32 ± 0.11	18
6/27/2006	2:00	10	fluorescent	none	10 ± 0.18	9.2 ± 0.16	518
6/27/2006	1:30	10	none	none	0.30 ± 0.12	0.27 ± 0.11	16
6/27/2006	2:10	10	fluorescent	none	9.9 ± 0.12	8.9 ± 0.11	512

[a] Values are means ± propagated error for TGM concentrations and fluxes.
[b] Theoretical in situ fluxes were estimated using mean measured TGM concentrations, the von Karman constant (0.41), the lowest value for friction velocities measured during our in situ experiments ($u^* = 0.20$ m s^{-1}), and assuming a neutral atmosphere ($\phi = 1$) over a 3 m vertical gradient.

Table 4.5 Raritan River I (Upstream): Sediment-Air Mercury Volatilization Fluxes[a].

experiment date	experiment length (h:mm)	temperature (ºC)	light source	filter	TGM concentration (ng m^{-3})	chamber TGM flux (ng m^{-2} h^{-1})	theoretical in situ flux[b] (ng m^{-2} h^{-1})
2/7/2007[c]	3:00	18	fluorescent	none	12	8.1	621
2/7/2007[c]	3:00	20	fluorescent	mylar	5.4	3.7	279
2/15/2007[c]	3:00	19	fluorescent	mylar	4.3	2.9	223
2/15/2007[c]	3:00	20	fluorescent	none	11	7.3	569

[a] Values are means ± propagated error for TGM concentrations and fluxes.
[b] Theoretical in situ fluxes were estimated using mean measured TGM concentrations, the von Karman constant (0.41), the lowest value for friction velocities measured during our in situ experiments (u* = 0.20 m s^{-1}), and assuming a neutral atmosphere ($\phi = 1$) over a 3 m vertical gradient.
[c] TGM was analyzed using the gold trap method.

Table 4.6 Hackensack River Upland Soil: Soil-Air Mercury Volatilization Fluxes[a].

experiment date	experiment length (h:mm)	temperature (ºC)	light source	filter	TGM concentration (ng m^{-3})	chamber TGM flux (ng m^{-2} h^{-1})	theoretical in situ flux[b] (ng m^{-2} h^{-1})
7/14/2006	3:20	10	fluorescent	none	19 ± 2.3	17 ± 2.1	983
7/14/2006	2:20	10	none	none	12 ± 1.2	11 ± 1.0	621
7/14/2006	2:20	10	fluorescent	none	15 ± 2.2	14 ± 1.9	776
7/14/2006	1:00	10	none	none	7.9 ± 0.33	7.1 ± 0.30	409
7/14/2006	1:10	10	fluorescent	none	11 ± 0.63	9.6 ± 0.57	569
7/14/2006	0:50	10	none	none	7.2 ± 0.64	6.5 ± 0.58	373
7/14/2006	3:10	10	fluorescent	none	9.6 ± 0.97	8.6 ± 0.87	497
7/15/2006	1:30	10	none	none	7.6 ± 0.62	6.8 ± 0.56	393
7/15/2006	2:00	10	fluorescent	none	10 ± 0.65	9.0 ± 0.59	518
4/25/2008	1:50	21	none	none	23 ± 1.6	21 ± 1.4	1190
4/25/2008	1:59	22	fluorescent	none	29 ± 1.5	26 ± 1.4	1501
4/25/2008	1:30	22	fluorescent	Lee 226	30 ± 0.34	27 ± 0.31	1553
4/26/2008	2:20	22	none	none	12 ± 0.73	10 ± 0.66	621
4/26/2008	1:20	21	fluorescent	none	19 ± 0.55	17 ± 0.50	983
4/26/2008	1:40	22	fluorescent	Lee 226	18 ± 0.15	16 ± 0.14	932

[a] Values are means ± propagated error for TGM concentrations and fluxes.
[b] Theoretical in situ fluxes were estimated using mean measured TGM concentrations, the von Karman constant (0.41), the lowest value for friction velocities measured during our in situ experiments ($u^* = 0.20$ m s^{-1}), and assuming a neutral atmosphere ($\phi = 1$) over a 3 m vertical gradient.

Table 4.7 Hackensack River: Sediment-Air Mercury Volatilization Fluxes[a].

experiment date	experiment length (h:mm)	temperature (ºC)	light source	filter	TGM concentration (ng m^{-3})	chamber TGM flux (ng m^{-2} h^{-1})	theoretical in situ flux[b] (ng m^{-2} h^{-1})
7/7/2006	3:40	10	none	none	0.28 ± 0.11	0.25 ± 0.10	14
7/7/2006	0:50	10	fluorescent	none	5.9 ± 0.06	5.3 ± 0.05	305
7/7/2006	0:50	10	none	none	0.25 ± 0.08	0.23 ± 0.07	13
7/7/2006	0:50	10	fluorescent	none	6.1 ± 0.18	5.5 ± 0.16	316
7/7/2006	0:50	10	none	none	0.28 ± 0.08	0.25 ± 0.07	14
7/8/2006	3:50	10	fluorescent	none	6.3 ± 0.08	5.7 ± 0.07	326
7/8/2006	1:20	10	none	none	0.26 ± 0.03	0.23 ± 0.03	13
7/8/2006	2:00	10	fluorescent	none	6.5 ± 0.13	5.9 ± 0.12	336
7/8/2006	1:30	10	none	none	0.21 ± 0.07	0.19 ± 0.06	11
7/8/2006	5:50	10	fluorescent	none	6.3 ± 0.13	5.7 ± 0.12	326
7/8/2006	3:30	10	none	none	0.18 ± 0.07	0.16 ± 0.06	9
7/8/2006	0:50	10	fluorescent	none	5.8 ± 0.12	5.2 ± 0.11	300
7/8/2006	0:40	10	none	none	0.20 ± 0.07	0.18 ± 0.06	10
7/8/2006	0:50	10	fluorescent	none	5.6 ± 0.08	5.1 ± 0.07	290
7/8/2006	0:40	10	none	none	0.20 ± 0.05	0.18 ± 0.05	10
7/9/2006	3:50	10	fluorescent	none	5.5 ± 0.07	5.0 ± 0.06	285
7/9/2006	1:20	10	none	none	0.20 ± 0.04	0.18± 0.04	10
7/9/2006	2:00	10	fluorescent	none	5.3 ± 0.09	4.8 ± 0.08	274

[a] Values are means ± propagated error for TGM concentrations and fluxes.
[b] Theoretical in situ fluxes were estimated using mean measured TGM concentrations, the von Karman constant (0.41), the lowest value for friction velocities measured during our in situ experiments ($u^* = 0.20$ m s^{-1}), and assuming a neutral atmosphere ($\phi = 1$) over a 3 m vertical gradient.

Table 4.8 Raritan River II (Downstream): Sediment-Air Mercury Volatilization Fluxes[a].

experiment date	experiment length (h:mm)	temperature (ºC)	light source	filter	TGM concentration (ng m^{-3})	chamber TGM flux (ng m^{-2} h^{-1})	theoretical in situ flux[b] (ng m^{-2} h^{-1})
6/13/2006	4:10	10	fluorescent	none	15 ± 0.19	14 ± 0.17	776
6/13/2006	0:20	10	none	none	1.2 ± 0.24	1.0 ± 0.22	62
6/13/2006	0:50	10	fluorescent	none	15 ± 0.50	13 ± 0.45	776
6/13/2006	1:30	10	none	none	0.77 ± 0.19	0.69 ± 0.17	40
6/13/2006	1:50	10	fluorescent	none	14 ± 0.17	12 ± 0.15	725
6/13/2006	3:40	10	none	none	0.41 ± 0.25	0.37 ± 0.23	21
6/14/2006	3:50	10	fluorescent	Lee 226	4.0 ± 0.15	3.6 ± 0.14	207
6/14/2006	0:20	10	none	none	0.90 ± 0.22	0.81 ± 0.20	47
6/14/2006	1:10	10	fluorescent	Lee 226	3.4 ± 0.15	3.0 ± 0.14	176
6/14/2006	1:40	10	none	none	0.55 ± 0.19	0.50 ± 0.17	28
6/14/2006	1:50	10	fluorescent	Lee 226	3.2 ± 0.08	2.9 ± 0.07	166
2/1/2007[c]	3:00	20	fluorescent	none	2.1	1.4	109
2/1/2007[c]	3:00	22	fluorescent	mylar	0.06	0.04	3

[a] Values are means ± propagated error for TGM concentrations and fluxes.
[b] Theoretical in situ fluxes were estimated using mean measured TGM concentrations, the von Karman constant (0.41), the lowest value for friction velocities measured during our in situ experiments ($u^* = 0.20$ m s^{-1}), and assuming a neutral atmosphere ($\phi = 1$) over a 3 m vertical gradient.
[c] TGM was analyzed using the gold trap method. All others were analyzed using the Tekran 2537A.

Table 4.9 Passaic River: Sediment-Air Mercury Volatilization Fluxes[a].

experiment date	experiment length (h:mm)	temperature (ºC)	light source	filter	TGM concentration (ng m^{-3})	chamber TGM flux (ng m^{-2} h^{-1})	theoretical in situ flux[b] (ng m^{-2} h^{-1})
6/15/2006	2:50	10	fluorescent	none	8.0 ± 1.5	7.2 ± 1.3	414
6/15/2006	1:40	10	none	none	0.24 ± 0.12	0.22 ± 0.11	12
6/15/2006	2:50	10	fluorescent	Lee 226	2.8 ± 0.16	2.5 ± 0.14	145
6/15/2006	2:30	10	none	none	0.22 ± 0.10	0.20 ± 0.09	11
6/15/2006	0:40	10	fluorescent	Lee 226	3.1 ± 0.11	2.8 ± 0.10	160
6/15/2006	1:40	10	none	none	0.19 ± 0.06	0.17 ± 0.05	10
6/16/2006	2:00	10	fluorescent	Lee 226	2.8 ± 0.14	2.5 ± 0.13	145
6/16/2006	0:50	10	none	none	0.37 ± 0.08	0.33 ± 0.07	19
6/16/2006	0:50	10	fluorescent	Lee 226	2.7 ± 0.06	2.5 ± 0.05	140
6/16/2006	1:20	10	none	none	0.29 ± 0.08	0.26 ± 0.07	15
6/16/2006	2:40	10	fluorescent	Lee 226	2.5 ± 0.07	2.3 ± 0.06	129
2/20/2007[c]	3:00	20	fluorescent	none	6.5	4.4	336
2/20/2007[c]	3:00	21	fluorescent	mylar	12.0	7.7	621
2/22/2007[c]	3:00	21	fluorescent	none	7.1	4.8	367
2/22/2007[c]	3:00	22	fluorescent	Lee 226	15	10	776
2/23/2007[c]	3:00	20	fluorescent	mylar	13	8.9	673
2/23/2007[c]	3:00	20	fluorescent	Lee 226	8.4	5.7	435
2/28/2007[c]	3:00	22	fluorescent	mylar	9.3	6.2	481
2/28/2007[c]	3:00	22	fluorescent	none	13	8.6	673
3/1/2007[c]	3:00	22	UV-A	none	2.8	1.9	145
3/1/2007[c]	3:00	23	UV-B	none	2.5	1.7	129
3/2/2007[c]	3:00	24	UV-A	none	1.6	1.1	83
3/2/2007[c]	3:00	26	UV-B	none	2.0	1.3	104
3/6/2007[c]	3:00	19	none	none	0.81	0.54	42
3/6/2007[c]	3:00	20	fluorescent	none	17	11	880

[a] Values are means ± propagated error for TGM concentrations and fluxes.
[b] Theoretical in situ fluxes were estimated using mean measured TGM concentrations, the von Karman constant (0.41), the lowest value for friction velocities measured during our in situ experiments ($u^* = 0.20$ m s^{-1}), and assuming a neutral atmosphere ($\phi = 1$) over a 3 m vertical gradient.
[c] TGM was analyzed using the gold trap method. All others were analyzed using the Tekran 2537A.

Table 4.10 Secaucus High School Marsh: Sediment-Air Mercury Volatilization Fluxes[a].

experiment date	experiment length (h:mm)	temperature (ºC)	light source	filter	TGM concentration (ng m^{-3})	chamber TGM flux (ng m^{-2} h^{-1})	theoretical in situ flux[b] (ng m^{-2} h^{-1})
7/25/2007	2:05	24	fluorescent	none	4.2 ± 0.33	9.5 ± 0.30	217
7/25/2007	0:55	25	fluorescent	mylar	4.0 ± 0.20	9.1 ± 0.18	207
7/26/2007	1:55	23	none	none	1.1 ± 0.10	2.4 ± 0.09	57
7/26/2007	2:25	24	fluorescent	none	4.9 ± 0.43	11 ± 0.39	254
7/26/2007	2:00	24	fluorescent	mylar	4.6 ± 0.41	10 ± 0.37	238
7/27/2007	2:00	23	none	none	0.85 ± 0.19	1.9 ± 0.17	44
7/27/2007	1:35	23	fluorescent	none	3.1 ± 0.39	7.0 ± 0.35	160
7/27/2007	1:35	25	fluorescent	mylar	5.9 ± 0.31	13 ± 0.28	305
7/31/2007	1:50	24	fluorescent	none	4.6 ± 0.37	10 ± 0.33	238
7/31/2007	2:05	25	fluorescent	Lee 226	4.0 ± 0.49	9.1 ± 0.44	207
7/31/2007	1:45	25	none	none	1.0 ± 0.31	2.3 ± 0.28	52
8/14/2007	1:30	23	none	none	0.47 ± 0.14	1.1 ± 0.13	24
8/14/2007	1:50	23	fluorescent	none	2.9 ± 0.25	6.4 ± 0.23	150
8/14/2007	1:45	23	fluorescent	mylar	2.7 ± 0.35	6.0 ± 0.32	140
8/16/2007	1:45	23	none	none	0.75 ± 0.25	1.7 ± 0.23	39
8/16/2007	1:50	23	fluorescent	none	4.8 ± 0.51	11 ± 0.46	248
8/16/2007	1:50	25	fluorescent	mylar	4.4 ± 0.43	9.9 ± 0.39	228
8/28/2007	2:35	23	none	none	0.64 ± 0.11	1.4 ± 0.10	33
8/28/2007	2:20	24	fluorescent	none	3.1 ± 0.44	7.0 ± 0.40	160
8/28/2007	3:05	25	fluorescent	mylar	3.2 ± 0.36	7.1 ± 0.32	166
8/30/2007	1:40	22	none	none	0.76 ± 0.21	1.7 ± 0.19	39
8/30/2007	2:00	23	fluorescent	none	5.1 ± 0.29	12 ± 0.26	264
8/30/2007	1:50	23	fluorescent	mylar	4.4 ± 0.13	9.9 ± 0.12	228
9/6/2007	1:40	22	none	none	0.84 ± 0.09	1.9 ± 0.08	43
9/6/2007	1:50	22	fluorescent	none	4.2 ±0.21	9.5 ± 0.19	217
9/6/2007	0:40	23	fluorescent	mylar	3.6 ± 0.15	8.0 ± 0.14	186
9/11/2007	1:30	25	none	none	0.61 ± 0.12	1.4 ± 0.11	32
9/11/2007	1:50	23	fluorescent	none	6.0 ± 0.50	14 ± 0.45	311
9/11/2007	2:00	23	fluorescent	Lee 226	4.3 ± 0.09	9.7 ± 0.08	223

[a] Values are means ± propagated error for TGM concentrations and fluxes.
[b] Theoretical in situ fluxes were estimated using mean measured TGM concentrations, the von Karman constant (0.41), the lowest value for friction velocities measured during our in situ experiments ($u^* = 0.20$ m s^{-1}), and assuming a neutral atmosphere ($\phi = 1$) over a 3 m vertical gradient.

Table 4.11 Berry's Creek II (Downstream): Sediment-Air Mercury Volatilization Fluxes[a].

experiment date	experiment length (h:mm)	temperature (ºC)	light source	filter	TGM concentration (ng m^{-3})	chamber TGM flux (ng m^{-2} h^{-1})	theoretical in situ flux[b] (ng m^{-2} h^{-1})
7/5/2005	0:30	17	none	none	2.3 ± 0.36	2.0 ± 0.32	119
7/5/2005	0:35	17	fluorescent	none	27 ± 2.0	24 ± 1.8	1397
7/5/2005	1:25	17	fluorescent	mylar	24 ± 0.27	22 ± 0.24	1242
7/5/2005	19:50	17	fluorescent	none	33 ± 1.4	30 ± 1.2	1708
7/6/2005	2:45	17	fluorescent	mylar	29 ± 0.40	26 ± 0.36	1501
9/21/2007	1:35	21	none	none	1.6 ± 0.28	3.7 ± 0.25	83
9/21/2007	1:30	22	UV-A	none	2.9 ± 0.49	6.5 ± 0.44	150
9/21/2007	1:45	23	UV-B	none	2.1 ± 0.47	4.7 ± 0.42	109

[a] Values are means ± propagated error for TGM concentrations and fluxes.
[b] Theoretical in situ fluxes were estimated using mean measured TGM concentrations, the von Karman constant (0.41), the lowest value for friction velocities measured during our in situ experiments ($u^* = 0.20$ m s^{-1}), and assuming a neutral atmosphere ($\phi = 1$) over a 3 m vertical gradient.

Table 4.12 Berry's Creek I (Upstream): Sediment-Air Mercury Volatilization Fluxes[a].

experiment date	experiment length (h:mm)	temperature (ºC)	light source	filter	TGM concentration (ng m^{-3})	chamber TGM flux (ng m^{-2} h^{-1})	theoretical in situ flux[b] (ng m^{-2} h^{-1})
2/25/2005	3:40	23	fluorescent	none	9.8 ± 0.40	8.8 ± 0.36	507
3/12/2005	5:05	17	fluorescent	none	14 ± 3.2	13 ± 2.9	725
3/13/2005	17:25	17	none	none	0.82 ± 0.17	0.74 ± 0.15	42
3/14/2005	6:55	17	fluorescent	none	13 ± 3.0	12 ± 2.7	673
3/17/2005	1:00	17	none	none	0.46 ± 0.07	0.42 ± 0.07	24
3/17/2005	1:20	17	fluorescent	none	13 ± 0.64	11 ± 0.57	673
3/17/2005	0:50	17	none	none	0.66 ± 0.16	0.59 ± 0.14	34
3/17/2005	1:10	17	fluorescent	none	12 ± 1.4	11 ± 1.2	621
3/17/2005	2:20	17	none	none	0.58 ± 0.13	0.52 ± 0.12	30
8/16/2005	17:10	23	none	none	1.0 ± 0.23	0.87 ± 0.21	52
8/17/2005	9:05	23	fluorescent	none	5.9 ± 1.1	5.3 ± 1.0	305
8/17/2005	10:15	23	none	none	1.6 ± 0.19	1.4 ± 0.17	83
8/18/2005	6:25	23	fluorescent	none	8.8 ± 0.81	7.9 ± 0.73	455
9/20/2007	1:55	20	none	none	2.1 ± 0.26	1.9 ± 0.23	109
9/20/2007	1:55	22	fluorescent	none	8.1 ± 0.26	7.3 ± 0.23	419
9/20/2007	1:55	22	fluorescent	Lee 226	7.4 ± 0.39	6.6 ± 0.35	383

[a] Values are means ± propagated error for TGM concentrations and fluxes.
[b] Theoretical in situ fluxes were estimated using mean measured TGM concentrations, the von Karman constant (0.41), the lowest value for friction velocities measured during our in situ experiments ($u^* = 0.20$ m s^{-1}), and assuming a neutral atmosphere ($\phi = 1$) over a 3 m vertical gradient.

Table 4.13 Chemical Site Information. OM is Organic Matter; AVS is Acid Volatile Sulfide; THg is Total Mercury[a].

site	THg content (ppm)	salinity (‰)	pore water pH	OM content (% OM)	water content (% WC)	AVS (µmol g^{-1} dry)
UNCONTAMINATED						
Tivoli South Bay (south end)	0.05	2	6.6	9.2	60	2.5
Tivoli South Bay (central)	0.09	2	6.4	8.3	61	1.7
SLIGHTLY CONTAMINATED						
Tivoli South Bay (north end)	0.25	2	6.7	23	71	0.89
Raritan River I (upstream)	0.25	13	5.0	9.0	50	2.0
Hackensack River (upland soil)	0.28	-	7.4	11	23	6.5
Hackensack River	0.32	19	6.5	8.0	52	6.6
CONTAMINATED						
Raritan River II	0.66	27	5.7	10	54	7.2
Passaic River	1.0	15	6.8	12	60	4.2
Secaucus High School Marsh	7.1	5	6.9	39	78	11
HIGHLY CONTAMINATED						
Berry's Creek II	20	4	6.8	14	55	9.6
Berry's Creek I (upstream)	51	4	6.9	13	63	20

[a] The sediment is considered uncontaminated with respect to Hg when it contains ≤ 0.1 ppm. The upper crustal abundance is ~0.06 ppm [Wedepohl 1995] with a small degree of anthropogenic influence assumed.

Table 4.14 Mean Particle Size Distributions Determined by Laser Diffraction.

site	particle size distribution		
	% clay (<2 μm)	% silt (2 - 50 μm)	% sand (50 - 2000 μm)
UNCONTAMINATED			
Tivoli South Bay (south end)	0	85	15
Tivoli South Bay (central)	1	84	15
SLIGHTLY CONTAMINATED			
Tivoli South Bay (north end)	0	88	12
Raritan River I (upstream)	16	84	0
Hackensack River (upland soil)	7	86	7
Hackensack River	11	89	0
CONTAMINATED			
Raritan River II	14	86	0
Passaic River	2	98	0
Secaucus High School Marsh	4	96	0
HIGHLY CONTAMINATED			
Berry's Creek II	8	85	7
Berry's Creek I (upstream)	14	86	0

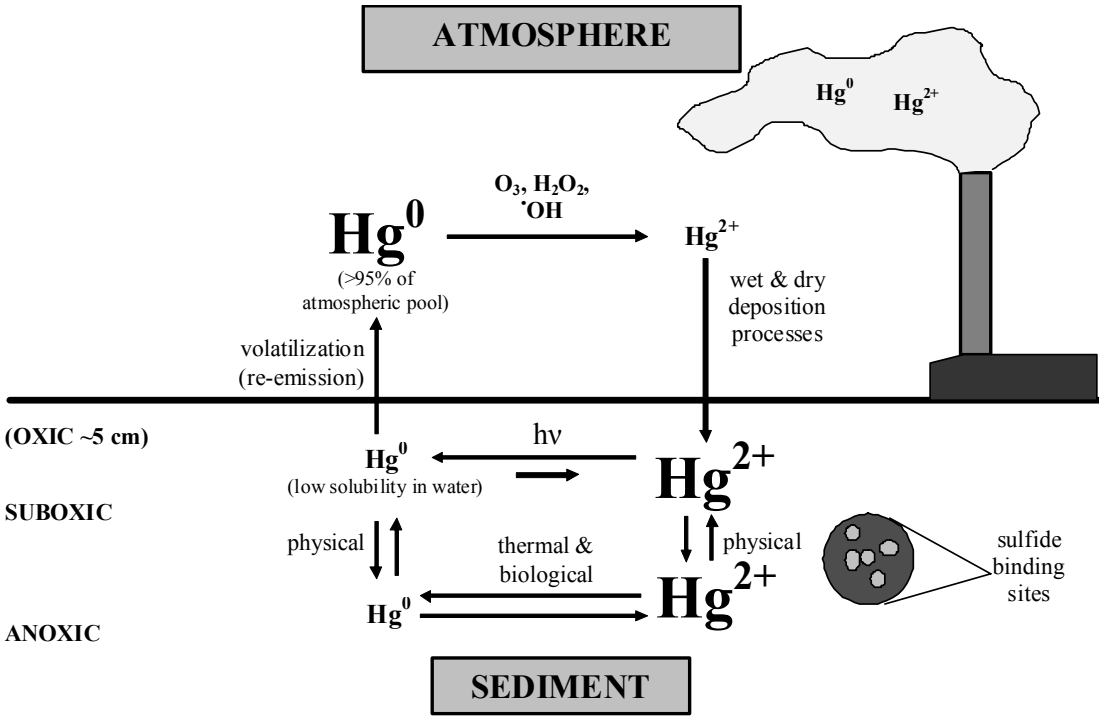

Figure 4.1 Conceptual model of Hg cycling between tidally-exposed sediments and the atmosphere.

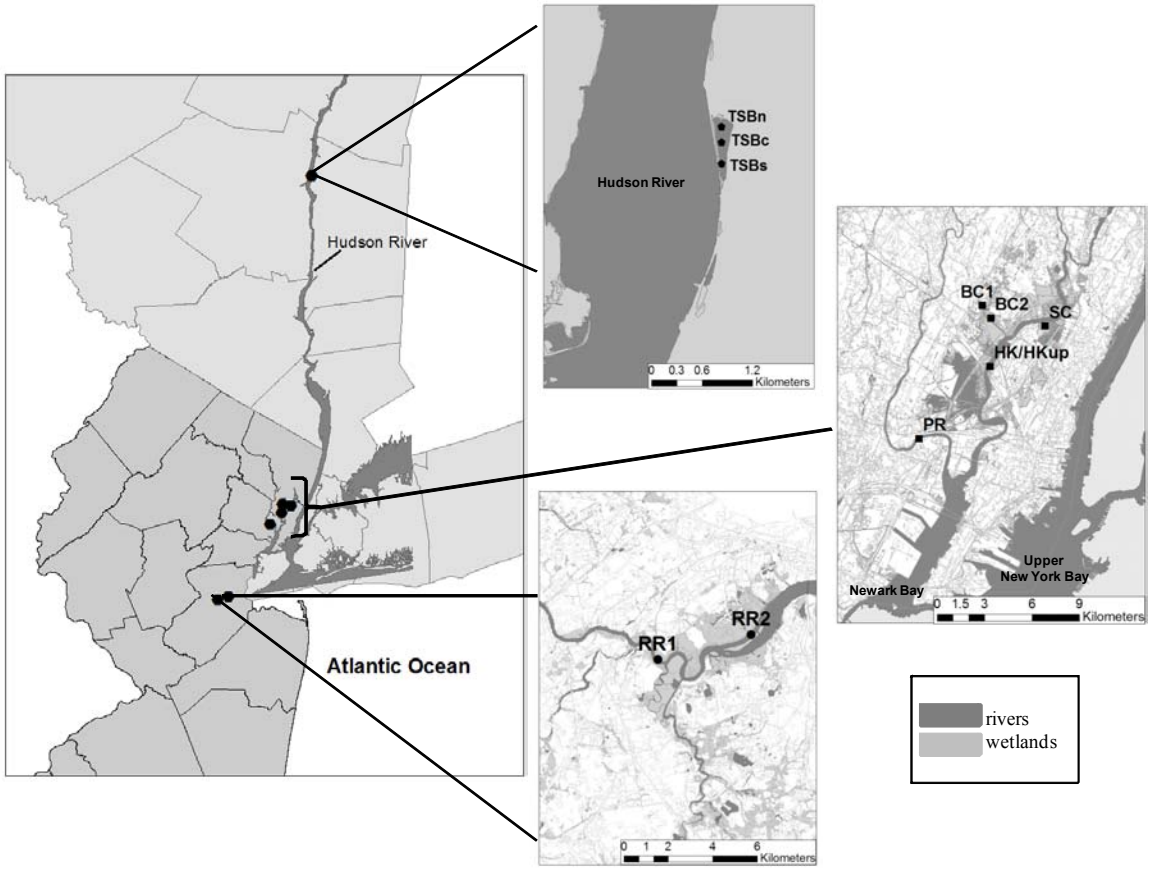

Figure 4.2 Map of sample collection sites. BC is Berry's Creek (BCI is upstream); HK is Hackensack River (sediment and upland soil samples); PR is Passaic River; RR is Raritan River (RRI is upstream); SC is Secaucus High School Marsh; TSB is Tivoli South Bay.

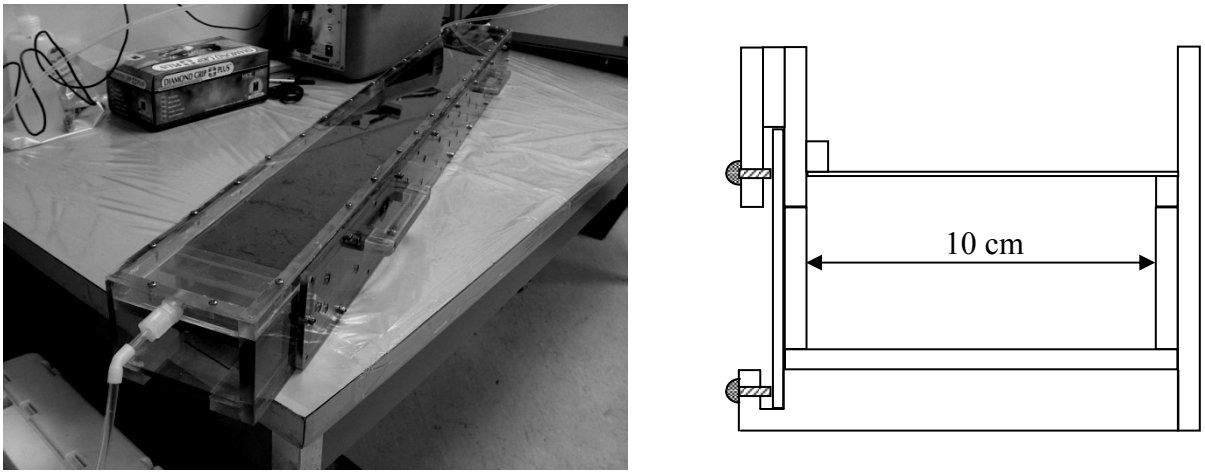

Figure 4.3 Sediment flux chamber with sediment inside viewed from the mercury-free air inlet end (A) and a schematic cross-section (B).

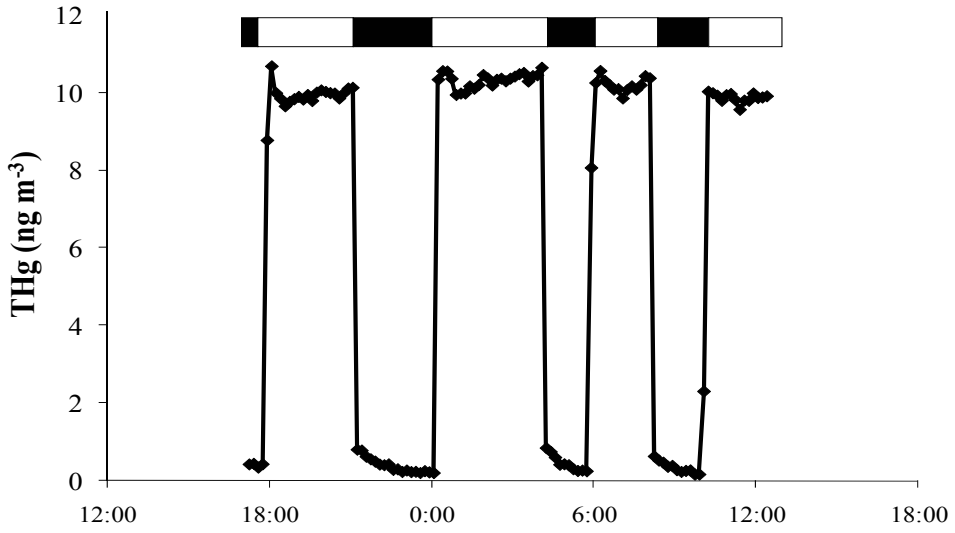

Figure 4.4 Hg Volatilization from Tivoli South Bay north (TSBn) sediments exposed to alternating light/dark conditions (visible + UV) as indicated by the open (light) and shaded (dark) figure above chart.

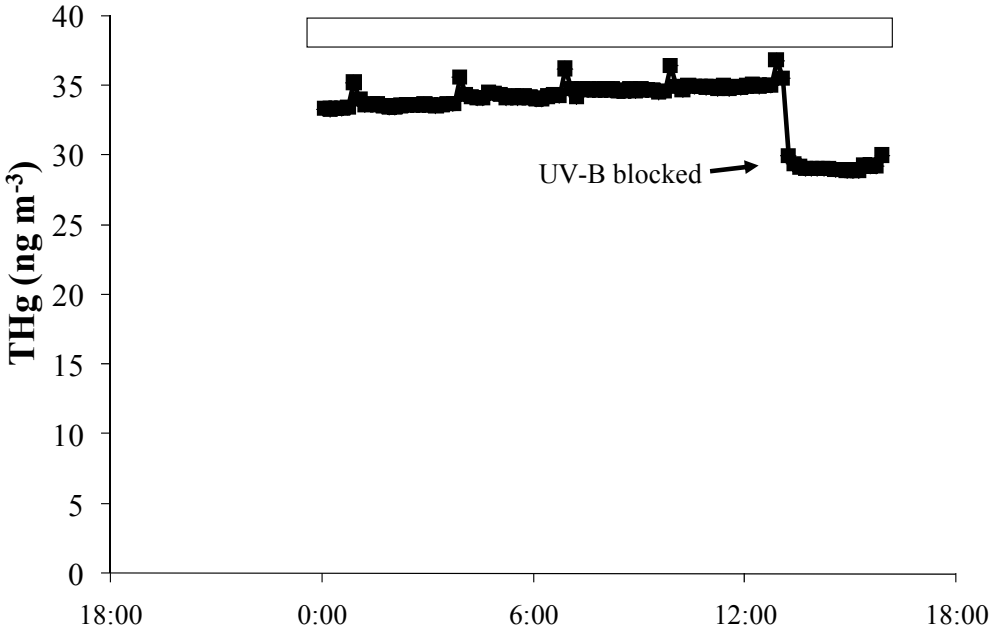

Figure 4.5 Hg volatilization from Berry's Creek II (BC II) sediments exposed to visible + UV light until UV-B is blocked by a mylar filter. Open figure above the chart indicates light was on during entire run.

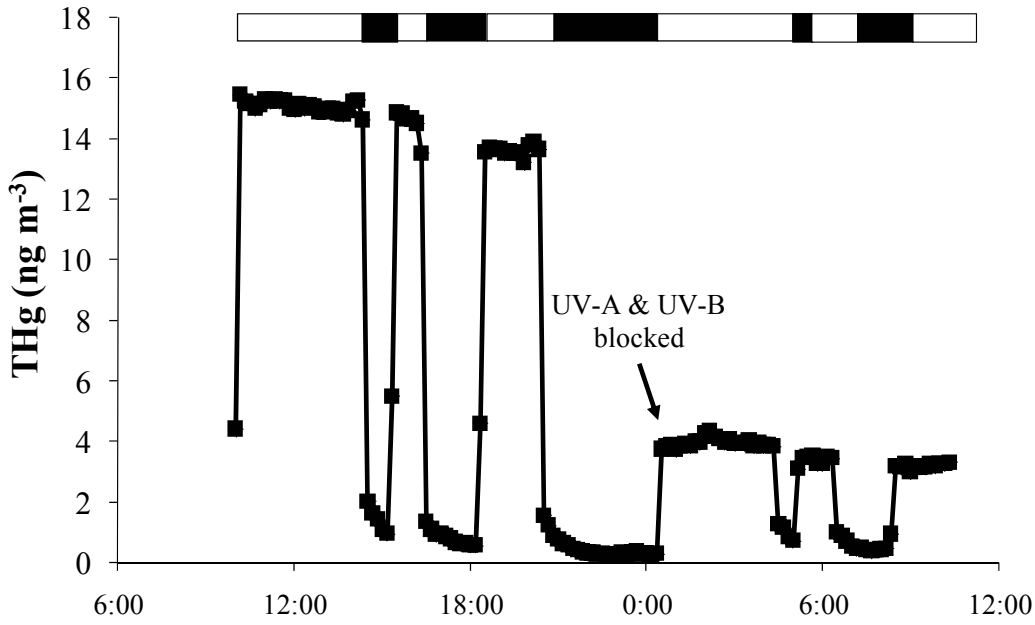

Figure 4.6 Hg Volatilization from Raritan River II (RR1) sediments exposed to alternating light/dark conditions (visible + UV) as indicated by the open (light) and shaded (dark) figure above chart. UV-A and UV-B light is blocked by a Lee model 226 filter.

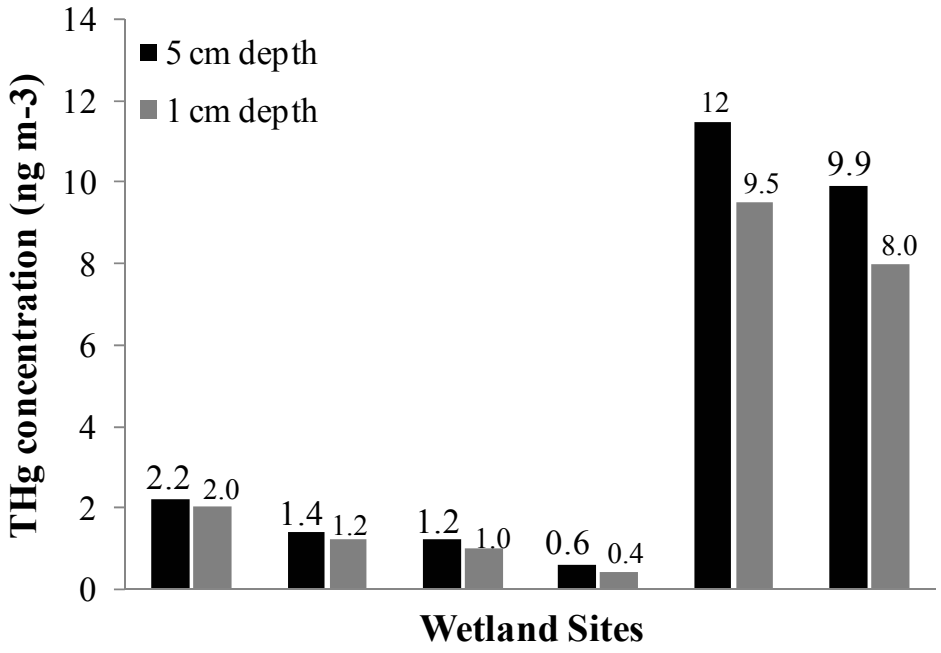

Figure 4.7 Comparison of THg concentrations between full chamber depth (5 cm) and 1 cm depth.

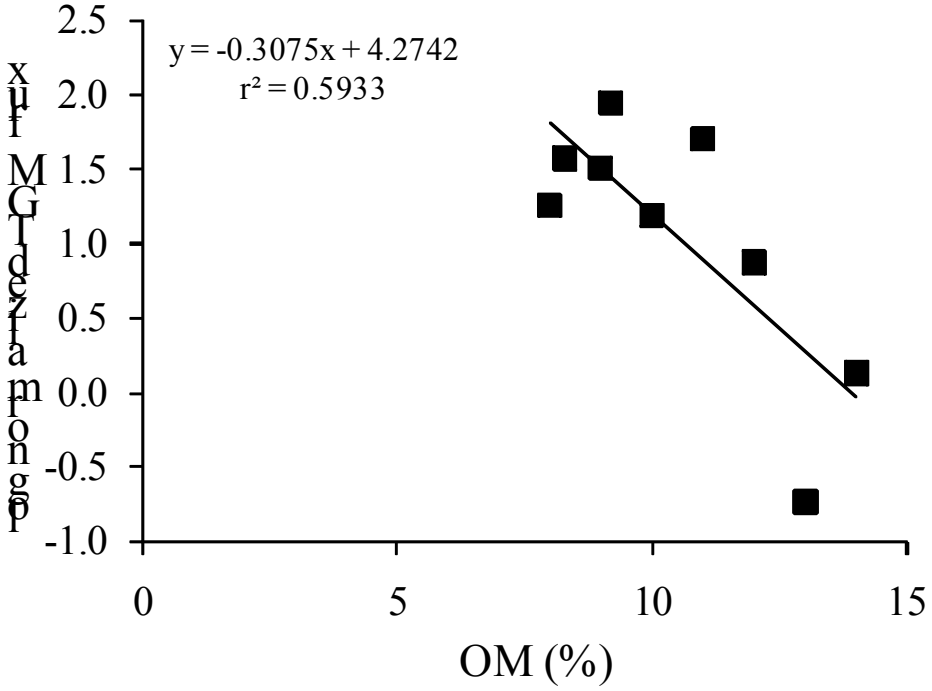

Figure 4.8 Relationship between light-driven mercury volatilization flux and sediment organic matter. Fluxes were normalized to sediment mercury content. Equation is the log-linear regression of the data excluding the Tivoli South Bay north and Secaucus High School Marsh samples (high %OM).

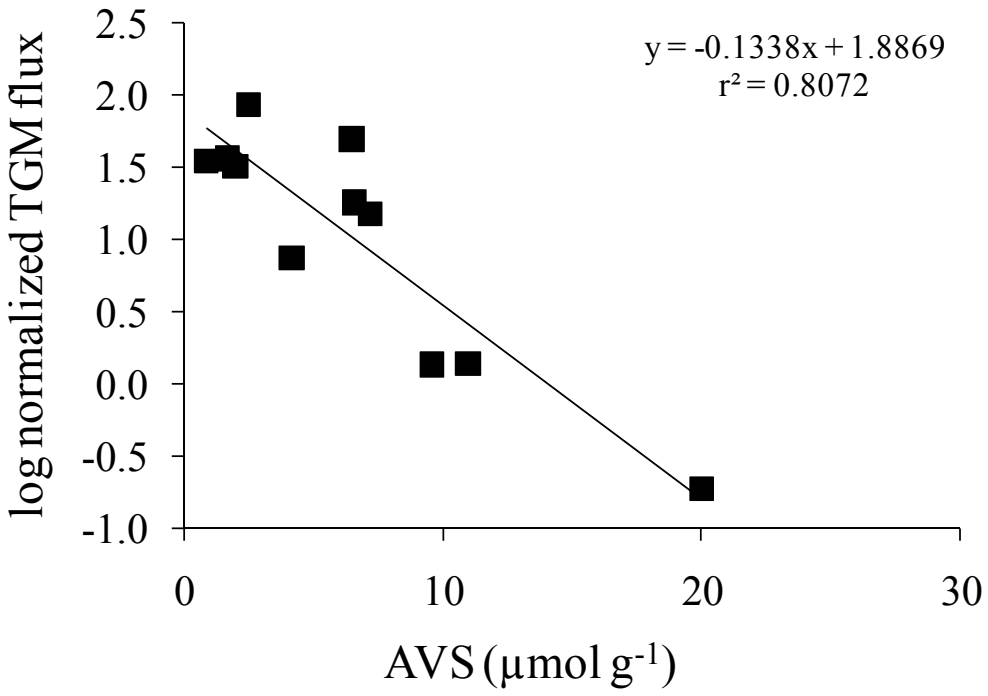

Figure 4.9 Relationship between light-driven mercury volatilization flux and sediment acid-volatile sulfide concentration. Volatilization fluxes were normalized to sediment mercury content. Equation is the log-linear regression of the data.

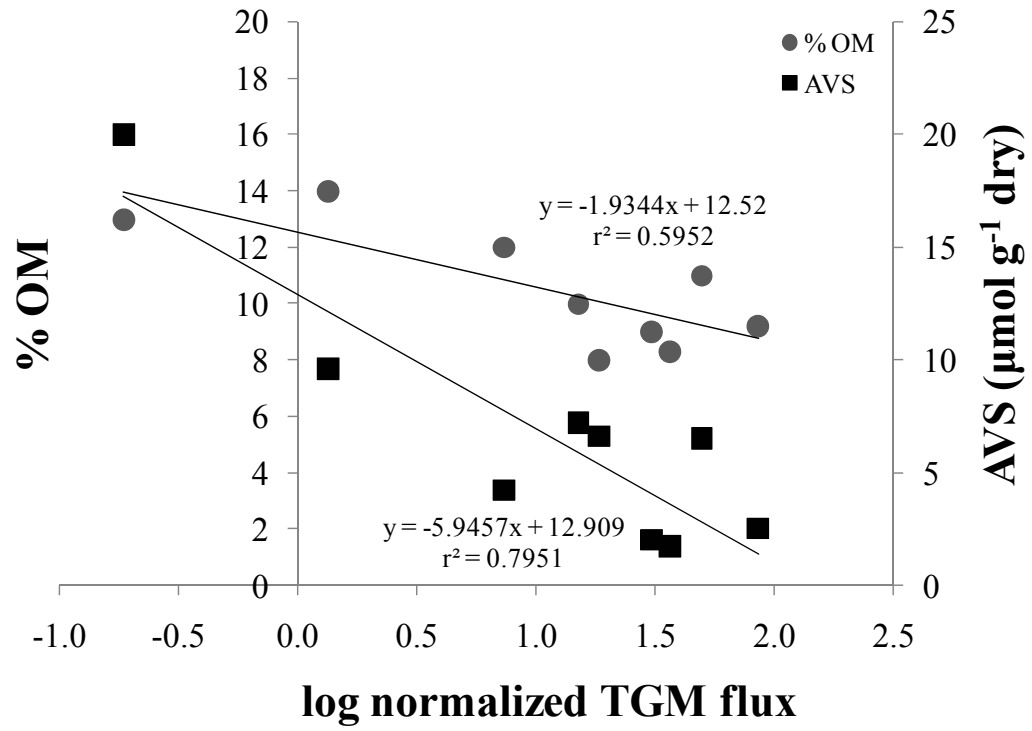

Figure 4.10 Relative contribution of %OM and AVS on light-driven mercury volatilization flux. Volatilization fluxes were normalized to sediment mercury content. Equation is the log-linear regression of the data. The relationship with AVS is significant ($p = 0.02$) but that with %OM is not ($p = 0.16$).

Chapter 5:

Conclusions

5.1 Conclusions

Mercury occurs in the environment as a result of natural and anthropogenic activities. Natural sources include volcanoes, forest fires, and vaporization of sea water while human-induced sources include waste incineration, precious metal mining, and fuel combustion. Both categories of mercury sources contribute to mercury in atmospheric deposition and the subsequent emission from the many surfaces of the Earth.

The main concern regarding mercury in the environment is its effect on humans. The organic monomethylmercury (MMHg) species is neurotoxic and can bioaccumulate in aquatic food chains. Consumers of upper trophic level aquatic species, including humans, are at the most risk. Understanding mercury transport and transformations in the aquatic environment is crucial to ultimately controlling its fate and protecting human health and the environment.

Research was conducted to better understand the land-air exchange of mercury in New Jersey wetland sediments, a reducing and highly organic environment capable of producing MMHg. Wet deposition studies were performed in two locations in NJ, one providing long-term trends to evaluate inputs to the system. These sample locations were compared with a National Atmospheric Deposition Program (NADP) Mercury Deposition Network (MDN) site in Pennsylvania. In addition, sediment-air flux experiments were performed in situ and in the laboratory to investigate the relative importance of photochemistry and such physicochemical parameters as sediment mercury and organic matter content, particle size distribution, pH, and salinity on the volatilization of mercury from tidally-exposed sediments (outputs).

Overall, the trend in New Brunswick, NJ was significantly decreasing between 1999 and 2006, with no discernable trends in Belvidere, NJ or Valley Forge, PA. However, wet deposition fluxes from the three sites remain elevated over global total atmospheric mercury fluxes, indicating that local sources are contributing. Indeed, in New Jersey, it appears that local and regional sources of particulate (Hg_p) and reactive gaseous mercury (RGM) likely explain the observed variances in wet deposition since larger scale phenomenon such as meteorology did not correlate. The Ohio River Valley, home to a number of coal-fired power plants, is a probable regional source.

Concentrations of trace metals co-emitted with mercury from various natural and man-made sources did not correlate with mercury concentrations, suggesting a variety of wet deposition contaminant sources to central NJ.

Micrometeorological studies were conducted in an impacted salt marsh wetland of the New Jersey Meadowlands (Secaucus, NJ) and in a natural background salt marsh, the Great Bay estuary (Tuckerton, NJ), by way of an eddy correlation system. Total gaseous mercury fluxes were higher in Secaucus than in Tuckerton, potentially reflecting the ten-fold higher sediment concentrations in Secaucus, but when averaged over the area of each wetland, Tuckerton had a more pronounced annual flux. Average ambient concentrations measured above both sites were elevated as compared with global background concentrations although measurements were only recorded during summer or summer-like conditions and may not be representative of average annual concentrations.

Strong positive correlations exist between cumulative mercury flux and cumulative PAR (Fig. 3.4), indicating that solar radiation was the most important factor controlling in situ volatilization of mercury from tidally-exposed sediments.

The magnitude of land-air mercury fluxes estimated in both Secaucus and Tuckerton suggest that mercury emission fluxes for large wetlands have the potential to rival industrial emissions and demonstrates that the emission of mercury from tidally-exposed wetland sediments is likely an important pathway in regional and perhaps global mercury biogeochemical cycles.

Controlled laboratory flux chamber studies were performed in an effort to investigate the importance of various wavelengths of light (visible and ultraviolet) and to evaluate several physicochemical properties of the sediments on the emission of gaseous elemental Hg from tidally-exposed sediments. Salt marsh, freshwater, and riverine sediments were collected from the New Jersey Meadowlands, Tivoli South Bay (New York) and the Raritan and Passaic Rivers, respectively.

In the presence of light, mercury flux from sediments was up to 50 times greater than in the dark, with the most enhanced emissions observed during visible + UV treatments. Most sediments volatilized between 1 and 14 ng m^{-2} h^{-1}, but Berry's Creek (NJ Meadowlands) sediments released considerably more elemental mercury (up to 30 ng m^{-2} h^{-1}) when exposed to visible + UV light. While sediment mercury concentration appeared to be an important factor in driving Hg^0 from sediments as in Chapter 3, other physicochemical characteristics may also be important. Moisture content may affect the amount of surface area with the atmosphere and subsequently, the amount of Hg volatilization from land surfaces as suggested in the comparison of sediments in this study with the cement stabilized sediments in Goodrow et al. [2005]. Hackensack River watershed upland soils (NJ Meadowlands), with half the moisture content of nearby

sediments in the Hackensack River, emitted up to four times more Hg when other sediment characteristics where nearly constant.

Light-driven mercury volatilization fluxes were significantly negatively correlated with acid volatile sulfide and organic matter content, indicating that AVS and OM are capable of sequestering Hg in sediments. However, a multiple linear regression showed that AVS was more important than OM in this process. Air temperature appeared to have an inverse effect on Hg evasion from sediments though sediment temperature may have provided a better correlation.

Studies have suggested that most of the actively cycling Hg resides in the top few millimeters to centimeters of soil where anthropogenic enrichment is greatest within the soil profile [Lindberg et al. 2007]. Indeed, sediment-air mercury fluxes were compared at two different depths in the flux chamber. Results showed that the top one cm of sediment was responsible for 73 to 91% of observed mercury volatilization fluxes as compared to the five cm depth. Using an average sediment density of 500 kg m^{-3} and average daytime fluxes in both the Secaucus High School Marsh and the Great Bay estuary, we estimated the percent of sediment Hg lost through volatilization for 1 and 5 cm sediment layers. In Secaucus, the 1 cm depth is expected to provide approximately 0.03% y^{-1} and the 5 cm depth, 0.006% y^{-1}. In the Great Bay, the contribution is greater with 0.14% y^{-1} and 0.03% y^{-1} of Hg volatilization from the 1 and 5 cm depths, respectively.

Theoretical in situ fluxes were estimated for flux chamber experiments using the measured near surface gaseous mercury concentration and conservative estimates for local micrometeorology using the modified Thornthwaite-Holtzman equation. Estimated in situ sediment-air Hg fluxes (visible + UV light) were reported (Chapter 4). The

magnitude of annual sediment-air mercury emissions to the global atmosphere using conservative micrometeorological values suggests that wetlands may indeed provide a larger portion of re-emitted mercury to the global pool than earlier studies have suggested.

A direct comparison of laboratory flux chamber fluxes and in situ micrometeorological fluxes was performed using sediment from the Secaucus High School Marsh. In situ fluxes in Secaucus ranged from 36 to 677 ng m^{-2} h^{-1}, excluding data collected in the presence of *Phragmites*. Using an average u* value of 0.2 m s^{-1}, chamber fluxes appear to be of the same order of magnitude as those measured in the field, ranging from 336 to 880 ng m^{-2} h^{-1}.

Light spectra and intensities were much greater in field studies. Sunlight is primarily visible (400 – 750 nm), with infrared (750 – 1E+06 nm), UV-A (315 – 400 nm), and trace amounts of UV-B (315 – 380 nm) and UV-C (100 – 280 nm). Measured light intensities in the field ranged from 0 (nighttime) to 2200 (afternoon) μmol m^{-2} s^{-1}. Laboratory studies were also conducted under primarily visible light (400 – 750 nm; 80 μmol m^{-2} s^{-1}), with UV-A (370 – 400 nm; 0.8 μmol m^{-2} s^{-1}), and essentially no UV-B, potentially adding to the observed greater in situ Hg fluxes.

We conclude that photochemistry is the most important force driving the volatilization of mercury from tidally-exposed sediments. The results of this study suggest that gaseous elemental mercury is released to the atmosphere at the greatest rate in the presence of both visible and ultraviolet radiation, as in the natural environment. With the depletion of the ozone layer, mechanisms and rates of photochemical processes occurring near the surface may be altered, potentially further enhancing mercury

volatilization from tidally-exposed wetland sediments to the global atmosphere. These studies indicate that the volatilization of elemental mercury from naturally enriched or industrially contaminated soils and sediments is an important pathway in the redistribution of mercury on watershed to global scales.

5.1.1. *Local, regional, global cycling*

In NJ, the largest input of both natural and anthropogenic mercury to the environment is believed to be atmospheric deposition (approximately 50% from nearby point sources; NJ DEP 2002) and the major output is volatilization. A mercury budget for NJ has been estimated (NJ DEP 2002), providing anthropogenically-derived point sources to the State on the order of 3 t y^{-1}.

The estimated wet deposition flux for NJ is approximately 0.3 t y^{-1}, which is comparable to recent estimates of 0.4 – 0.5 t y^{-1} [Reinfelder 2000]. The Mercury Task Force report [NJ DEP 2002] did not provide an estimate of mercury fluxes from historical repositories, such as sediments. Using conservative fluxes, salt marsh sediments contribute an estimated 0.3 t y^{-1}. At the high end of observed in situ fluxes, this estimate may reach 4 t y^{-1}. Freshwater wetland sediments (estimated from fluxes in Tivoli South Bay, NY) could contribute an additional 4 t y^{-1}.

Since the approximation of mercury volatilization from tidally-exposed wetland sediments appears to be elevated over atmospheric deposition without the inclusion of volatilization from other land surfaces, it appears that New Jersey is a net source of mercury to the atmosphere as concluded in the NJ DEP [2002] Mercury Task Force report.

5.2. Data gaps and suggested future research

The natural environment is highly variable, an inherent uncertainty in any environmental estimation. Several factors that may have differed between study sites include: salinity, water content, and sediment temperature. While air temperature did not appear to correlate with Hg emission, sediment temperature may have been a better measure. The effects of these parameters on mercury volatilization should be elucidated in future studies.

Further investigation of the effects UV light is suggested, including a combination of visible light with a number of different wavelengths in both the UV-A and UV-B ranges. A mercury flux per photon estimation would be beneficial in comparing sites with varying degrees of light intensity.

The evaluation of organic matter composition and different types of minerals on Hg emission rates is suggested to better our understanding of the relationships mercury has with other nutrients in the natural ecosystem. In fact, isotope fractionation of Hg in sediments may aid in determining the specific isotopes of volatile mercury species in sediments as lighter isotopes are expected to be preferentially enriched in the gas phase [Zheng et al. 2007].

Direct uptake of mercury by plants from soil and water has been observed [Maury-Brachet et al. 1990; Ericksen et al. 2003]. Differences in size and species of plants in Secaucus High School Marsh compared with those in the Great Bay estuary may have contributed to varying uptake and release rates of mercury. Determining the role of vascular plants in mercury cycling would be valuable to future research since plant uptake has the potential to contribute substantially to mercury in food webs.

While a diurnal trend over tidally-exposed wetland sediments was observed, it would also be beneficial to investigate whether a diurnal trend exists over wetland grasses.

Finally, we need to develop a more robust method of measuring mercury in dry deposition and conduct long term studies comparing wet and dry deposition processes. Without dry deposition data, a large data gap exists in the source attribution of mercury in atmospheric deposition.

References

Ericksen, J., M.S. Gustin, D. Schorran, D. Johnson, S. Lindberg, and J. Coleman (2003), Accumulation of atmospheric mercury in forest foliage, *Atmos. Environ., 37,* 1613-1622.

Goodrow, S., R. Miskewitz, R.I. Hires, S.J. Eisenreich, W.S. Douglas, and J.R. Reinfelder (2005), Mercury emissions from cement-stabilized dredged material, *Environ. Sci. Technol., 39,* 8185-8190.

Kim, K.-H., S.E. Lindberg, and T.P. Meyers (1995), Micrometeorological measurements of mercury vapor fluxes over background forest soils in eastern Tennessee, *Atmos. Environ., 29(2)*, 267-282.

Lindberg et. al 2007

Maury-Brachet, R., F. Ribeyre, and A. Boudou (1990), Actions and reactions of temperature and photoperiod on Hg accumulation by *Elodea densa* from sediment source, *Ecotoxicol. Environ. Saf., 10,* 141-155.

NJ DEP (2002), Sources of mercury in New Jersey, New Jersey Mercury Task Force, Vol. III.

Reinfelder, J.R. (2000), Atmospheric deposition of mercury to the New York - New Jersey harbor estuary and watershed. In: M.P. Weinstein, K.E. Kosko, and L.S. Young, eds., Proceedings – The Significance of Atmospheric Pollutant Loading to the New York-New Jersey Harbor Estuary and Watershed (April 13, 2000), NJSG-00-443. New Jersey Marine Sciences Consortium and New Jersey Department of Environmental Protection.

Zheng, W., D. Foucher, and H. Hintelmann (2007), Mercury isotope fractionation during volatilization of Hg(0) from solution into the gas phase, *J. Analyt. Atom. Spectros., 22,* 1097-1104.

Appendix A

Meteorological Data

A.1 New Brunswick, NJ: Meteorological parameters averaged (median wind direction) over sample period at Rutgers Gardens. Dash (-) indicates no data available.

date	wind speed (10m) (m/s)	wind direction (10m) (deg)	T (deg C)	pressure (mb)	RH (%)
27-Nov-99	1.7	197	8	1016	80
8-Dec-99	1.7	274	5	1018	68
20-Dec-99	2.0	188	3	1016	76
13-Jan-00	2.0	244	2	1012	70
26-Jan-00	2.2	287	-6	1012	63
5-Feb-00	2.1	276	-5	1013	65
19-Feb-00	1.8	227	-1	1015	69
14-Mar-00	2.0	233	5	1015	69
24-Mar-00	2.4	110	3	1022	73
6-Apr-00	2.4	229	10	1005	67
17-Apr-00	1.8	161	8	1014	72
29-Apr-00	-	-	-	-	-
5-Jun-00[a]	1.6	126	15	1012	78
17-Jun-00	2.1	210	20	1015	81
30-Jun-00	1.5	217	24	1013	77
22-Jul-00	1.4	218	23	1011	73
28-Jul-00	1.4	84	21	1018	83
4-Aug-00	1.5	127	25	1015	88
15-Aug-00	1.5	215	25	1012	81
29-Aug-00	1.3	229	22	1016	79
8-Sep-00	1.6	126	22	1018	82
21-Sep-00	1.5	220	21	1012	79
2-Oct-00	1.2	200	14	1016	82
8-Nov-00	1.4	247	11	1016	75
21-Nov-00	1.9	249	7	1009	75
2-Dec-00	2.0	268	2	1015	71
17-Dec-00	1.9	223	0	1018	73
5-Jan-01[b]	2.3	247	1	-	69
21-Jan-01	-	-	-	-	-
1-Feb-01	-	-	-	-	-
23-Feb-01	2.0	251	1	1017	70
9-Mar-01	2.1	272	1	1009	74
20-Mar-01	2.1	258	4	1011	70
28-Mar-01	2.8	282	3	1009	67
5-Apr-01	1.7	203	5	1013	76

12-Apr-01	2.0	131	8	1014	85
21-May-01	1.8	220	15	981	72
30-May-01	1.9	73	16	1010	86
21-Jun-01	1.5	219	24	1012	70
5-Jul-01	1.5	221	28	1016	73
26-Jul-01	1.4	221	27	1012	70
15-Aug-01	1.4	202	25	1016	72
19-Sep-01	1.2	206	21	1015	74
3-Oct-01	1.4	202	17	1012	80
24-Oct-01	1.5	213	14	1016	73
12-Dec-01	1.6	223	10	1018	71
8-Jan-02	1.9	263	2	1009	67
29-Jan-02	1.9	236	4	1010	69
26-Feb-02	1.6	203	5	1014	64
19-Mar-02	1.7	191	6	1016	69
13-Apr-02	1.8	236	8	1016	66
6-May-02	1.3	265	14	1012	69
24-May-02	1.9	248	14	1014	68
21-Jun-02	1.8	192	20	1012	76
17-Jul-02	1.4	239	26	1013	70
12-Aug-02	1.6	203	24	1015	70
3-Sep-02	1.5	198	24	1015	75
30-Sep-02	1.4	210	20	1015	75
22-Oct-02	1.8	203	15	1015	80
19-Feb-03	2.1	242	-3	1013	71
3-Mar-03	1.9	197	0	1012	74
26-Mar-03	2.0	206	5	1012	71
8-Apr-03	2.6	97	6	1014	79
19-Apr-03	3.1	83	10	1016	73
14-May-03	1.9	201	13	1009	75
27-May-03	1.9	81	13	1018	82
6-Jun-03	1.6	223	16	1005	-
30-Jun-03	1.4	203	21	1011	83
25-Jul-03	1.5	222	24	1012	80
20-Sep-03	1.5	202	23	1015	85
5-Oct-03	1.4	225	17	1014	84
28-Oct-03	1.7	232	12	1009	79
21-Nov-03	1.7	226	10	1015	82
16-Dec-03	1.7	247	3	1012	78
8-Jan-04	1.0	230	4	1012	76
20-Mar-04	2.0	265	0	1013	69
16-Apr-04	2.4	206	7	1011	75
10-May-04	2.2	210	15	1015	76

2-Jun-04	1.6	193	18	1012	86
24-Jun-04	1.6	218	21	1014	79
8-Jul-04	1.4	216	23	1013	76
19-Jul-04	1.6	229	21	1009	86
11-Aug-04	1.4	205	23	1013	84
4-Sep-04	1.3	202	23	1015	85
29-Sep-04	1.6	137	20	1017	86
22-Oct-04	1.3	223	13	1013	85
17-Nov-04	1.5	244	9	1016	77
12-Dec-04	2.0	217	8	1011	85
3-Jan-05	1.8	241	1	1017	75
26-Jan-05	2.0	254	-1	1015	82
19-Feb-05	1.7	244	0	1016	74
14-Mar-05	2.3	268	0	1006	73
7-Apr-05	2.2	205	6	1009	77
27-May-05	1.8	201	13	1011	74
20-Jun-05	1.7	216	21	1011	74
13-Jul-05	1.5	207	23	1014	75
5-Aug-05	0.9	266	26	1014	73
30-Aug-05	1.1	208	24	1014	73
23-Sep-05	1.3	211	22	1015	70
17-Oct-05	1.5	175	17	1014	80
10-Nov-05	1.2	222	11	1010	73
5-Dec-05	1.5	233	5	1012	67
28-Dec-05	1.3	260	-1	1013	69
20-Jan-06	1.4	221	3	1007	77
14-Feb-06	1.9	245	2	1009	69
3-Apr-06	2.1	259	2	1013	57
28-Apr-06	2.0	236	12	1009	60
26-May-06	1.8	204	14	1008	63
14-Jun-06	1.3	224	19	1009	76
11-Jul-06	1.5	217	23	1014	73
18-Jul-06	1.2	222	26	1012	74
25-Jul-06	1.6	204	24	1012	79

[a]Data from 16-May-00 through 5-Jun-00 only.
[b]Data from 17-Dec-00 through 25-Dec-00 only.

Appendix B

Mean Mercury Concentrations in Wet Deposition

B.1 New Brunswick, NJ: sample collection dates, sample intervals, sample volumes, rain depths, blank corrected mean concentrations, and fluxes. Dash (-) indicates data unavailable. Data from 27-Nov-99 through 22-Oct-02 from Zhuang [2004].

sample end date	sample interval (d)	sample volume (L)	rain depth (cm)	mean concentration (ng L^{-1})	flux (ng/m^2/d)
27-Nov-99	12	0.81	4.5	7.2	5.4
8-Dec-99	11	0.36	2.0	4.2	1.5
20-Dec-99	12	1.0	5.8	40	39
13-Jan-00	24	0.77	4.3	13	4.8
26-Jan-00	13	0.28	1.6	3.5	0.9
5-Feb-00	10	0.42	2.4	3.3	1.5
19-Feb-00	14	0.87	4.8	6.2	4.3
14-Mar-00	24	0.77	4.3	10	3.7
24-Mar-00	10	0.70	3.9	7.8	6.1
6-Apr-00	13	0.78	4.3	11	7.6
17-Apr-00	11	0.82	4.6	12	10
29-Apr-00	12	0.73	4.1	12	7.9
5-Jun-00	37	0.45	2.5	13	1.8
17-Jun-00	12	1.0	5.8	4.7	4.5
30-Jun-00	13	0.41	2.3	7.7	2.7
22-Jul-00	22	0.83	4.6	18	7.5
28-Jul-00	6	1.1	6.0	11	23
4-Aug-00	7	1.0	5.8	18	30
15-Aug-00	11	1.9	11	11	22
29-Aug-00	14	0.20	1.1	18	2.8
8-Sep-00	10	0.66	3.7	14	10
21-Sep-00	13	1.1	6.0	27	25
2-Oct-00	11	0.70	3.9	12	8.5
8-Nov-00	37	0.37	2.0	14	1.5
21-Nov-00	13	0.96	5.3	18	15
2-Dec-00	11	0.95	5.3	6.0	5.7
17-Dec-00	15	1.1	6.0	13	10
5-Jan-01	19	0.72	4.0	5.4	2.3
21-Jan-01	16	1.2	6.5	15	12
1-Feb-01	11	0.42	2.3	6.8	2.9
23-Feb-01	22	1.0	5.8	13	6.7
9-Mar-01	14	0.62	3.5	12	6.2

20-Mar-01	11	0.92	5.1	15	14
28-Mar-01	8	0.93	5.1	4.6	5.9
5-Apr-01	8	1.1	6.0	7.5	11
12-Apr-01	7	0.90	5.0	19	28
21-May-01	39	0.21	1.2	16	1.0
30-May-01	9	1.2	6.5	13	20
21-Jun-01	22	2.6	14	25	33
5-Jul-01	14	1.1	6.0	19	16
26-Jul-01	21	0.90	5.0	37	18
15-Aug-01	20	1.4	7.9	23	18
19-Sep-01	35	1.1	6.0	34	12
3-Oct-01	14	0.85	4.7	6.4	4.3
24-Oct-01	21	0.21	1.2	12	1.4
12-Dec-01	49	1.0	5.8	10	2.5
8-Jan-02	27	1.0	5.8	11	4.8
29-Jan-02	21	0.72	4.0	8.6	3.3
26-Feb-02	28	0.50	2.8	9.8	2.0
19-Mar-02	21	1.1	6.0	3.6	2.0
13-Apr-02	25	1.1	6.0	5.6	2.7
6-May-02	23	1.5	8.1	1.6	1.1
24-May-02	18	1.1	6.0	0.7	0.5
21-Jun-02	28	1.6	9.1	0.0	0.0
17-Jul-02	26	0.43	2.4	0.2	0.0
12-Aug-02	26	1.8	10	0.5	0.4
3-Sep-02	22	1.1	6.0	27	15
30-Sep-02	27	1.5	8.4	12	7.2
22-Oct-02	22	1.1	6.0	12	6.8
19-Feb-03	24	0.75	4.2	2.4	0.8
3-Mar-03	12	1.0	5.8	8.1	7.8
26-Mar-03	23	1.0	5.8	31	16
8-Apr-03	13	0.83	4.6	15	11
19-Apr-03	11	0.58	3.2	7.5	4.4
14-May-03	25	0.59	3.3	11	2.8
27-May-03	13	1.4	7.6	7.6	9.0
6-Jun-03	10	1.8	10	7.3	15
30-Jun-03	24	1.1	5.9	15	7.4
25-Jul-03	25	1.1	6.0	20	10
20-Sep-03	57	0.27	1.5	11	0.6
5-Oct-03	15	1.0	5.7	9.2	7.1
28-Oct-03	23	1.4	8.0	8.8	6.2

21-Nov-03	24	1.1	6.0	3.6	1.8
16-Dec-03	25	1.0	5.5	6.4	2.9
8-Jan-04	23	1.0	5.7	6.2	3.1
20-Mar-04	72	1.1	5.9	15	2.5
16-Apr-04	27	1.0	5.8	13	5.8
10-May-04	24	1.6	9.0	9.9	7.4
2-Jun-04	23	1.4	7.6	14	9.2
24-Jun-04	22	0.70	3.9	7.8	2.8
8-Jul-04	14	1.0	5.7	8.2	6.8
19-Jul-04	11	-	-	5.4	-
11-Aug-04	23	1.4	5.7	4.0	2.0
4-Sep-04	24	1.0	5.8	8.8	4.3
29-Sep-04	25	1.0	5.8	12	5.8
22-Oct-04	23	0.83	4.6	12	4.8
17-Nov-04	26	1.2	6.8	4.4	2.3
12-Dec-04	25	3.1	17	4.2	5.9
3-Jan-05	22	0.38	2.1	3.4	0.7
26-Jan-05	23	1.1	6.1	6.6	3.5
19-Feb-05	24	0.83	4.6	4.6	1.8
14-Mar-05	23	0.98	5.5	4.2	2.0
7-Apr-05	24	1.1	5.9	8.6	4.2
27-May-05	50	0.97	5.4	12	2.5
20-Jun-05	24	0.77	4.3	12	4.4
13-Jul-05	23	3.4	19	6.2	10
5-Aug-05	23	1.0	5.8	8.8	4.5
30-Aug-05	25	0.53	2.9	8.8	2.1
23-Sep-05	24	0.84	4.7	14	5.6
17-Oct-05	24	2.8	15	5.4	7.0
10-Nov-05	24	1.2	6.8	5.8	3.3
5-Dec-05	25	-	-	4.6	-
28-Dec-05	23	1.1	6.1	5.2	2.8
20-Jan-06	23	1.4	7.8	5.2	3.6
14-Feb-06	25	1.4	7.9	12	7.9
3-Apr-06	48	0.51	2.8	16	1.9
28-Apr-06	25	1.3	7.3	17	10
26-May-06	28	1.1	6.2	7.6	3.4
14-Jun-06	19	1.2	6.8	14	10
11-Jul-06	27	1.2	6.6	13	6.3
18-Jul-06	7	0.59	3.3	9.2	8.6
25-Jul-06	7	0.69	3.8	19	21

B.2 Belvidere, NJ: sample collection dates, sample intervals, sample volumes, rain depths, blank corrected mean concentrations, and fluxes. Dash (-) indicates data unavailable.

sample end date	sample interval (d)	sample volume (L)	rain depth (cm)	mean concentration (ng L^{-1})	flux ($ng/m^2/d$)
15-Nov-02	12	0.83	4.6	7.6	5.9
26-Nov-02	11	1.0	5.8	4.8	5.1
8-Dec-02	12	0.49	2.7	3.1	1.4
21-Dec-02	13	1.1	5.9	8.7	7.9
2-Jan-03	12	1.1	6.0	6.7	6.8
13-Jan-03	11	0.38	2.1	6.0	2.3
25-Jan-03	12	0.05	0.3	18	0.7
6-Feb-03	12	0.22	1.2	19	3.8
19-Feb-03	13	0.68	3.8	9.2	5.3
3-Mar-03	12	1.0	5.7	4.5	4.3
14-Mar-03	11	1.0	5.8	3.7	4.0
26-Mar-03	12	0.86	4.8	3.1	2.5
8-Apr-03	13	0.83	4.6	14	10
19-Apr-03	11	0.61	3.4	6.8	4.2
1-May-03	12	0.29	1.6	6.1	1.6
14-May-03	13	0.49	2.7	15	6.2
25-May-03	11	0.51	2.8	4.5	2.3
6-Jun-03	12	1.8	9.7	11	17
18-Jun-03	12	1.1	6.2	9.4	10
30-Jun-03	12	1.1	5.9	13	13
12-Jul-03	12	0.16	0.9	15	2.2
25-Jul-03	13	1.3	7.0	17	18
5-Aug-03	11	1.1	5.9	8.7	9.3
17-Aug-03	12	0.31	1.7	15	4.1
29-Aug-03	12	0.21	1.1	9.7	1.8
10-Sep-03	12	0.91	5.0	11	10
18-Sep-03	8	0.45	2.5	12	7.2
20-Sep-03	2	0.34	1.9	13	25
5-Oct-03	15	1.2	6.4	12	10
16-Oct-03	11	0.87	4.8	8.7	7.6
28-Oct-03	12	1.0	5.8	7.2	7.0

9-Nov-03	12	1.0	5.8	4.7	4.6
21-Nov-03	12	1.1	6.0	13	13
3-Dec-03	12	0.98	5.5	8.4	7.7
16-Dec-03	13	1.1	6.2	2.6	2.5
28-Dec-03	12	1.1	5.9	3.5	3.5
8-Jan-04	11	0.55	3.0	9.0	5.0
20-Jan-04	12	0.28	1.6	> 77 [1]	-
1-Feb-04	12	0.28	1.6	> 77 [1]	-
13-Feb-04	12	0.31	1.7	5.2	1.5
9-Mar-04	25	0.83	2.8	7.6	1.7
20-Mar-04	11	0.57	3.2	2.7	1.6
3-Apr-04	14	0.70	3.9	6.3	3.5
16-Apr-04	13	0.62	3.5	5.7	3.0
10-May-04	24	1.1	5.9	17	8.4
20-May-04	10	0.82	4.5	13	12
2-Jun-04	13	0.88	4.9	15	12
12-Jun-04	10	0.73	4.1	10	8.4
24-Jun-04	12	0.35	2.0	9.9	3.2
7-Jul-04	13	0.29	1.6	9.1	2.3
18-Jul-04	11	1.3	7.5	1.2	1.7
30-Jul-04	12	1.2	6.6	7.9	8.7
11-Aug-04	12	0.64	3.6	29	17
23-Aug-04	12	1.9	11	6.1	11
16-Sep-04	24	1.1	6.1	3.8	1.9
27-Sep-04	11	2.6	15	6.3	17
10-Oct-04	13	1.1	5.9	2.4	2.2
22-Oct-04	12	0.88	4.9	9.5	7.8
17-Nov-04	26	0.85	4.8	6.0	2.2
27-Nov-04	10	0.38	2.1	7.1	3.0
9-Dec-04	12	1.0	5.8	3.9	3.7
22-Dec-04	13	0.48	2.7	4.1	1.7
3-Jan-05	12	0.53	3.0	1.8	0.9
14-Jan-05	11	1.0	5.7	13	14
26-Jan-05	12	0.52	2.9	2.4	1.2
19-Feb-05	24	0.75	4.2	5.1	1.8
3-Mar-05	12	0.71	3.9	2.8	1.9
26-Mar-05	23	0.77	4.3	6.7	2.5
7-Apr-05	12	1.0	5.7	3.2	3.1
19-Apr-05	12	0.26	1.5	7.7	1.9
2-May-05	13	1.0	5.7	12	10
27-May-05	25	0.68	3.8	11	3.5
7-Jun-05	11	0.86	4.8	15	13

20-Jun-05	13	0.52	2.9	15	6.8
30-Jun-05	10	0.47	2.6	25	13
13-Jul-05	13	1.1	6.2	10	10
25-Jul-05	12	0.69	3.8	10	6.5
18-Aug-05	24	0.74	4.1	13	4.6
13-Sep-05	26	0.37	2.1	12	1.9
23-Sep-05	10	1.1	6.4	6.5	8.3
17-Oct-05	24	1.0	5.7	8.9	4.2
28-Oct-05	11	1.0	5.8	5.3	5.5
11-Nov-05	14	0.27	1.5	13	2.7

[1]Sample contained unusually high concentrations of Hg, causing it to exceed the upper limit of detection. The value reported is the upper limit of detection for the day of analysis.
[2]High sample volume due to hurricane Jeanne.

B.3 Valley Forge, PA (MDN): sample collection dates, sample intervals, sample volumes, rain depths, blank corrected mean concentrations, and fluxes.

sample end date	sample interval (d)	sample volume (L)	rain depth (cm)	mean concentration (ng L^{-1})	flux (ng/m^2/d)
30-Nov-99	7	0.49	4.1	8.17	1.14
7-Dec-99	7	0.21	1.8	6.2	0.38
13-Dec-99	6	0.05	0.4	3.82	0.14
21-Dec-99	8	0.54	4.5	9.32	1.52
11-Jan-00	7	0.37	3.1	3.82	0.45
18-Jan-00	7	0.02	0.2	20.64	0.39
26-Jan-00	7	0.09	0.8	9.43	0.92
1-Feb-00	6	0.28	2.4	12.91	1.14
8-Feb-00	7	0.04	0.4	8.69	0.12
15-Feb-00	7	0.17	1.4	7.71	0.40
22-Feb-00	7	0.32	2.7	5.78	0.65
29-Feb-00	7	0.10	0.8	8.68	0.27
14-Mar-00	7	0.31	2.5	14.91	1.28
21-Mar-00	7	0.33	2.7	5.94	0.68
28-Mar-00	7	1.41	11.8	5.28	2.00
4-Apr-00	7	0.14	1.2	10.71	0.49
11-Apr-00	7	0.16	1.3	16.49	0.98
18-Apr-00	7	0.42	3.5	16.99	2.12
25-Apr-00	7	0.19	1.6	18.19	0.93
2-May-00	7	0.04	0.4	34.61	0.45
16-May-00	7	0.34	2.8	18.54	1.82
23-May-00	7	0.57	4.7	15.51	2.47
30-May-00	7	0.31	2.5	14.71	1.27
6-Jun-00	7	0.15	1.3	3.7	0.16
14-Jun-00	8	0.48	4.0	11.47	1.79
20-Jun-00	6	0.36	3.0	9.17	0.98
27-Jun-00	7	0.41	3.4	10.33	1.30
4-Jul-00	7	0.14	1.2	15.69	0.60
11-Jul-00	7	0.08	0.6	12.39	0.28
18-Jul-00	7	0.26	2.1	17	1.24
25-Jul-00	7	0.14	1.2	32.81	1.37
1-Aug-00	7	1.16	9.7	2.84	1.02
8-Aug-00	7	0.49	4.1	11.68	1.60
15-Aug-00	7	0.34	2.9	10.3	1.03

22-Aug-00	7	0.02	0.2	19.87	0.19
29-Aug-00	7	0.04	0.4	10.34	0.20
5-Sep-00	8	0.11	0.9	19.79	0.49
20-Sep-00	8	1.24	10.3	8.48	2.89
26-Sep-00	6	0.56	4.7	8.2	1.62
3-Oct-00	7	0.05	0.4	13.27	0.22
10-Oct-00	7	0.25	2.1	11.69	0.88
24-Oct-00	7	0.12	1.0	14.77	1.01
14-Nov-00	7	0.30	2.5	14.39	1.32
21-Nov-00	7	0.05	0.4	5.7	0.08
28-Nov-00	7	0.39	3.3	12.75	1.52
5-Dec-00	7	0.04	0.4	4.31	0.06
12-Dec-00	7	0.00	0.0	154.73	0.07
19-Dec-00	7	1.26	10.5	12.24	4.45
26-Dec-00	7	0.03	0.2	9.68	0.07
9-Jan-01	7	0.06	0.5	6.56	0.11
16-Jan-01	7	0.05	0.4	10.06	0.16
23-Jan-01	7	0.51	4.2	17.67	3.15
31-Jan-01	8	0.22	1.9	7.1	0.43
6-Feb-01	6	0.50	4.2	2.61	0.43
13-Feb-01	7	0.01	0.1	20.5	0.06
20-Feb-01	7	0.15	1.2	3.98	0.18
27-Feb-01	7	0.15	1.3	21.46	1.30
6-Mar-01	7	0.24	2.0	19.18	1.25
13-Mar-01	7	0.32	2.6	4.56	0.41
20-Mar-01	7	0.24	2.0	12.34	0.65
27-Mar-01	7	0.37	3.1	3.05	0.33
3-Apr-01	7	0.59	4.9	5.66	1.03
10-Apr-01	7	0.16	1.4	21.54	0.88
17-Apr-01	7	0.27	2.3	20.23	1.83
24-Apr-01	7	0.07	0.6	16.18	0.39
22-May-01	7	0.53	4.5	16.23	2.30
29-May-01	7	0.48	4.0	8.84	1.38
5-Jun-01	7	0.27	2.2	10.54	0.70
12-Jun-01	7	0.01	0.1	37.76	0.10
19-Jun-01	7	0.88	7.3	9.59	2.22
26-Jun-01	7	0.06	0.5	12.2	0.22
3-Jul-01	7	0.46	3.8	13.4	1.69
17-Jul-01	7	0.00	0.0	44.24	0.08
24-Jul-01	7	0.31	2.6	13.48	1.05
31-Jul-01	7	0.02	0.1	32.25	0.15
7-Aug-01	7	0.18	1.5	11.67	0.59

14-Aug-01	7	0.39	3.3	13.79	1.51
11-Sep-01	7	0.05	0.5	15.84	0.26
18-Sep-01	7	0.17	1.5	7.46	0.41
2-Oct-01	7	0.04	0.4	10.02	0.13
9-Oct-01	7	0.03	0.2	10.86	0.10
16-Oct-01	6	0.09	0.7	5.05	0.15
6-Nov-01	7	0.03	0.3	4.17	0.04
18-Dec-01	14	0.56	4.6	10.24	1.83
26-Dec-01	8	0.13	1.1	2.08	0.08
8-Jan-02	6	0.35	2.9	3.55	0.42
15-Jan-02	7	0.11	0.9	2.39	0.09
22-Jan-02	7	0.17	1.4	4.16	0.22
29-Jan-02	7	0.25	2.1	6.69	0.51
5-Feb-02	7	0.14	1.1	9.84	0.40
12-Feb-02	7	0.04	0.3	21.14	0.29
26-Feb-02	7	0.06	0.5	10.12	0.19
5-Mar-02	7	0.32	2.7	2.17	0.23
12-Mar-02	7	0.04	0.3	10.83	0.15
19-Mar-02	7	0.29	2.4	31.52	3.06
26-Mar-02	7	0.28	2.3	6.06	0.54
2-Apr-02	7	0.30	2.5	9.5	0.85
9-Apr-02	7	0.01	0.1	50.51	0.35
23-Apr-02	6	0.24	2.0	14.89	2.89
8-May-02	15	0.59	4.9	13.13	1.26
14-May-02	6	0.57	4.8	19.26	3.31
21-May-02	7	0.51	4.3	7.14	1.15
28-May-02	7	0.02	0.2	37.07	0.26
11-Jun-02	7	0.60	5.0	9.11	1.69
18-Jun-02	7	0.25	2.1	15.77	1.32
25-Jun-02	7	0.35	2.9	15.23	1.81
2-Jul-02	7	0.28	2.3	6.94	0.61
16-Jul-02	7	0.09	0.8	16.53	0.42
23-Jul-02	7	0.12	1.0	14.58	0.61
30-Jul-02	7	0.02	0.1	54.32	0.25
6-Aug-02	7	0.03	0.2	31.97	0.32
20-Aug-02	7	0.03	0.2	41.18	0.41
27-Aug-02	7	0.16	1.3	17.63	0.91
3-Sep-02	7	0.63	5.3	2.83	0.58
24-Sep-02	14	0.11	1.0	14.68	0.62
1-Oct-02	7	0.77	6.4	2.63	0.66
8-Oct-02	7	0.06	0.5	30.72	0.70
5-Nov-02	7	0.42	3.5	4.93	0.64

12-Nov-02	7	0.18	1.5	6.18	0.36
19-Nov-02	7	0.99	8.3	2.67	0.87
26-Nov-02	7	0.09	0.7	2.71	0.07
3-Dec-02	7	0.10	0.9	5.56	0.18
10-Dec-02	7	0.25	2.1	1.97	0.14
17-Dec-02	7	0.71	5.9	5.38	1.24
24-Dec-02	7	0.19	1.6	6.16	0.33
31-Dec-02	7	0.46	3.8	4.06	1.75
7-Jan-03	7	0.46	3.8	7.34	1.14
4-Feb-03	7	0.05	0.4	8.09	0.19
11-Feb-03	7	0.23	1.9	5.06	0.09
18-Feb-03	7	0.28	2.3	5.48	0.46
25-Feb-03	7	0.65	5.4	4.02	0.83
4-Mar-03	7	0.22	1.8	11.92	0.76
11-Mar-03	7	0.29	2.4	7.15	0.66
25-Mar-03	8	0.42	3.5	20.15	2.72
1-Apr-03	7	0.28	2.3	10.83	1.12
8-Apr-03	7	0.09	0.7	12.02	0.59
22-Apr-03	7	0.07	0.6	13.06	0.24
29-Apr-03	7	0.07	0.5	8.43	0.25
6-May-03	7	0.02	0.1	71.87	0.89
13-May-03	7	0.19	1.6	18.37	1.08
20-May-03	7	0.11	0.9	14.51	0.48
27-May-03	7	0.83	6.9	7.36	1.74
3-Jun-03	7	0.39	3.2	4.09	0.49
10-Jun-03	7	0.79	6.6	8.81	2.14
17-Jun-03	7	0.55	4.6	14.64	2.47
24-Jun-03	7	1.01	8.5	11.09	3.32
1-Jul-03	7	0.01	0.1	44.73	0.08
8-Jul-03	7	0.10	0.8	9.67	0.30
15-Jul-03	7	0.07	0.6	13.45	0.25
22-Jul-03	7	0.10	0.8	21.63	0.65
29-Jul-03	7	0.04	0.3	19.17	0.26
5-Aug-03	7	0.80	6.7	9.94	2.14
12-Aug-03	7	1.45	12.1	6.52	2.85
22-Aug-03	10	0.03	0.3	31.64	0.35
2-Sep-03	7	0.47	3.9	8.88	1.22
9-Sep-03	7	0.24	2.0	11.27	0.79
16-Sep-03	7	0.82	6.9	8.16	2.02
23-Sep-03	7	0.75	6.3	8.11	1.92
1-Oct-03	8	0.21	1.8	24.22	1.42
21-Oct-03	7	0.56	4.7	6.93	1.17

28-Oct-03	7	0.87	7.3	4.3	1.15
4-Nov-03	7	0.50	4.2	2.6	0.42
11-Nov-03	7	0.54	4.5	8.85	1.42
18-Nov-03	7	0.11	0.9	13.47	0.54
25-Nov-03	7	0.61	5.1	6.95	1.27
2-Dec-03	7	0.25	2.1	6.76	0.56
23-Dec-03	7	0.27	2.3	1.48	0.14
30-Dec-03	7	0.27	2.3	3.95	0.34
6-Jan-04	7	0.15	1.3	23.51	1.42
20-Jan-04	7	0.19	1.6	4.74	0.33
3-Feb-04	7	0.07	0.6	1.96	0.07
10-Feb-04	7	0.76	6.4	5.26	1.24
2-Mar-04	7	0.04	0.3	12.51	0.17
9-Mar-04	7	0.38	3.2	11.83	1.38
16-Mar-04	7	0.02	0.1	12.56	0.16
23-Mar-04	7	0.46	3.8	30.97	4.53
30-Mar-04	7	0.04	0.4	15.73	0.26
4-May-04	14	0.88	7.3	8.46	2.28
11-May-04	7	0.07	0.6	17.93	0.44
25-May-04	7	0.20	1.7	14.9	0.60
1-Jun-04	7	0.22	1.8	22.45	1.49
15-Jun-04	14	0.34	2.8	15.81	1.75
22-Jun-04	7	0.16	1.3	19.12	0.96
29-Jun-04	7	0.46	3.8	8.76	1.20
6-Jul-04	7	0.01	0.1	34.56	0.06
13-Jul-04	7	1.04	8.7	8.15	2.64
20-Jul-04	7	0.70	5.8	7.7	1.66
26-Jul-04	6	0.35	2.9	7.37	0.74
3-Aug-04	8	1.58	13.2	9.19	4.20
10-Aug-04	7	0.10	0.8	12.51	0.34
17-Aug-04	7	0.10	0.8	19.26	0.65
24-Aug-04	7	0.11	0.9	12.47	0.64
31-Aug-04	7	0.45	3.8	9.05	1.24
14-Sep-04	7	0.14	1.2	9.59	0.39
21-Sep-04	7	1.06	8.9	3.7	1.23
28-Sep-04	7	0.06	0.5	6.61	0.07
5-Oct-04	7	1.43	11.9	5.15	2.18
19-Oct-04	7	0.51	4.3	11.42	1.65
26-Oct-04	7	0.05	0.4	14.49	0.29
2-Nov-04	7	0.16	1.4	7.03	0.34
9-Nov-04	7	0.31	2.6	5.02	0.46
16-Nov-04	7	0.43	3.6	4.14	0.56

23-Nov-04	7	0.08	0.6	17.09	0.39
29-Nov-04	6	0.88	7.3	2.64	0.64
7-Dec-04	8	0.41	3.4	8.67	1.07
14-Dec-04	7	0.98	8.2	4.86	1.44
4-Jan-05	13	0.32	2.7	4.81	0.46
11-Jan-05	7	1.22	10.1	6.02	2.20
25-Jan-05	7	0.02	0.1	11.1	0.06
2-Feb-05	8	0.01	0.1	5.66	0.02
16-Feb-05	8	0.31	2.6	4.19	0.42
22-Feb-05	6	0.20	1.7	5.5	0.38
1-Mar-05	7	0.11	0.9	3.23	0.28
8-Mar-05	7	0.07	0.6	17.33	0.57
16-Mar-05	7	0.03	0.2	13.93	0.04
23-Mar-05	7	0.17	1.4	7.22	0.35
29-Mar-05	6	0.74	6.1	5.47	1.24
5-Apr-05	7	1.02	8.5	4.68	1.41
12-Apr-05	7	0.16	1.3	8.25	0.26
27-Apr-05	6	0.62	5.2	4.83	0.90
4-May-05	7	0.22	1.9	8.58	0.64
25-May-05	8	0.26	2.2	9.48	0.82
31-May-05	6	0.06	0.5	11.51	0.14
7-Jun-05	7	0.93	7.8	14.93	3.61
14-Jun-05	7	0.02	0.1	29.66	0.14
28-Jun-05	7	0.19	1.6	8.55	0.20
4-Jul-05	6	0.01	0.1	23.1	0.06
13-Jul-05	9	0.77	6.4	9.6	1.83
19-Jul-05	6	0.40	3.3	16.4	1.46
26-Jul-05	7	0.03	0.2	33.1	0.27
2-Aug-05	7	0.07	0.6	58.6	0.21
16-Aug-05	7	0.13	1.1	9.2	0.14
23-Aug-05	7	0.10	0.8	22.6	0.74
30-Aug-05	7	0.09	0.7	5.7	0.16
22-Sep-05	8	0.29	2.4	32.5	2.53
27-Sep-05	5	0.05	0.4	13.5	0.23
4-Oct-05	7	0.02	0.2	23.04	0.19
25-Oct-05	7	0.66	5.5	7.47	1.61
1-Nov-05	7	0.05	0.4	3.99	0.09
8-Nov-05	7	0.04	0.3	13.31	0.13
15-Nov-05	7	0.03	0.2	9.73	0.08
22-Nov-05	7	0.55	4.6	5.11	0.89
29-Nov-05	7	0.04	0.3	11.14	0.13
6-Dec-05	7	0.42	3.5	6.59	0.79

13-Dec-05	7	0.07	0.6	3.62	0.22
20-Dec-05	7	0.51	4.3	12.62	1.85
3-Jan-06	14	0.74	6.1	8.22	1.82
12-Jan-06	9	0.12	1.0	5.85	0.21
17-Jan-06	5	0.14	1.2	5.83	0.30
24-Jan-06	7	0.60	5.0	5.49	0.98
31-Jan-06	7	0.06	0.5	10.81	0.17
7-Feb-06	7	0.25	2.1	14.5	1.17
14-Feb-06	7	0.14	1.2	3.42	0.25
22-Feb-06	8	0.02	0.2	29.53	0.16
28-Feb-06	6	0.01	0.1	39.07	0.25
7-Mar-06	7	0.08	0.6	15.78	0.32
14-Mar-06	7	0.13	1.1	20.08	0.83
28-Mar-06	7	0.05	0.4	8.34	0.15
4-Apr-06	7	0.09	0.7	10.28	0.29
20-Apr-06	9	0.01	0.1	41.8	0.15
26-Apr-06	6	0.81	6.8	14.62	3.48
10-May-06	7	0.03	0.2	48.97	0.54
18-May-06	8	0.73	6.1	17.21	3.86
23-May-06	5	0.05	0.5	20.67	0.34
1-Jun-06	9	0.06	0.5	11	0.18
7-Jun-06	6	0.64	5.3	9	1.56
13-Jun-06	6	0.05	0.4	12.48	0.32
20-Jun-06	7	0.19	1.6	12.04	0.66
4-Jul-06	7	0.86	7.2	4.22	1.04
11-Jul-06	7	0.40	3.3	6.63	0.70
25-Jul-06	7	0.28	2.3	12.69	1.02

Appendix C

Concentrations of Trace Metals

in New Brunswick, New Jersey Wet Deposition

C.1 New Brunswick, NJ: sample volumes, rain depths, and trace metal concentrations in precipitation[a]. NA is not analyzed; ND is non-detect; dash (-) is data unavailable. Data from 27-Jul-99 through 22-Oct-02 from Zhuang [2004].

sample end date	sample volume	rain depth	trace metal concentration (ug L^{-1})															
	(mL)	(cm)	Mg	Pd	Ag	Cd	Sb	Pb	Al	V	Cr	Mn	Fe	Co	Ni	Cu	Zn	As
27-Jul-99	308	1.7	NA	0.010	0.010	0.130	0.090	3.20	42.4	0.550	0.800	4.13	67.6	0.090	2.99	7.78	25.6	0.160
10-Aug-99	191	1.1	NA	0.010	0.010	0.150	0.150	5.06	115	0.640	0.980	13.8	171	0.200	1.17	3.99	34.8	0.230
21-Aug-99	801	4.5	NA	0.010	0.002	0.030	0.020	0.380	10.2	0.230	0.150	0.700	10.0	0.020	0.220	0.450	3.40	0.060
14-Sep-99	733	4.1	NA	0.020	0.00004	0.020	0.050	1.54	6.84	0.380	0.100	0.790	10.7	0.020	0.250	0.490	2.78	0.110
21-Sep-99	923	5.1	NA	0.010	0.003	0.010	0.030	0.300	8.12	0.240	0.160	0.740	12.8	0.020	0.230	0.490	2.68	0.020
9-Oct-99	821	4.6	NA	0.020	0.005	0.020	0.060	1.32	6.51	0.340	0.280	0.630	9.28	0.070	0.240	0.610	3.29	0.100
21-Oct-99	681	3.8	NA	0.030	0.110	0.040	0.070	0.590	4.38	0.230	0.080	0.430	7.32	0.020	0.230	0.670	4.04	0.080
2-Nov-99	176	1.0	NA	0.010	0.010	0.020	0.040	0.480	13.8	0.100	0.080	3.25	17.7	0.040	0.210	0.360	0.98	0.070
15-Nov-99	445	2.5	NA	0.088	0.004	0.010	0.010	0.220	16.9	0.050	0.090	0.230	3.48	0.040	0.300	0.800	5.22	0.020
27-Nov-99	698	3.9	NA	0.020	0.0004	0.020	0.060	0.490	4.78	0.310	0.080	0.720	5.25	0.040	0.260	0.550	8.76	0.080
8-Dec-99	330	1.8	14.3	0.003	0.006	0.048	0.058	0.437	7.96	0.277	0.063	0.689	11.6	0.011	0.661	0.373	0.46	0.003
20-Dec-99	913	5.1	73.5	0.004	0.005	0.029	0.107	0.849	9.20	0.457	0.154	1.15	28.1	0.033	0.940	0.959	5.31	0.007
13-Jan-00	674	3.7	25.4	0.004	0.006	0.040	0.079	1.28	12.5	0.291	0.137	1.87	19.3	0.018	0.646	0.562	5.28	0.001
26-Jan-00	216	1.2	54.1	0.012	0.008	0.194	0.101	1.97	15.9	0.742	0.172	2.62	27.7	0.076	1.35	2.99	15.1	0.001
5-Feb-00	408	2.3	32.2	0.010	0.007	0.058	0.066	0.937	6.03	0.592	0.063	0.817	9.54	0.034	0.954	0.647	5.43	0.005
19-Feb-00	781	4.3	30.9	0.001	0.006	0.036	0.068	0.934	9.79	0.600	0.089	1.34	12.3	0.026	0.831	0.559	5.78	0.007
14-Mar-00	690	3.8	84.0	0.006	0.004	0.042	0.084	1.15	24.5	0.729	0.231	4.18	28.1	0.031	0.841	0.883	5.21	0.007
24-Mar-00	598	3.3	42.2	0.002	0.005	0.020	0.057	0.657	6.71	0.503	0.066	0.963	10.6	0.020	0.672	0.528	0.90	0.004
6-Apr-00	621	3.5	103	0.002	0.001	0.063	0.094	1.94	16.9	0.618	0.081	2.40	15.0	0.028	1.25	1.06	6.68	0.004
17-Apr-00	599	3.3	87.1	0.007	0.002	0.056	0.099	1.82	37.4	0.384	0.164	4.48	37.0	0.028	0.187	1.03	7.97	0.288
29-Apr-00	654	3.6	123	0.009	0.002	0.040	0.090	0.986	33.7	0.800	0.069	3.11	28.8	0.036	0.221	0.682	2.22	0.072
5-Jun-00	305	1.7	101	0.003	0.00003	0.070	0.101	2.66	24.4	0.403	0.139	7.35	28.6	0.043	0.255	1.14	9.58	0.204
17-Jun-00	898	5.0	47.6	0.004	0.004	0.024	0.068	1.64	14.8	0.268	0.082	2.71	22.1	0.019	0.111	0.597	5.83	0.006
30-Jun-00	318	1.8	31.0	0.009	0.001	0.023	0.087	1.41	11.4	0.434	0.069	1.11	11.0	0.048	0.552	1.20	5.15	0.104
22-Jul-00	661	3.7	52.1	0.006	0.003	0.041	0.103	2.67	13.9	0.294	0.048	1.48	17.4	0.032	0.246	1.31	5.95	0.027
28-Jul-00	1082	6.0	15.0	0.003	0.002	0.018	0.039	1.03	1.86	0.383	0.062	0.537	2.49	0.004	0.087	0.391	7.73	0.001
4-Aug-00	1015	5.6	20.2	0.002	0.001	0.018	0.072	0.680	7.33	0.432	0.028	0.362	6.56	0.012	0.109	0.393	7.83	0.036
15-Aug-00	1920	10.7	17.7	0.007	0.001	0.016	0.038	0.535	8.86	0.237	0.035	0.631	9.89	0.022	0.076	0.325	3.10	0.018
29-Aug-00	142	0.8	40.6	0.015	0.0003	0.083	0.165	3.46	39.3	0.434	0.122	5.15	39.9	0.045	0.429	1.63	56.5	0.172
8-Sep-00	550	3.1	65.2	0.006	0.003	0.064	0.059	1.14	12.3	0.428	0.040	1.71	13.5	0.025	0.316	1.00	1.19	0.074
21-Sep-00	1011	5.6	39.4	0.002	0.001	0.034	0.087	0.929	15.8	0.330	0.099	1.44	25.3	0.015	0.284	0.426	1.43	0.053
2-Oct-00	504	2.8	54.2	0.022	0.003	0.031	0.089	0.735	13.6	0.485	0.069	0.862	22.5	0.040	0.474	2.07	4.35	0.038
8-Nov-00	272	1.5	305	0.016	0.022	0.079	0.160	1.54	32.5	0.576	0.231	5.04	53.6	0.061	0.713	1.71	9.12	0.181
21-Nov-00	699	3.9	26.2	0.005	0.301	0.036	0.070	0.529	7.96	0.539	0.038	0.885	10.4	0.015	0.211	0.423	1.62	0.109
2-Dec-00	845	4.7	77.2	0.009	0.796	0.024	0.028	0.466	2.66	0.209	0.044	1.06	5.73	0.008	0.079	0.370	1.79	0.039
17-Dec-00	1076	6.0	111	0.028	0.115	1.20	0.209	5.22	72.2	0.516	0.326	3.09	30.2	0.328	10.3	25.83	42.8	0.002
5-Jan-01	490	2.7	25.7	0.026	0.005	0.026	0.063	1.91	19.8	0.740	0.092	1.20	18.6	0.034	0.486	0.665	103	0.006
21-Jan-01	1163	6.5	38.6	0.016	0.020	0.040	0.120	1.33	25.6	0.877	0.193	3.91	28.7	0.051	0.656	1.45	7.90	0.004
1-Feb-01	317	1.8	30.7	0.008	0.002	0.032	0.080	0.684	14.9	0.624	0.133	1.25	16.8	0.013	0.302	0.564	2.70	0.002
23-Feb-01	885	4.9	49.1	0.016	0.005	0.040	0.107	1.22	20.8	0.723	0.161	2.09	31.2	0.050	0.558	1.09	4.83	0.003
9-Mar-01	513	2.9	314	0.026	0.006	0.065	0.111	2.23	25.7	1.07	0.261	3.58	41.6	0.056	0.626	1.13	9.02	0.001
20-Mar-01	757	4.2	38.5	0.029	0.004	0.042	0.068	1.62	26.4	0.543	0.110	1.91	26.9	0.028	0.291	0.690	7.07	0.001
28-Mar-01	835	4.6	59.6	0.019	0.006	0.021	0.078	0.925	19.9	0.816	0.156	0.891	31.6	0.061	0.667	0.858	7.35	0.007
5-Apr-01	1078	6.0	23.0	0.014	0.007	0.022	0.060	4.13	11.2	0.633	0.072	0.570	13.4	0.024	0.332	0.554	0.687	0.007
12-Apr-01	708	3.9	103	0.060	0.008	0.083	0.156	3.28	43.9	1.07	0.140	4.28	43.0	0.056	0.455	1.25	13.1	0.006
21-May-01	124	0.7	438	0.238	0.017	0.204	0.314	9.10	202	1.80	0.442	29.3	176	0.327	1.54	3.80	24.7	0.006
30-May-01	1177	6.5	54.9	0.077	0.011	0.062	0.173	4.23	47.1	1.26	0.262	3.93	54.3	0.042	0.543	1.28	11.4	0.006
21-Jun-01	2550	14.2	73.5	0.012	0.005	0.032	0.050	1.69	36.1	0.496	0.215	4.47	64.1	0.036	0.383	1.02	5.75	0.117
5-Jul-01	1070	5.9	15.2	0.002	0.003	0.022	0.026	0.461	20.2	0.194	0.037	0.703	22.1	0.015	0.219	0.165	1.64	0.049
26-Jul-01	799	4.4	52.2	0.006	0.022	0.062	0.174	1.66	49.5	1.09	0.149	2.42	75.0	0.066	0.728	1.06	6.64	0.197
15-Aug-01	1414	7.9	30.3	0.002	0.011	0.020	0.070	0.933	35.7	0.407	0.096	1.91	55.2	0.039	0.384	0.496	4.74	0.084
19-Sep-01	1080	6.0	65.7	0.005	0.082	0.041	0.151	1.62	101	0.682	0.246	3.30	155	0.081	0.731	1.17	6.60	0.119
3-Oct-01	786	4.4	40.3	0.003	0.002	0.017	0.027	1.73	18.3	0.229	0.030	0.403	16.8	0.015	0.168	0.514	5.30	0.053
24-Oct-01	210	1.2	62.4	0.004	0.002	0.041	0.052	1.03	18.6	0.402	0.047	1.50	22.1	0.037	0.341	0.770	7.85	0.120
12-Dec-01	873	4.9	137	0.006	0.003	0.062	0.198	3.03	48.1	1.04	0.322	4.91	69.1	0.059	0.675	1.80	13.4	0.117
8-Jan-02	884	4.9	51.6	0.009	0.003	0.030	0.097	1.64	16.8	0.527	0.112	1.82	36.9	0.033	0.457	0.901	11.2	0.105
29-Jan-02	528	2.9	34.0	0.003	0.004	0.028	0.082	0.634	38.5	0.456	0.165	1.83	36.0	0.041	0.477	1.11	7.18	0.099
26-Feb-02	376	2.1	173	0.008	0.016	0.088	0.097	4.93	86.8	1.72	0.274	7.58	115	0.091	1.09	2.65	28.7	0.165
19-Mar-02	1073	6.0	91.1	0.003	0.001	0.036	0.058	2.12	59.1	0.577	0.067	3.44	44.8	0.036	0.360	1.38	6.97	0.093
13-Apr-02	1079	6.0	127	0.004	0.007	0.038	0.093	2.31	109	0.997	0.223	4.12	121	0.060	0.601	2.03	7.18	0.161
6-May-02	1460	8.1	116	0.004	0.002	0.048	0.062	4.35	128	0.844	0.185	6.13	133	0.089	0.653	2.55	8.23	0.164
24-May-02	1075	6.0	55.6	0.003	0.001	0.034	0.092	1.36	45.1	0.944	0.074	2.90	54.3	0.039	0.406	0.993	4.54	0.144
21-Jun-02	1635	9.1	55.1	0.005	0.003	0.048	0.088	2.08	27.0	0.397	0.057	3.89	42.7	0.035	0.272	1.08	8.03	0.092
17-Jul-02	332	1.8	109	0.006	0.002	0.052	0.109	1.89	83.0	0.854	0.112	6.11	98.9	0.097	0.719	2.10	11.0	0.163
12-Aug-02	1797	10.0	79.5	0.012	0.010	0.153	0.150	2.82	120	1.23	0.381	4.20	197	0.104	0.954	1.93	7.30	0.157
3-Sep-02	1078	6.0	111	0.005	0.004	0.026	0.132	1.82	137	1.44	0.469	4.58	206	0.097	0.949	2.08	5.05	0.087
30-Sep-02	1507	8.4	20.6	0.001	0.002	0.014	0.076	0.566	17.5	0.352	0.050	0.821	35.1	0.025	0.272	2.38	3.48	0.040
22-Oct-02	1074	6.0	107	0.003	0.003	0.031	0.142	2.23	43.4	0.886	0.259	3.06	92.3	0.068	0.534	1.57	6.35	0.100

22-Feb-03	-	-	21.9	0.016	0.008	0.028	0.025	4.17	95.8	1.37	0.389	2.31	119	0.035	0.285	1.40	8.34	0.015
8-Apr-03	928	5.2	93.2	0.023	0.007	0.039	0.082	1.56	56.9	0.781	0.307	3.75	61.4	0.050	0.349	1.05	8.68	0.019
18-Sep-03	314	1.7	153	0.010	0.004	0.017	0.054	1.16	12.1	0.345	0.451	1.51	16.5	0.090	0.822	0.503	9.53	6.00
5-Oct-03	925	5.1	33.4	0.015	0.001	0.026	0.021	0.115	1.43	0.066	0.076	0.386	4.27	0.006	0.138	0.122	9.83	0.026
28-Oct-03	1038	5.8	43.3	0.009	0.003	0.015	0.044	0.490	24.8	0.181	0.369	0.845	25.2	0.018	0.116	0.454	2.57	0.066
16-Dec-03	1933	10.7	195	0.015	0.006	0.025	0.083	0.903	28.5	0.438	0.155	1.55	26.0	0.029	0.383	0.949	5.71	0.070
8-Jan-04	1126	6.3	50.3	0.012	0.002	0.020	0.090	0.376	13.5	0.441	0.122	0.552	13.0	0.026	0.334	0.529	3.83	0.069
20-Mar-04	1065	5.9	49.2	0.029	0.008	0.050	0.187	1.77	76.4	0.790	0.329	3.01	65.8	0.075	0.641	1.89	14.5	0.113
10-May-04	1072	6.0	114	0.026	0.006	0.044	0.127	1.16	43.4	0.342	0.438	3.87	34.1	0.042	0.242	0.888	7.92	9.03
2-Jun-04	1371	7.6	88.9	0.027	0.008	0.046	0.206	2.21	90.4	1.04	0.321	5.52	94.0	0.097	0.716	1.69	11.5	0.176
24-Jun-04	-	-	94.6	0.024	0.006	0.041	0.167	1.74	50.1	0.648	0.376	4.45	58.5	0.074	0.591	1.39	8.26	0.103
8-Jul-04	1058	5.9	29.3	0.029	0.028	0.049	0.107	1.51	21.0	0.307	0.173	1.26	25.4	0.032	0.195	0.726	4.15	0.118
19-Jul-04	-	-	28.7	0.009	0.0003	0.015	0.066	0.283	5.02	0.111	0.196	0.528	3.82	0.034	0.244	0.481	5.00	0.057
11-Aug-04	1554	8.6	18.7	0.012	0.005	0.021	0.073	0.382	9.86	0.292	0.326	0.677	15.4	0.018	0.255	0.526	3.65	0.070
29-Sep-04	3696	20.5	35.9	0.005	0.003	0.009	0.045	0.505	17.5	0.220	0.145	0.701	16.6	0.011	0.106	0.910	3.77	0.022
22-Oct-04	661	3.7	86.8	0.020	0.006	0.034	0.271	1.31	31.7	1.25	0.228	2.15	46.7	0.094	0.872	1.96	8.96	0.144
17-Nov-04	1095	6.1	25.7	0.014	0.002	0.025	0.086	0.423	12.3	0.201	0.154	0.855	14.4	0.027	0.315	0.797	7.09	0.033
12-Dec-04	2115	11.8	87.9	0.012	0.003	0.020	0.095	0.751	10.9	0.490	0.156	1.79	17.5	0.022	0.237	0.679	5.37	0.071
3-Jan-05	372	2.1	119	0.014	0.001	0.023	0.078	1.67	23.1	0.243	0.135	1.22	21.3	0.025	0.170	0.867	4.54	0.058
26-Jan-05	960	5.3	41.2	0.012	0.002	0.020	0.103	0.712	17.3	0.427	0.167	1.27	21.1	0.032	0.352	0.732	4.36	0.080
13-Feb-05	-	-	29.1	0.009	0.006	0.015	0.092	0.882	20.2	0.355	0.154	1.70	28.5	0.028	0.258	0.886	3.63	0.053
19-Feb-05	632	3.5	41.4	0.019	0.006	0.033	0.116	0.748	22.3	0.378	0.157	1.21	28.2	0.030	0.310	1.03	5.34	0.068
14-Mar-05	1051	5.8	36.2	0.019	0.002	0.032	0.086	0.873	27.4	0.425	0.184	1.85	45.6	0.054	1.98	2.63	8.83	0.015
7-Apr-05	948	5.3	70.0	0.016	0.004	0.028	0.106	0.832	19.8	0.561	0.179	1.67	23.7	0.032	0.327	0.688	3.74	0.080
2-May-05	1079	6.0	58.4	0.022	0.004	0.038	0.104	1.02	31.5	0.458	0.178	4.00	36.2	0.035	0.276	1.83	5.86	0.122
27-May-05	726	4.0	72.2	0.024	0.013	0.040	0.118	1.02	27.6	0.425	0.180	8.47	37.8	0.045	0.347	1.81	7.94	0.200
20-Jun-05	617	3.4	66.9	0.017	0.023	0.029	0.100	1.71	26.0	0.465	0.219	8.49	34.7	0.038	1.19	0.977	8.60	0.070
5-Aug-05	1110	6.2	19.7	0.010	0.002	0.016	0.094	0.625	12.0	0.364	0.114	1.43	14.2	0.019	0.457	0.783	3.03	0.126
30-Aug-05	412	2.3	63.8	0.019	0.011	0.032	0.217	1.90	47.9	0.779	0.244	2.95	50.5	0.073	0.572	1.92	7.95	0.209
23-Sep-05	685	3.8	104	0.010	0.001	0.018	0.085	0.636	98.0	0.680	0.219	4.03	61.8	0.070	0.335	1.03	3.74	0.088
17-Oct-05	4718	26.2	42.0	0.004	0.002	0.008	0.060	0.441	14.3	0.425	0.106	0.487	13.7	0.021	0.278	0.544	1.92	0.022
10-Nov-05	1331	7.4	56.4	0.013	0.005	0.022	0.124	0.567	9.88	0.550	0.107	1.50	14.9	0.031	0.309	0.924	3.75	0.060
5-Dec-05	1149	6.4	48.2	0.026	0.001	0.045	0.049	0.575	6.94	0.132	0.133	0.868	9.55	0.010	0.159	0.420	3.37	0.032
28-Dec-05	1092	6.1	86.1	0.008	0.006	0.014	0.076	0.386	9.23	0.400	0.101	0.783	10.9	0.019	0.300	0.594	4.30	0.045
20-Jan-06	1716	9.5	105	0.010	0.003	0.018	0.076	0.426	9.21	0.349	0.098	0.819	8.04	0.023	0.294	0.522	3.25	0.066
14-Feb-06	1407	7.8	78.5	0.022	0.001	0.038	0.121	1.47	15.2	0.455	0.090	6.14	14.9	0.029	0.362	0.848	7.03	0.088
3-Apr-06	310	1.7	145	0.055	0.006	0.094	0.322	2.63	93.3	1.15	0.284	8.82	91.3	0.110	0.630	2.49	15.7	0.291
28-Apr-06	1061	5.9	188	0.024	0.004	0.040	0.109	1.33	30.3	0.398	0.134	5.28	32.9	0.037	0.261	1.05	5.46	0.130
26-May-06	1209	6.7	76.4	0.013	ND	0.023	0.092	0.861	13.7	0.420	0.059	2.78	11.0	0.026	0.277	0.939	3.73	0.078
14-Jun-06	1083	6.0	33.9	0.018	0.008	0.031	0.201	1.80	31.8	0.432	0.145	2.54	48.9	0.040	0.305	1.59	7.64	0.104
11-Jul-06	1775	9.9	49.0	0.013	0.004	0.022	0.192	1.12	18.7	0.233	0.105	1.63	22.6	0.023	0.225	1.15	3.70	0.103
18-Jul-06	534	3.0	16.8	0.013	0.003	0.022	0.105	0.495	17.6	0.257	0.068	1.18	16.8	0.023	0.274	0.472	4.63	0.104
25-Jul-06	567	3.2	37.4	0.014	0.003	0.025	0.116	1.07	29.4	0.354	0.113	2.34	30.2	0.040	0.316	0.735	3.80	0.124

Curriculum Vita

Lora M. Smith

Education

2008 Ph.D. in Environmental Sciences, Rutgers University
Dissertation: Land-atmosphere exchange of mercury in temperate wetlands
2001 B.S. in Environmental Sciences, Rutgers University
1999 A.S. in Chemistry, Middlesex County College

Principal Occupations and Positions

October 2007 to present - Intern, human health risk assessor (Superfund program), US EPA, New York, NY
September 2002 to present - Graduate fellow/assistant, The Graduate School – New Brunswick, Rutgers University
September 2003 to December 2003 - Teaching assistant, Department of Environmental Sciences, Rutgers University, Course: Chemical Principles of Environmental Science
January 2003 to May 2003 - Teaching assistant, Department of Environmental Sciences, Rutgers University, Course: Soils and Water lab
August 2001 to August 2002 - Environmental Scientist, URS Corporation, Cranford, NJ

Publications

Smith, L.M. and J.R. Reinfelder (in prep), Mercury volatilization fluxes from salt marsh sediments, Environ. Sci. Technol.